ISRIC
World Soil Information

# How well does Digital Soil Mapping represent soil geography? An investigation from the USA

*Part 2: Case Studies*

ISRIC Report 2021/03
revised September 2022

David G. Rossiter
Dylan Beaudette
Zamir Libohova
Laura Poggio

Director, ISRIC - World Soil Information
Droevendaalsesteeg 3 (building 101)
6708 PB Wageningen
The Netherlands
E-mail: soils@isric.org



**Citation**

Rossiter, David G; Beaudette, Dylan ; Libohova,Zamir; Poggio, Laura, 2022. How well does Digital Soil Mapping represent soil geography? An investigation from the USA. Case Studies. Report 2021/03 (revised 05-September-2022), ISRIC – World Soil Information, Wageningen (doi: 10.17027/isric-wdc-202103)

# How well does Digital Soil Mapping represent soil geography? An investigation from the USA Part 2: Case Studies

David G. Rossiter[1, 2], Dylan Beaudette[3], Zamir Libohova[4], and Laura Poggio[1]

[1]ISRIC-World Soil Information, Postbus 353, Wageningen 6700 AJ, NL
[2]Section of Soil & Crop Sciences, New York State College of Agriculture and Life Sciences, 233 Emerson Hall, Cornell University, Ithaca NY 14853 USA
[3]USDA-NRCS-National Soil Survey Center, 100 Centennial Mall North, Room 152, Lincoln, NE 68508-3866 USA
[4]USDA-ARS, Dale Bumpers Small Farms Research Center, 6883 South State Hwy 23, Booneville, AR 72927 USA

**Correspondence:** David G. Rossiter (david.rossiter@isric.org)

**Abstract.** We present four case studies in the contiguous USA illustrating the application of methods, developed in a companion paper in the journal SOIL (https://doi.org/10.5194/soil-8-559-2022), to evaluate the spatial patterns of the geographic distribution of soil properties as shown in gridded maps produced by digital soil mapping (DSM) at global (SoilGrids v2), national (Soil Properties and Class 100m Grids of the USA), and regional (POLARIS soil properties) scales, and compare them to spatial patterns known from detailed field survey (gNATSGO and gSSURGO). These case studies reveal substantial differences in the performance of DSM related to (1) the study area and its soil geomorphology; (2) the soil property being predicted; (3) the depth interval being predicted. Each case is unique and reveals different aspects of the reference and DSM products. A set of R Markdown scripts is provided so that readers can apply the analysis for areas and soil properties of their interest.



**Contents**

## 1 Introduction

Digital Soil Mapping (DSM) has been defined as "as the development of a numerical or statistical model of the relationship among environmental variables and soil properties, which is then applied to a geographic data base to create a predictive map" (Scull et al., 2003; McBratney et al., 2003; Minasny and McBratney, 2016). The key question addressed here in to what degree DSM products represent the actual soil landscape spatial pattern and, more importantly, the underlying pedogenetic and geomorphic processes. This report complements an article in SOIL which presents methods and an example (Rossiter et al., 2022). A previous version of that paper, with reviewer and community comments and authors' replies, is in SOIL Discussions (Rossiter et al., 2021).

Here we present representative case studies from four regions of the contiguous USA (CONUS). The DSM products evaluated in this report are **SoilGrids v2.0** (further **SG2**) (ISRIC - World Soil Information, 2020; Poggio et al., 2021), **Soil Properties**

**and Class 100m Grids of the United States** (further **SPCG**) (Ramcharan et al., 2018), **POLARIS soil properties** (Chaney et al., 2019) (further **PSP**). These sources are described in the SOIL article. The objective of this report is to evaluate the landscape and detailed spatial patterns produced by DSM developed for global (SG2), national (SPCG), and regional (PSP) spatial extents, with digital soil maps produced directly from map unit-based field survey: the regional gNATSGO (NRCS Soils, 2020) and local gSSURGO (Natural Resources Conservation Service, n.d.).

These comparisons may be useful in the context of current plans (Thompson et al., 2020) for updating and completing the USA soil survey using DSM methods and GlobalSoilMap (GSM) specifications (Arrouays et al., 2014). They should also be useful for developing realistic expectations for what DSM can and cannot deliver (Arrouays et al., 2020).

The case studies are from four quite different areas, each for locally-important soil properties. Each case study discusses the success of the various DSM methods in their own soil geographic context as well as reasons for their performance. The studies also compare the performance of DSM for different properties and depth intervals. A final Conclusions section discusses the overall success of DSM in these contexts. Data sources and evaluation methods are described in detail in the companion article in SOIL (Rossiter et al., 2022).

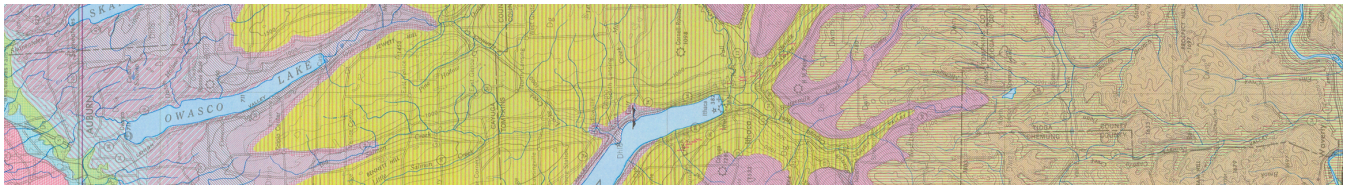


**Figure 1.** Bedrock geology of Central New York State, transect from N–43° N (left) – 42° , centred on -76° 30’ E. Orientation N (left) to S (right). Source: (New York State Geological Survey, 1970)

## 2 Central New York State

This case study expands on the abbreviated example of the main text and puts it in its soil geographic context. The example area is in central New York State, bounding box (-77 – -76° E), (42–43° N); the subtile for pattern evaluation was (-76.8 – -76.6° E), (42.2–42.4° N) The regional geomorphology is described by Bloom (2018). The underlying bedrock is a sedimentary sequence from Ordovician (north) to upper Devonian (south), with a wide variety of sedimentary facies. A north-south transect of the bedrock geology map (New York State Geological Survey, 1970) is shown in Fig. 1. This shows a chronological and topographic sequence from Upper Silurian (N) through Upper Devonian (S) sedimentary rocks, notably the Onondaga limestone (green “Don”) and Tully limestone (crosshatched red, “Dt”), which were spread southward as glacial till.

The entire area has been glaciated, but the portion north of about 42° 15’ (Valley Heads terminal moraines) somewhat more recently than the southern portion. Many glacial features are present: ground moraine, deep glacial troughs with proglacial lake sediments, beach lines, outwash valley trains, kame terraces and hanging deltas. Soil reaction in the northern half is largely controlled by limestone spread by the glacier from outcrops of the Onondaga and Tully limestones, decreasing to the south. A fragment of the surficial geology map (New York State Geological Survey, 1986) is shown in Fig. 2. This shows the strongly-expressed glacial features ground moraine (pink), proglacial lakes (brown), organic swamps (green), bedrock or very thin soil cover (red), till moraine (purple), kame moraines (yellow), and outwash sand and gravel (yellow). These features are well-known to the field soil surveyors.

A soil property with strong spatial expression and with major importance for land use is pH. We present an analysis of pH in the 0–5 and 30–60 cm layers. The pH in the 0–5 cm layer is the example in the SOIL article; here we contrast it with the subsoil (30–60 cm) layer, to see if DSM is, in this case, equally effective in mapping the surface and subsurface.

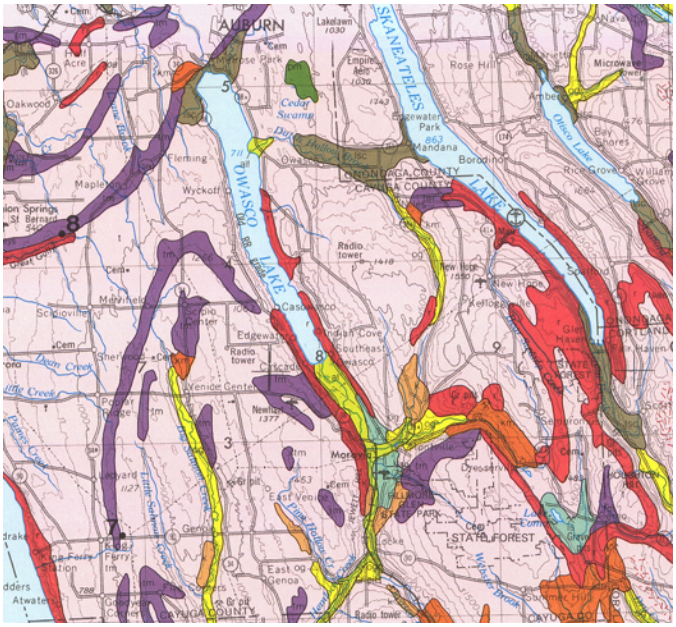


**Figure 2.** Surficial geology of Central New York State near Moravia NY. Legend: ground moraine (pink; if stippled shallow over bedrock), proglacial lakes (brown), organic swamps (dark green), bedrock or very thin soil cover (red), till moraine (purple), kame moraines (orange), lacustrine sand (light green), outwash sand and gravel (yellow). Source: (New York State Geological Survey, 1986)

### 2.1 Regional spatial patterns

### 2.1.1 Regional maps

Table 1 shows the statistical differences between gNATSGO (reference) and the DSM products, along with the predictions of pH in the two depth intervals. Figs. 3 and 4 shows their histograms, and Figs. 5 the pairwise Pearson correlations between all maps.

| Product | MD | RMSD | RMSD.Adjusted |
|---|---|---|---|
| SG2 | 3.796 | 6.111 | 4.789 |
| PSP | 3.843 | 4.908 | 3.052 |
| SPCG | 4.815 | 6.693 | 4.649 |

| Product | MD | RMSD | RMSD.Adjusted |
|---|---|---|---|
| SG2 | 0.564 | 4.681 | 4.647 |
| PSP | 2.736 | 3.996 | 2.913 |
| SPCG | 2.475 | 5.18 | 4.55 |

**Table 1.** Statistical differences between gNATSGO and DSM products, pHx10, 0–5 cm (top), 30–60 cm (bottom)

The DSM products under-predict topsoil pH with respect to gNATSGO, by about 0.38–0.48 pH units, and subsoil pH by about 0.05–0.27 units; SG2 is almost unbiased in the subsoil. The RMSD is substantial also, on the order of 0.49–0.67 (surface) and 0.40–0.51 (subsoil) pH units, somewhat less than this when corrected for bias.

The histograms show that PSP has a bimodal distributions, and predicts few pH values around 5.8 pH in both the top and subsoil. The other distributions are fairly symmetric, except for gNATSGO in the subsoil, which also has a bimodal distribution, however with a minimum around pH 6.2.

The products are overall well-correlated, especially for the subsoil. SG2 and SPCG are very closely correlated, since they use similar mapping methods, despite the additional covariates used by SPCG. PSP and gNATSGO are also closely-correlated. Note however that these close correlations do not account for bias. They do however show that the maps are similar in their overall pattern.

Figs. 6 and 7 show gNATSGO (reference) along with the predictions of pH in the two depth intervals (0-5 cm, 30–60 cm, respectively) of the PSP products Figs. 8 and 9 show these as difference maps.

These figures reveal substantial differences between products. The most obvious difference is in the detail of the spatial pattern. Despite having been upscaled to regional resolution, gNATSGO shows finer detail than the other products, especially PSP.

Compared to gNATSGO, SG2 and SPCG underestimate pH in the higher hills in the NE portion of the map, and in the glacio-lacustrine sediments along the lakeshores. SG2 misses the soils derived from Onondaga limestone glacial till towards the southern end of the till plain. SG2 has no information on parent material and uses global models. SPCG has very similar differences, despite using SSURGO-derived parent material as a covariate.

PSP predictions are closer to gNATSGO than are those of SG2, which is not surprising since PSP also uses gSSURGO as its primary information source. This product has removed some of the fine variation of gNATSGO. However the disaggregation by DSMART results in quite some discrepancies with gNATSGO. In particular, the Homer-Tully outwash valley (northeast side of map) is under-predicted by one pH unit, and the surrounding hills over-predicted by almost as much. Many of the valley trains

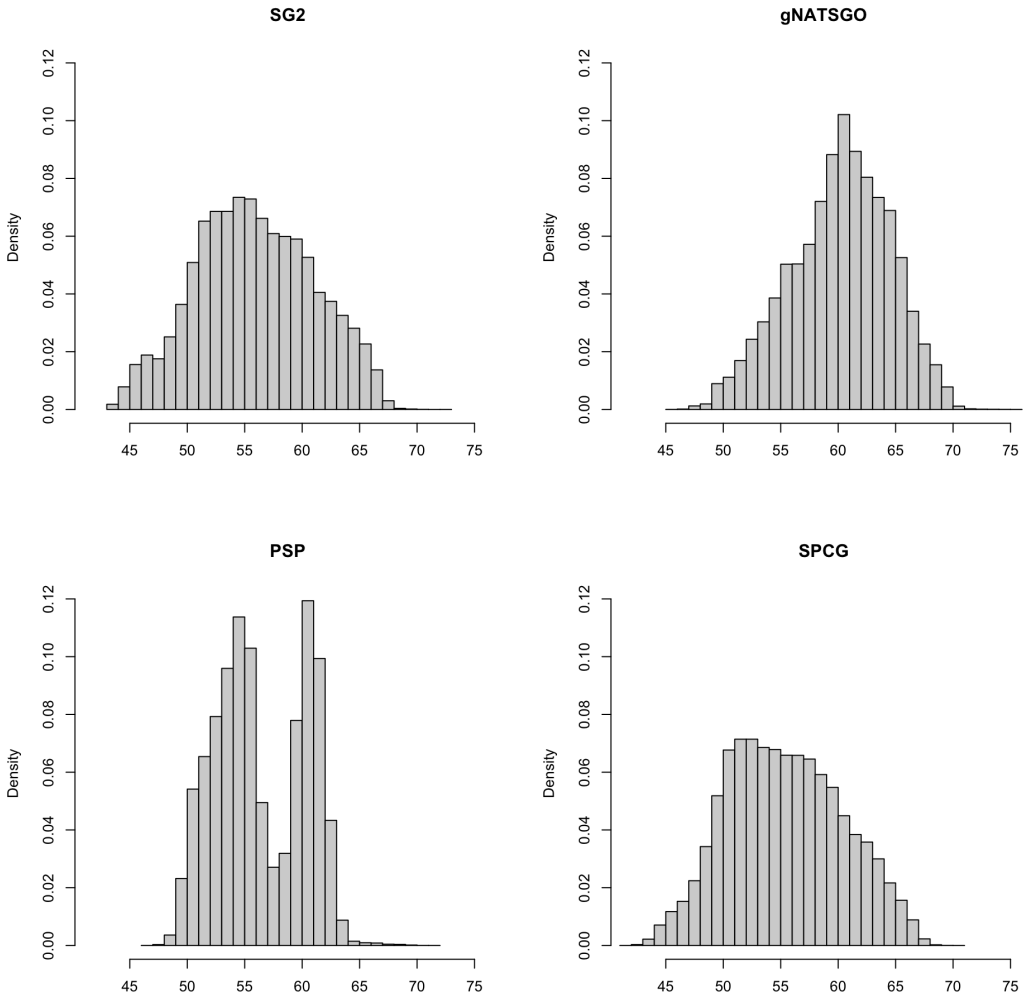


**Figure 3.** Histograms of topsoil (0-5 cm) pHx10

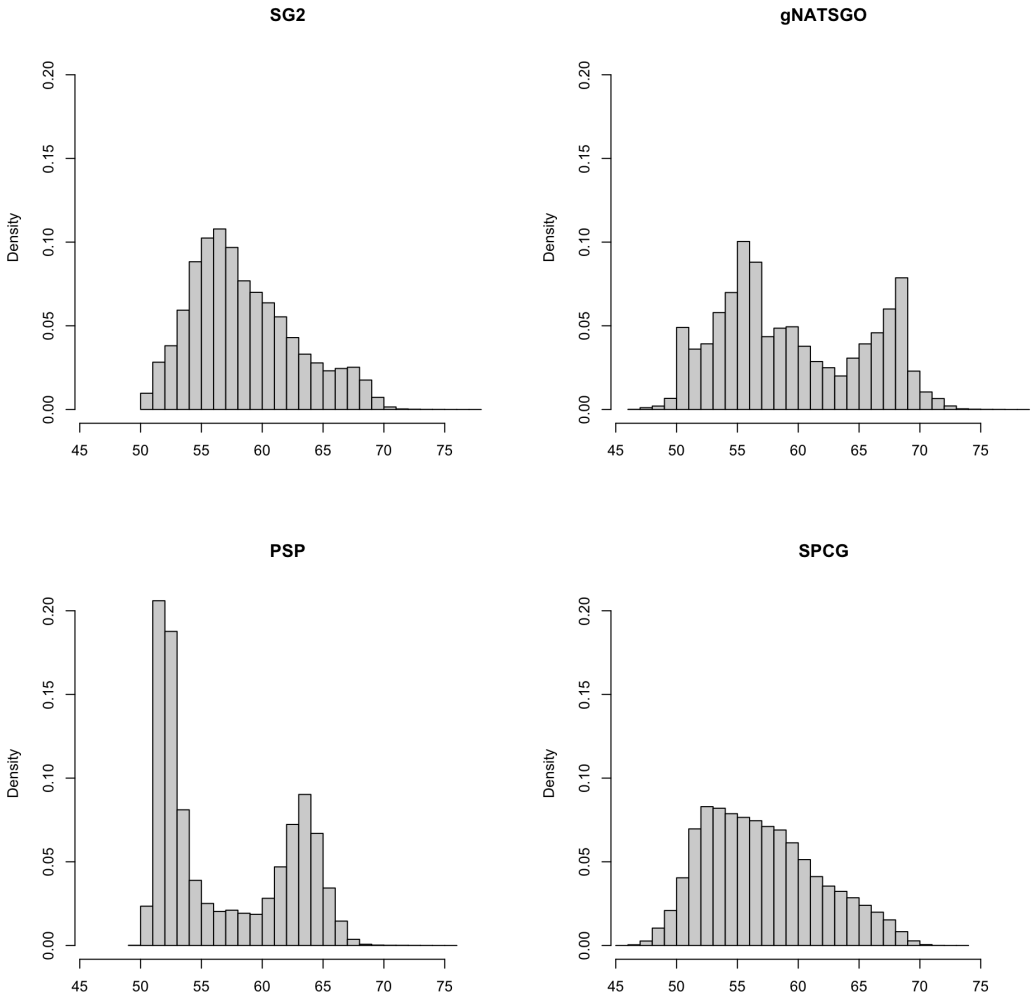


**Figure 4.** Histograms of subsoil (30-60 cm) pHx10

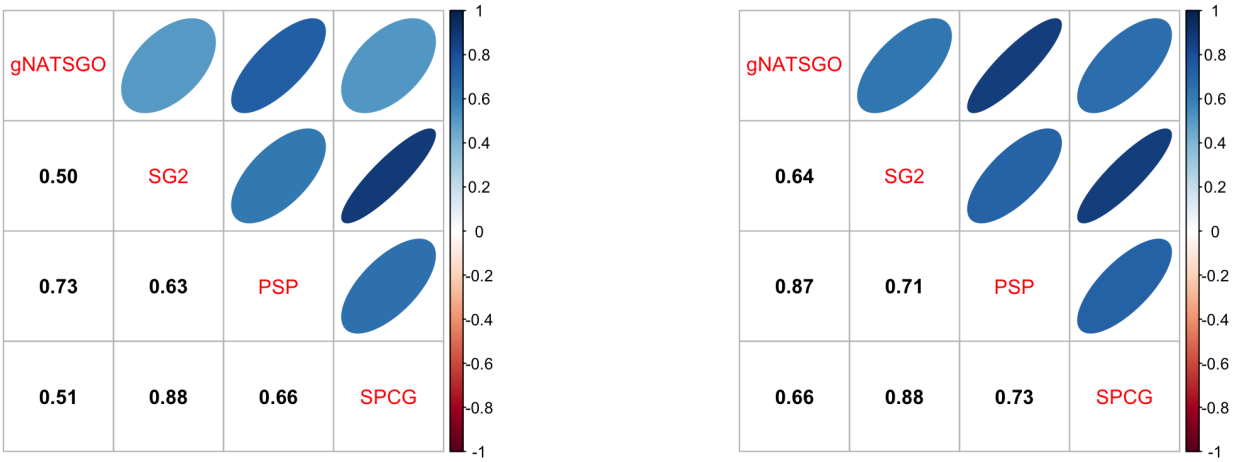


**Figure 5.** Pearson correlations between all products, pHx10, 0–5 cm (left), 30–60 cm (right)

are under-predicted. This is likely due to PSP's soil series predictions, which are based on estimated map unit composition, but random selection of series locations within map units for DSM calibration.

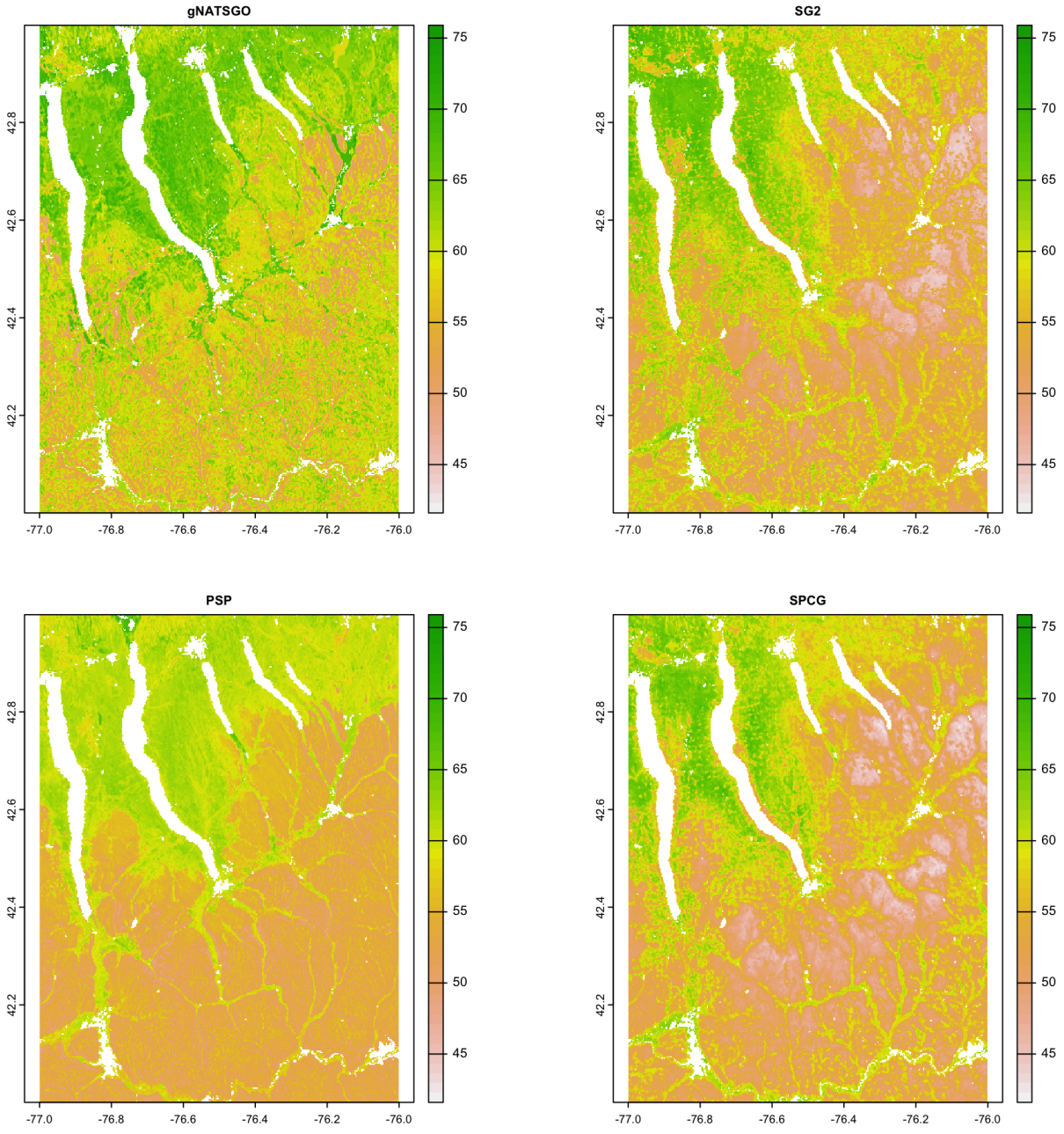


**Figure 6.** Topsoil (0-5 cm) pHx10, according to gNATSGO and DSM products

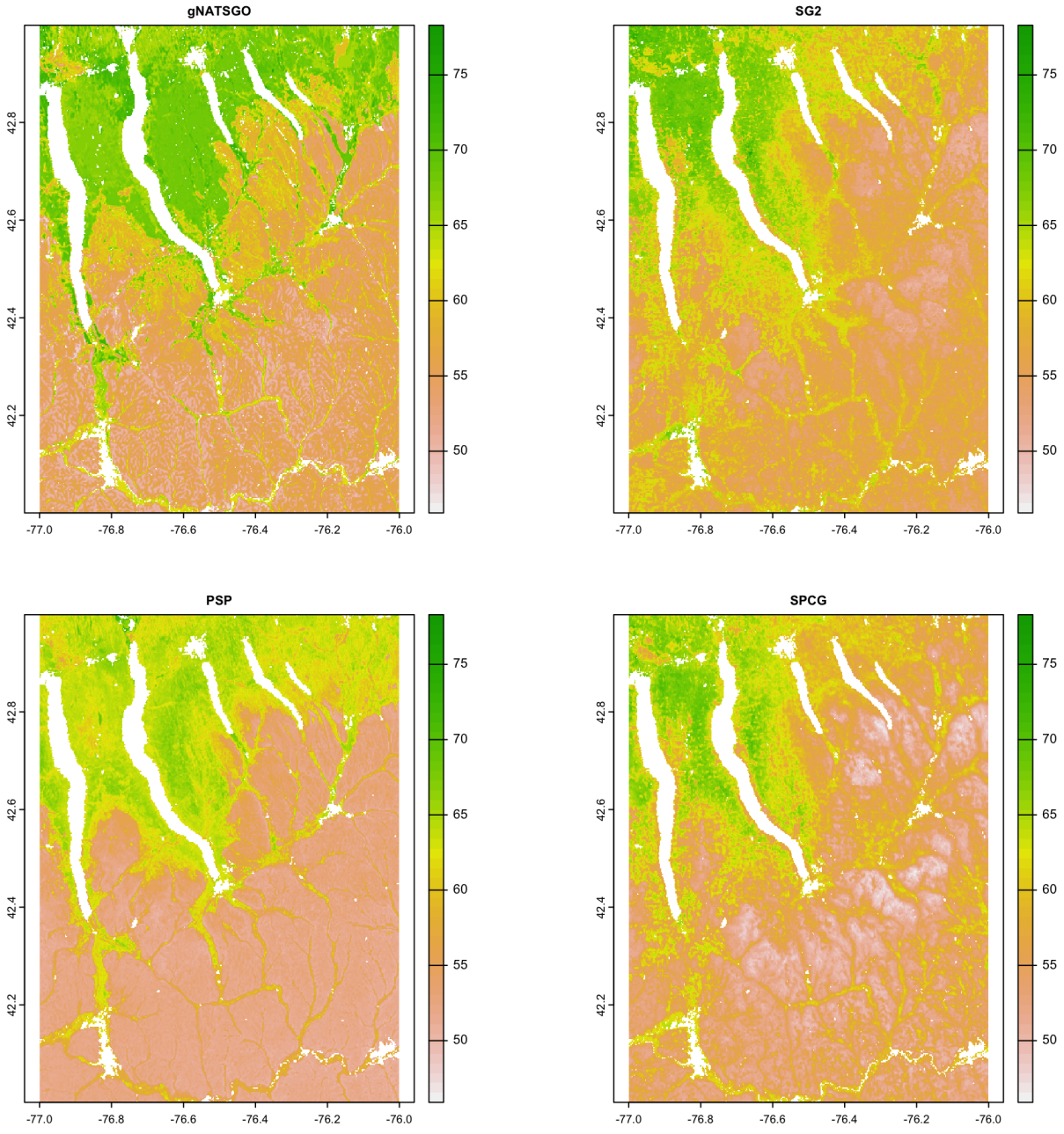


**Figure 7.** Subsoil (30-60 cm) pHx10, according to gNATSGO and DSM products

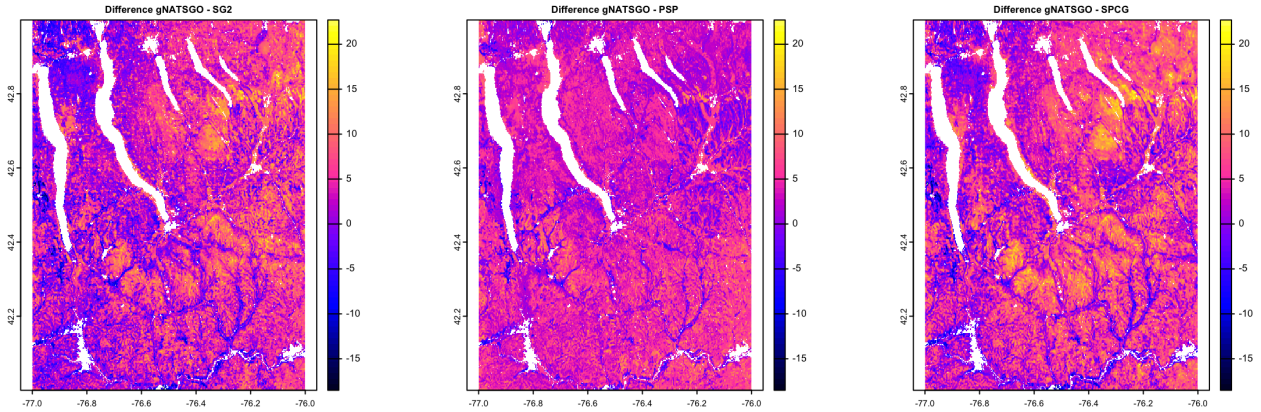


**Figure 8.** Difference between gNATSGO and DSM products, pHx10, 0–5 cm

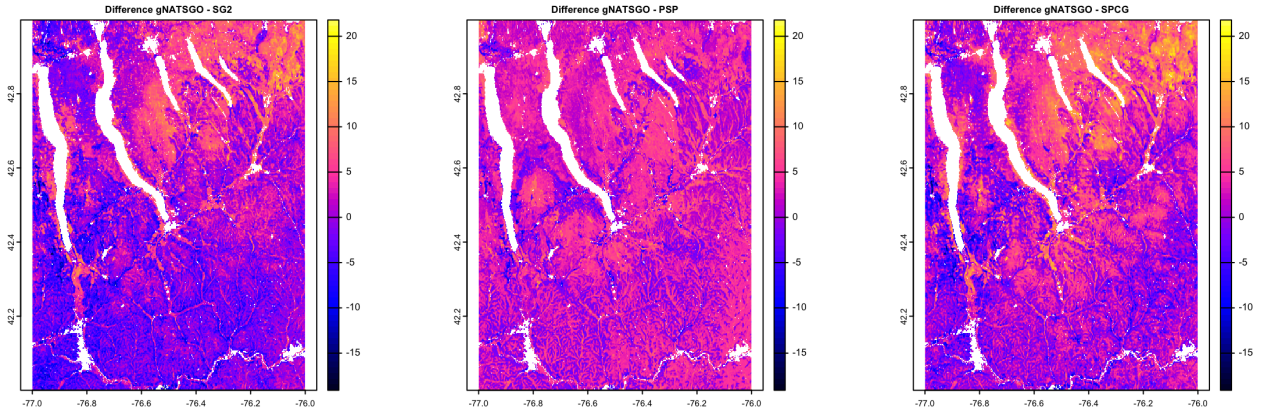


**Figure 9.** Difference between gNATSGO and DSM products, pHx10, 30–60 cm

### 2.1.2 Uncertainty

Only SG2 and PSP provide uncertainty estimates that can be used to construct confidence intervals, as inter-quantile ranges (IQR), from the 5% to the 95% quantiles. These are computed as part of the random forest machine learning model.

The 5%, 50%, and 95% prediction quantile maps are shown in Fig. 10 (PSP) and 11 (SG2); each figure has its own stretch. The "low", "representative" and "high" values from gNATSGO are shown in Fig. 12

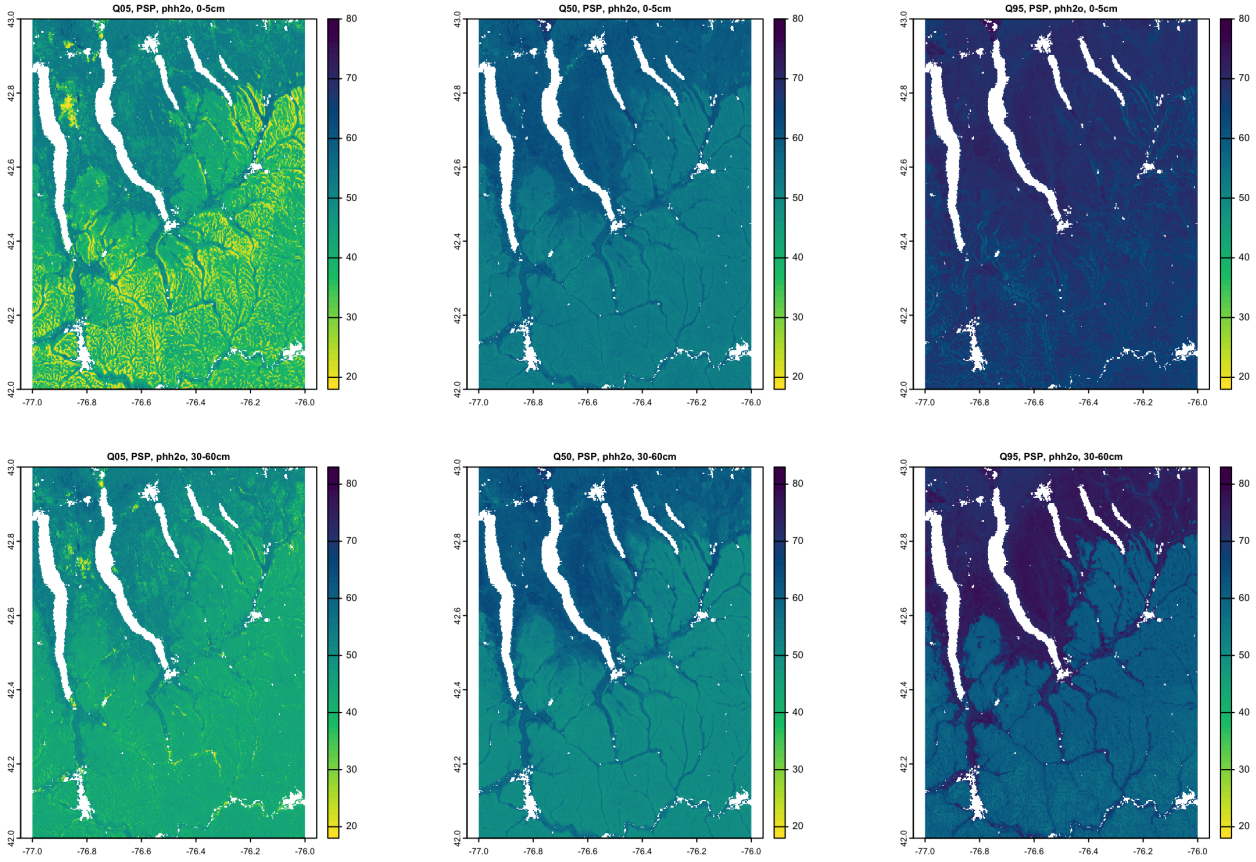


**Figure 10.** Quantiles of the prediction, PSP, pHx10, 0–5 cm (top), 30–60 cm (bottom)

Fig. 13 shows the inter-quartile range 5–95% (IQR), along with the low-high range for gNATSGO, for the two products at the two depth intervals.

SG2 has a fairly consistent IQR, mostly from about 2.5 to 3.5 pH, whereas PSP has a much wider range of uncertainties, mostly from about 1.5 to 4.5 pH, and shows much more spatial pattern. PSP has the widest ranges on the steep valley sides and especially in the Seneca Army Depot at the north inter-lake area, and the lowest on the broad till plains and through valleys.

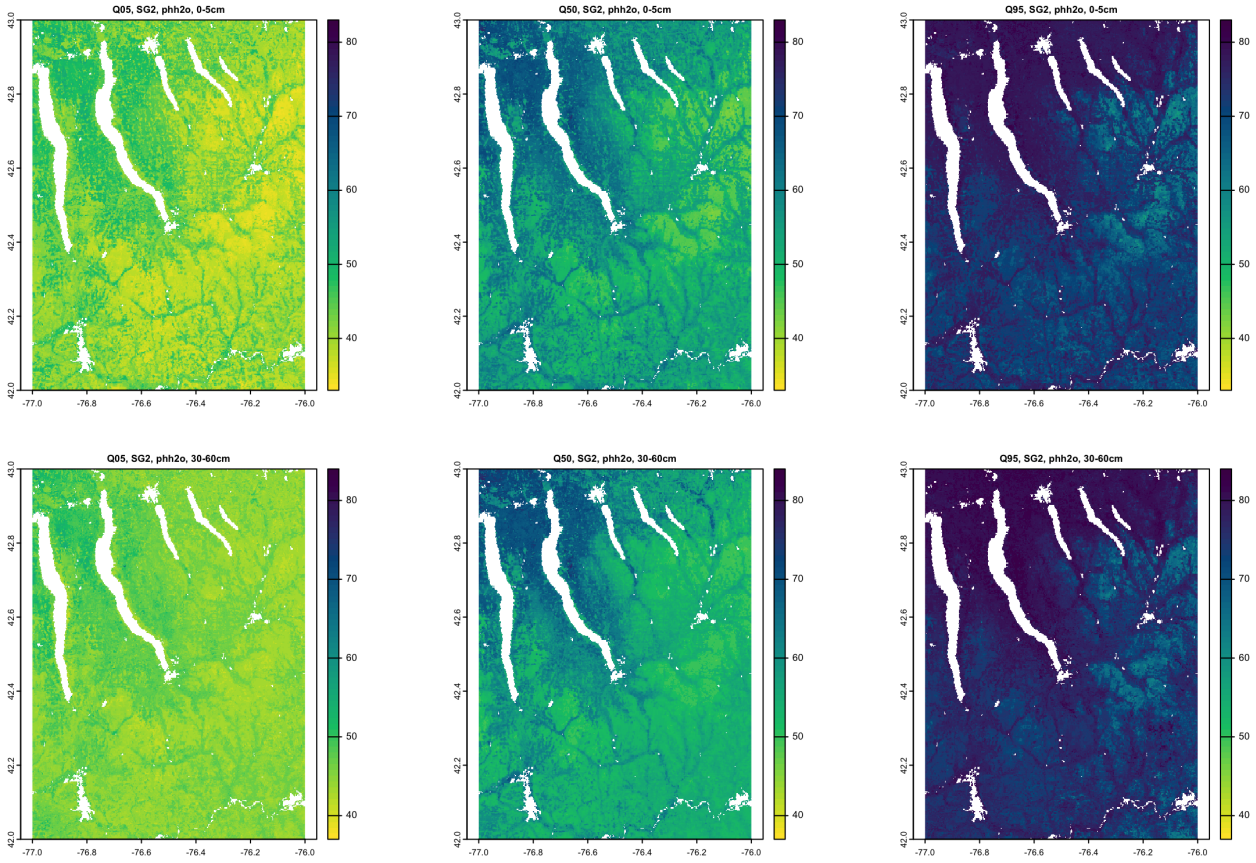


**Figure 11.** Quantiles of the prediction, SG2, pHx10, 0–5 cm (top), 30–60 cm (bottom)

These are wide ranges, and although an honest reflection of the DSM models, should give pause to map users. The wide ranges of these DSM products are due to the modelling method: the random forest includes some bad individual trees, due to random data splitting and variable selection. Apparently the worst 5% of the trees at both extremes give highly unrealistic values. This suggests that the GlobalSoilMap specifications for uncertainty (Arrouays et al., 2014) are unduly pessimistic.

Fig. 14 shows the spatial differences between the two IQR at the two depth intervals.

For the surface layer PSP gives narrower IQR than SG2 in the broad till plains and through valleys, but higher on some of the steeper hills. For the subsurface PSP gives narrower IQR than SG2 almost everywhere. The overall conclusion is that sources for uncertainty assessment (SG2: training points and global covariates, PSP: mapped soil series and national covariates) lead to greatly different results.

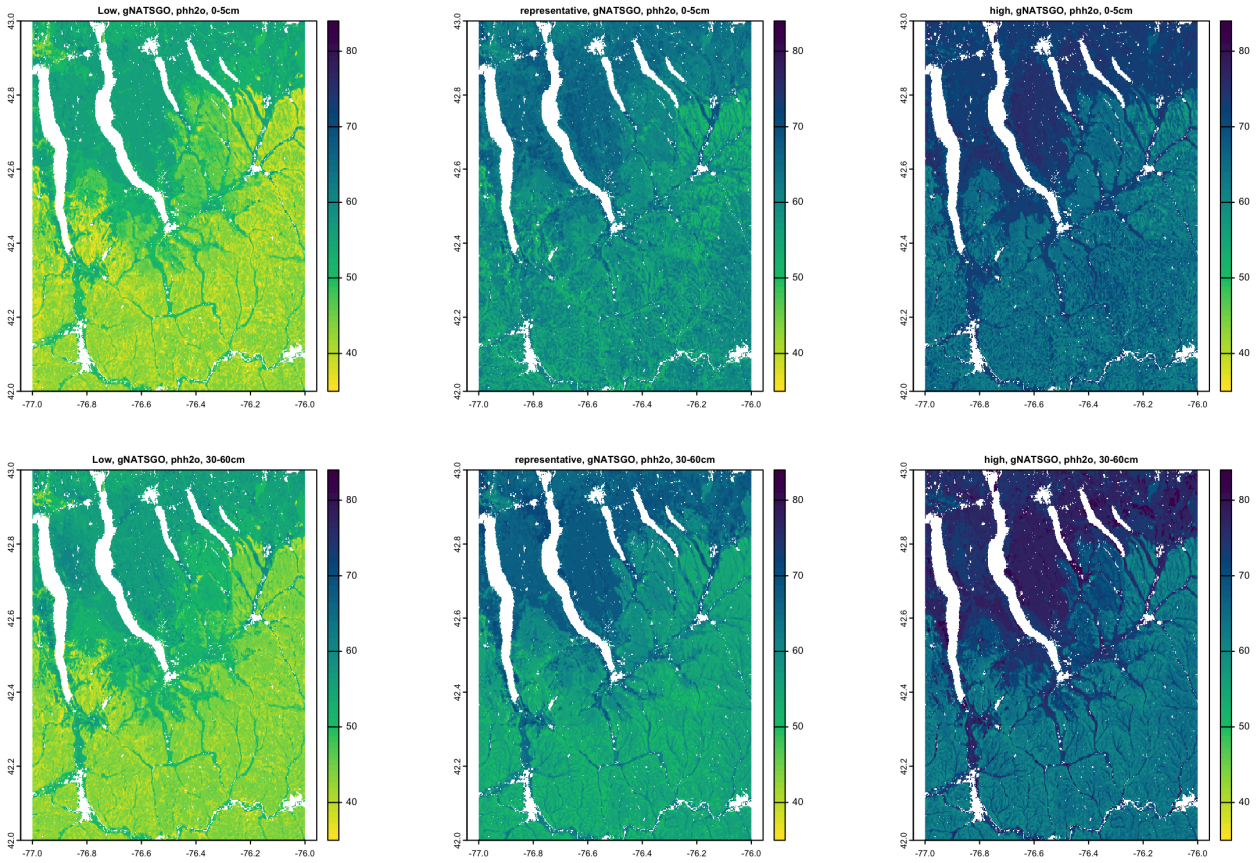


**Figure 12.** Low, representative, high values from gNATSGO, pHx10, 0–5 cm

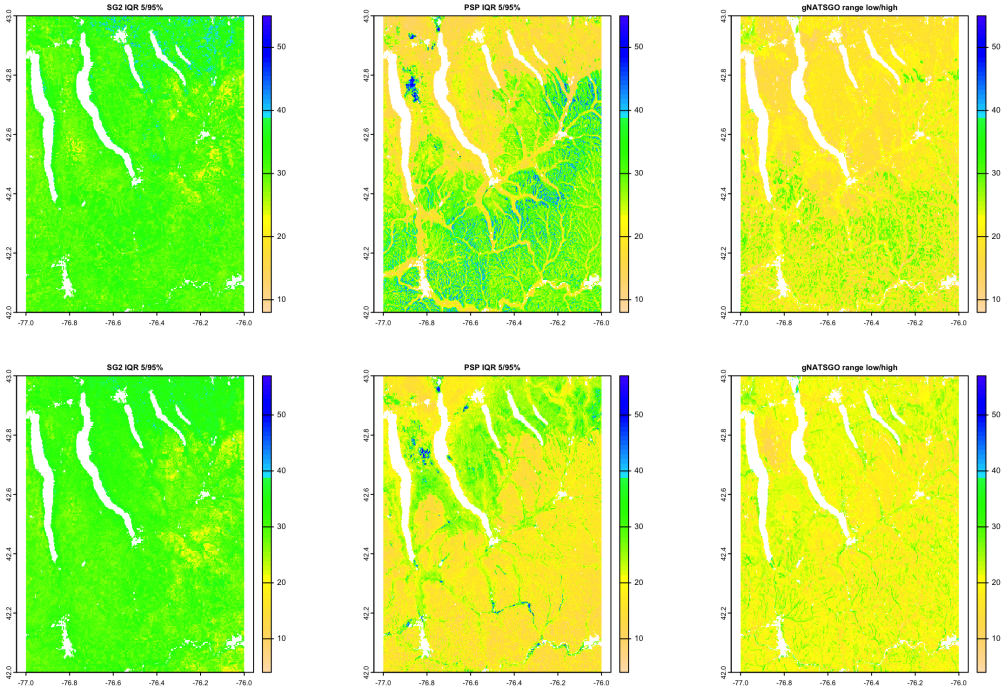


**Figure 13.** Inter-quantile ranges 0.05–0.95, pHx10, 0–5 cm (top), 30–60 cm (bottom)

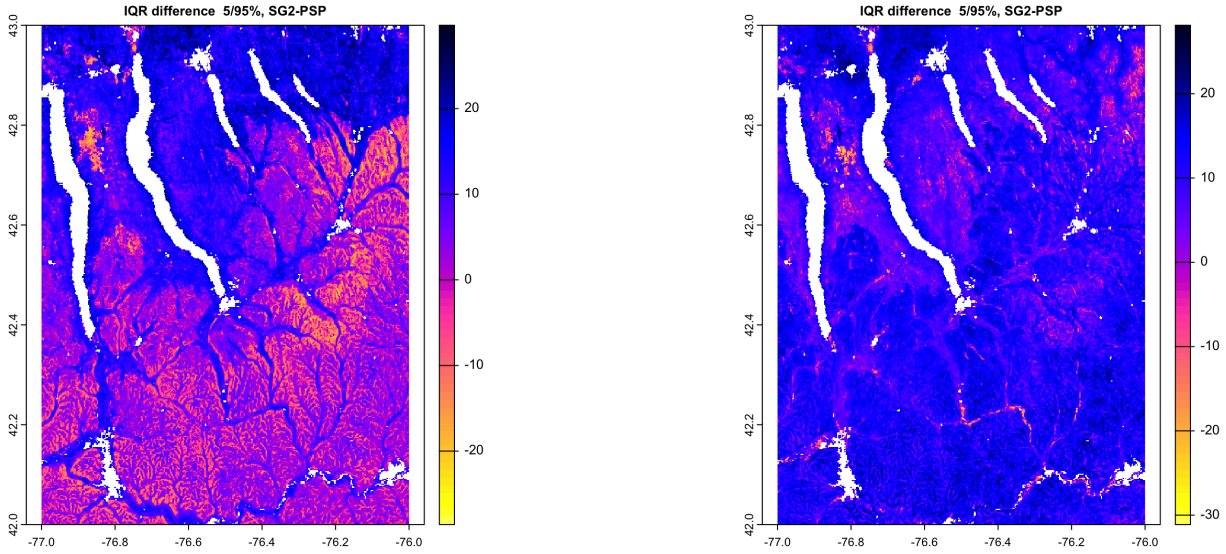


**Figure 14.** Difference between Inter-quantile range 0.05–0.95, Δ(pHx10), 0–5 cm (left), 30–60 cm (right)

### 2.1.3 Local spatial autocorrelation

The local variograms and their fitted exponential models are shown in Figs. 15 and 16. Table 2 shows their statistics.

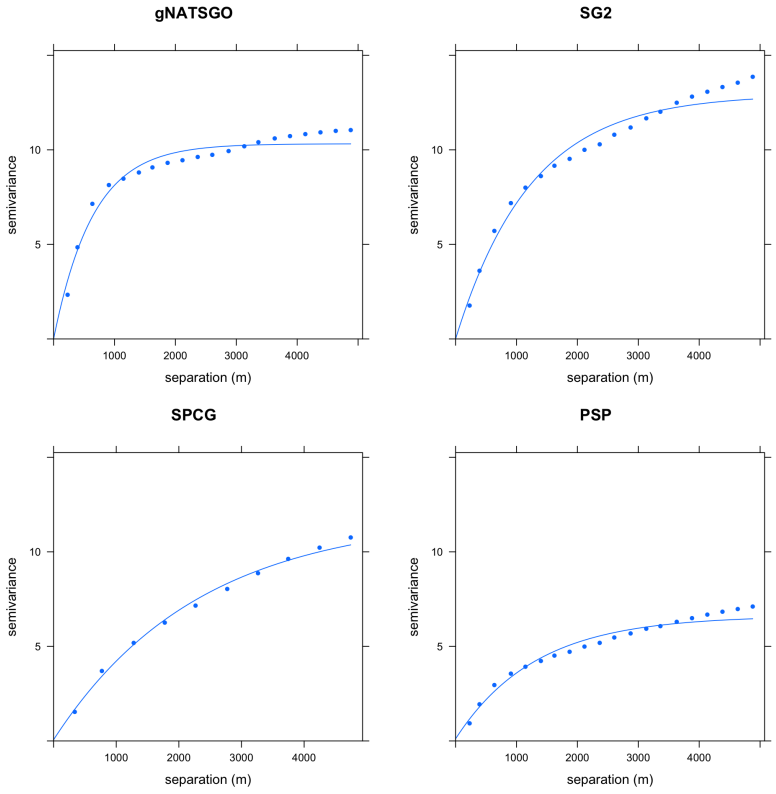


**Figure 15.** Fitted variograms, pH 0–5 cm (top), 30–60 cm (bottom), central NY. Semivariance units $(\mathrm{pH}x10)^2$

gNATSGO has the shortest effective range for both topsoil and subsoil pH. This indicate fine-scale structure at 250 $\mathrm{m}$ resolution. The DSM products have longer ranges, showing that these models do not well capture fine-scale variation. These show a smoothing effect, likely due to spatial continuity in the covariates. PSP has a long range and low sill, due to the harmonization from DSMART. The low proportional nuggets are due to the relatively coarse resolution.

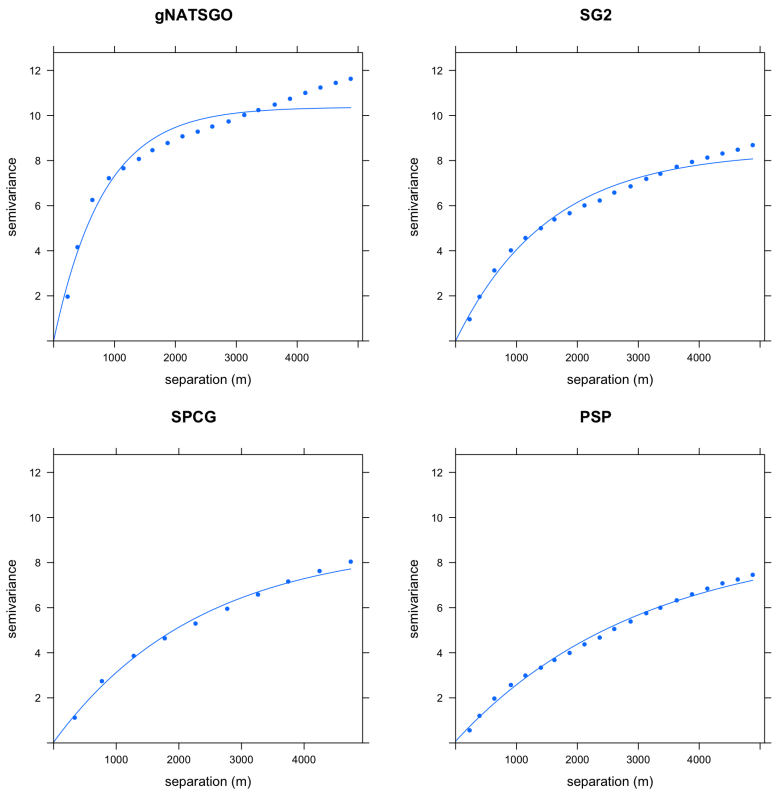


**Figure 16.** Fitted variograms, pH 0–5 cm (top), 30–60 cm (bottom), central NY. Semivariance units $(\mathrm{pH}x10)^2$

| Product | Effective range | Structural Sill | Proportional Nugget |
|---|---|---|---|
| gNATSGO | 1938.00 | 10.32 | 0.00 |
| SG2 | 3699.00 | 12.93 | 0.00 |
| SPCG | 6924.00 | 11.81 | 0.01 |
| PSP | 3918.00 | 6.50 | 0.02 |

| Product | Effective range | Structural Sill | Proportional Nugget |
|---|---|---|---|
| gNATSGO | 2454.00 | 10.37 | 0.00 |
| SG2 | 4581.00 | 8.42 | 0.00 |
| SPCG | 6966.00 | 8.83 | 0.00 |
| PSP | 9123.00 | 8.93 | 0.01 |

**Table 2.** Fitted variogram parameters, pH0-5 cm (top), 30–60 cm (bottom). Effective range in $\mathrm{m}$; structural sill in $(\mathrm{pH}x10)^2$, proportional nugget on $[0 \ldots 1]$

| DSM_products | V_measure | Homogeneity | Completeness |
|---|---|---|---|
| gNATSGO vs. SG2 | 0.0128 | 0.0143 | 0.0116 |
| gNATSGO vs. SPCG | 0.0258 | 0.0275 | 0.0243 |
| gNATSGO vs. PSP | 0.084 | 0.0897 | 0.079 |
| SPCG vs. SG2 | 0.3342 | 0.3495 | 0.3201 |

| DSM_products | V_measure | Homogeneity | Completeness |
|---|---|---|---|
| gNATSGO vs. SG2 | 0.06 | 0.0565 | 0.064 |
| gNATSGO vs. SPCG | 0.0649 | 0.0653 | 0.0646 |
| gNATSGO vs. PSP | 0.1235 | 0.1164 | 0.1314 |
| SPCG vs. SG2 | 0.3462 | 0.324 | 0.3716 |

**Table 3.** V-measure statistics, pHx10 0–5 cm (top), 30–60 cm (bottom)

### 2.1.4 Classification

Figs. 17 and 18 shows the topsoil and subsoil pH, respectively, classified into eight histogram-equalized classes in a 0.2 x 0.2° sub-area, with limits $(-76.8 \cdots -76.6)^\circ$ E, $(42.2 \cdots 42.3)^\circ$ N, centred just south of Cayuta, NY. The higher pH are shown in the darker blue. Class limits for the surface soil are approximately 5.01, 5.14, 5.27, 5.40, 5.54, 5.71, and 6.02 pH, with the extreme values of 4.52 and 6.96 pH, and for the subsoil are approximately 5.15, 5.21, 5.29, 5.40, 5.53, 5.67, and 5.93, with the extreme values of 4.74 and 7.16 pH. In general, the subsoil is predicted to be somewhat less acid than the surface soil. The maps show obvious spatial differences in class distribution. gNATSGO shows more areas in the highest pH class than the PSP products. The products based on gSSURGO, i.e., gNATSGO and PSP, show a finer spatial pattern than the purely DSM products, i.e., SG2 and SPCG. But SPCG shows large homogeneous areas of the lowest class, covering the highest hills, whereas SG2 presents a more nuanced view.

### 2.1.5 V-measure

Table 3 shows the statistics from several V-measure comparisons, based on the histogram-equalized class maps. Only SG2 and SPCG have somewhat comparable patterns. gNATSGO is considerably different from all other products, due to its detailed spatial pattern based on field survey.

Figs. 19 (0-5 cm) and 20 (30-60 cm) show the computed homogeneity and completeness of the SG2 pH class map, with respect to the gNATSGO pH class map. In the yellow areas of the homogeneity map one, one gNATSGO predicted class is contained in the SG2 region; in the blue areas many are. Overall the agreement is fairly good.

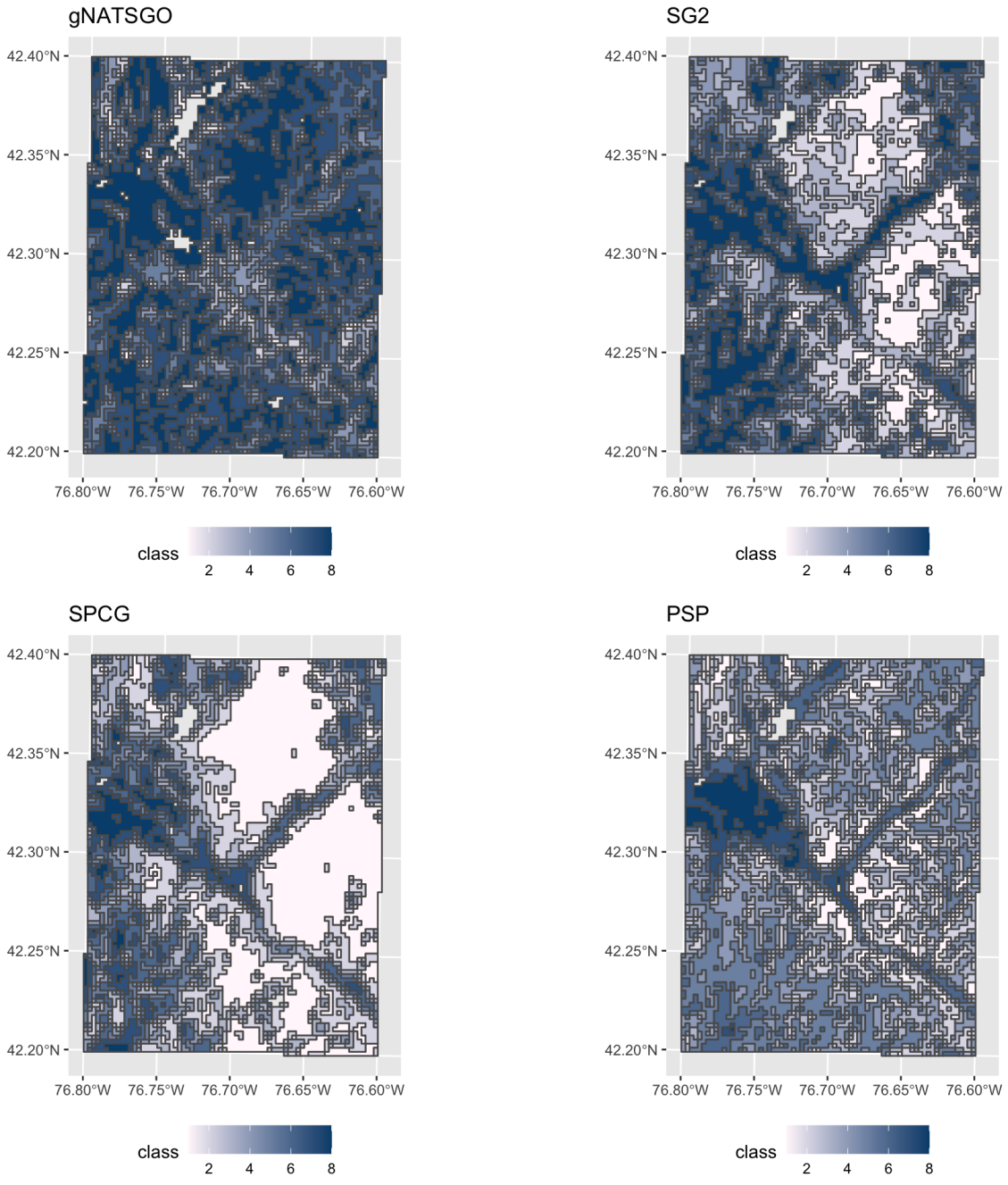


**Figure 17.** pH classes, 0–5 cm, central NY, detail

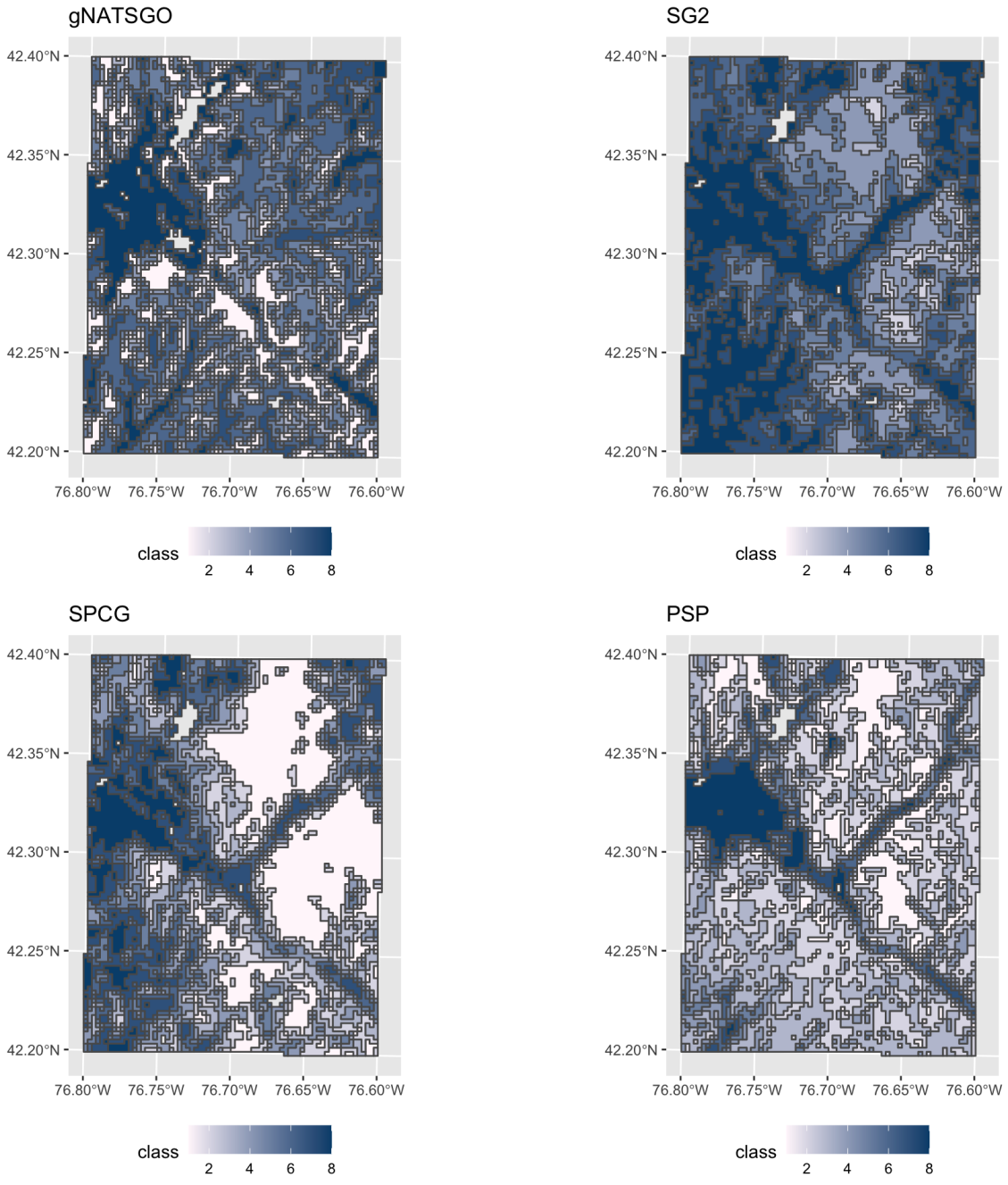


**Figure 18.** pH classes, 30–60 cm, central NY, detail

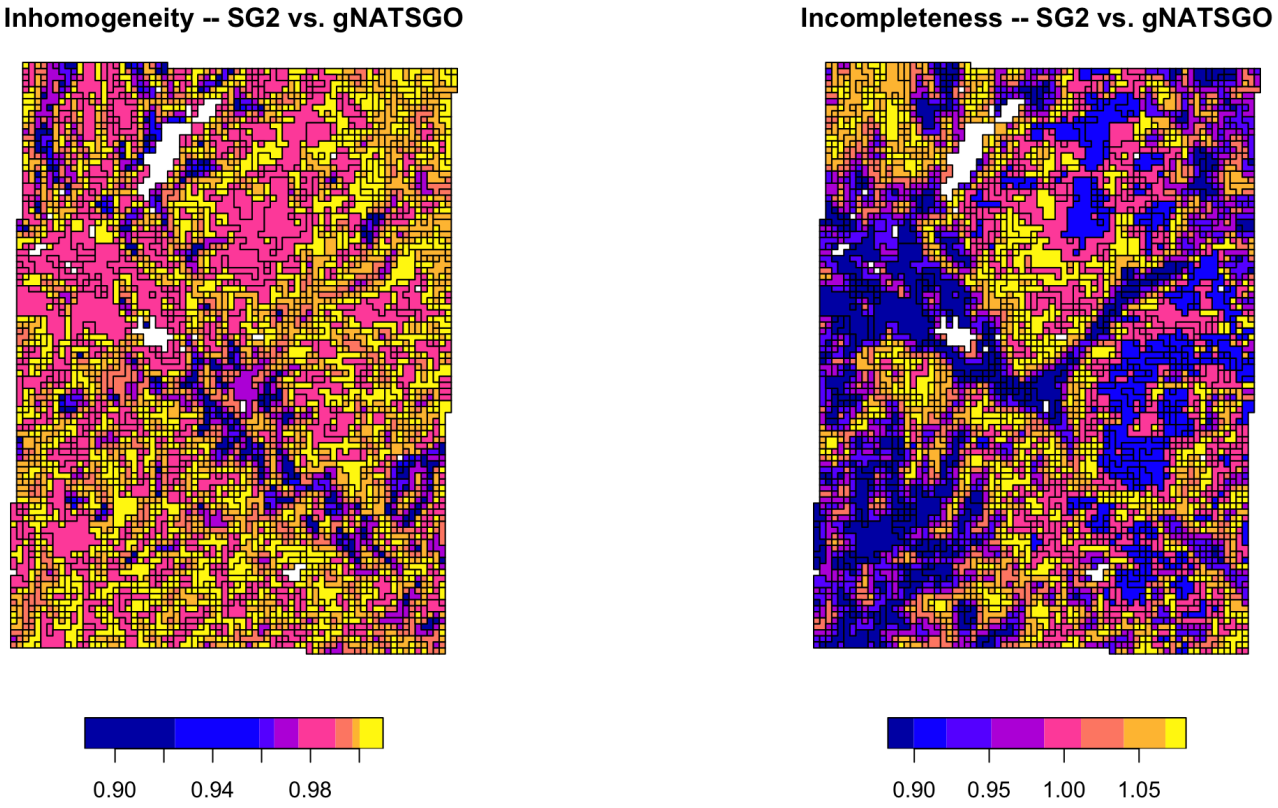


**Figure 19.** Homogeneity (left) and Completeness (right) of the SG2 pH class map, with respect to gNATSGO pH class map, 0–5 cm

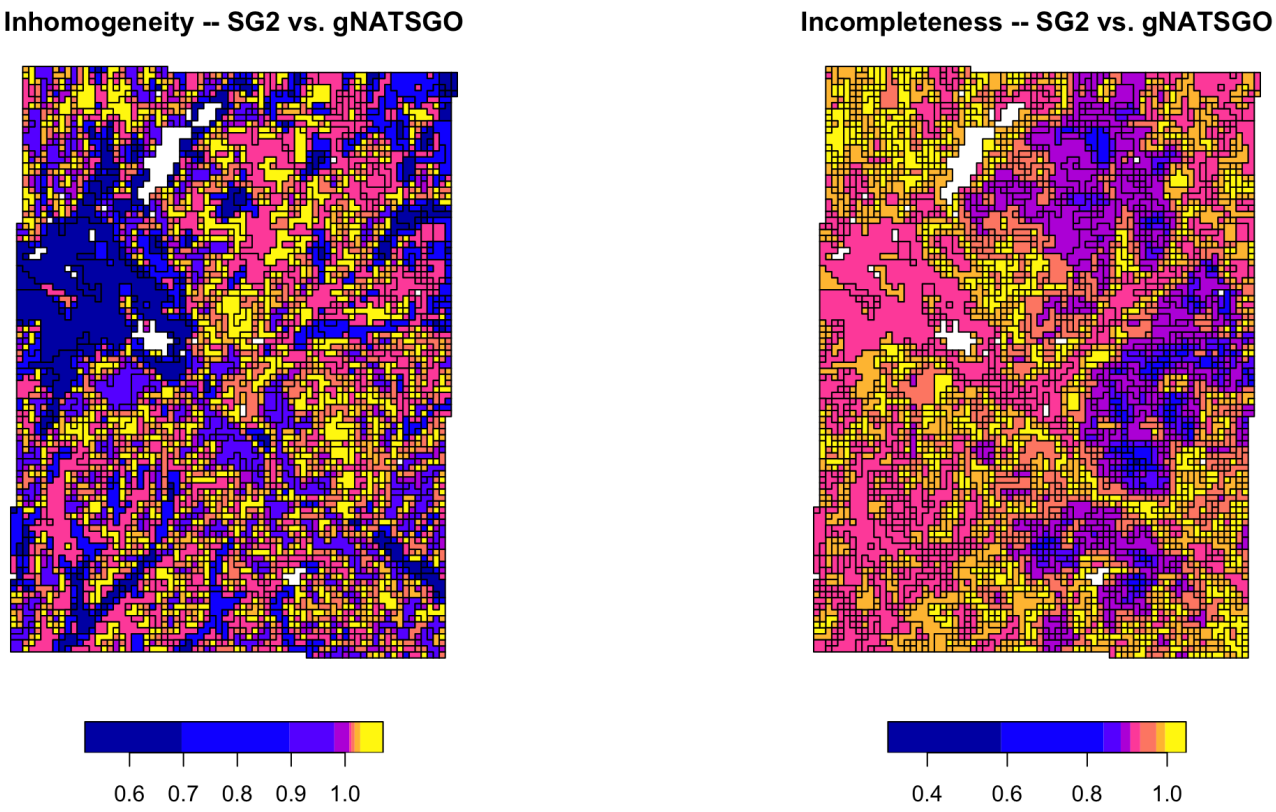


**Figure 20.** Homogeneity (left) and Completeness (right) of the SG2 pH class map, with respect to gNATSGO pH class map, 30–60 cm

| product | ai | frac_mn | lsi | shdi | shei |
|---|---|---|---|---|---|
| gNATSGO | 48.188 | 1.034 | 22.602 | 1.666 | 0.801 |
| SG2 | 50.659 | 1.034 | 21.768 | 2.06 | 0.991 |
| SPCG | 58.483 | 1.041 | 18.557 | 1.887 | 0.907 |
| PSP | 47.025 | 1.04 | 23.232 | 1.898 | 0.913 |

| product | ai | frac_mn | lsi | shdi | shei |
|---|---|---|---|---|---|
| gNATSGO | 44.062 | 1.029 | 24.34 | 1.991 | 0.957 |
| SG2 | 62.46 | 1.043 | 16.934 | 1.754 | 0.844 |
| SPCG | 56.041 | 1.039 | 19.587 | 2.013 | 0.968 |
| PSP | 54.278 | 1.035 | 20.247 | 1.773 | 0.853 |

**Table 4.** Landscape metrics statistics, pH 0–5 cm (top); 30–60 cm (bottom). `frac_mn`: Mean Fractal Dimension; `lsi`: Landscape Shape Index; `shdi`: Shannon Diversity; `shei`: Shannon Evenness; `ai`: Aggregation Index

| | gNATSGO | SG2 | SPCG | PSP |
|---|---|---|---|---|
| gNATSGO | 0.000 | 0.149 | 0.281 | 0.261 |
| SG2 | 0.149 | 0.000 | 0.067 | 0.087 |
| SPCG | 0.281 | 0.067 | 0.000 | 0.111 |
| PSP | 0.261 | 0.087 | 0.111 | 0.000 |

| | gNATSGO | SG2 | SPCG | PSP |
|---|---|---|---|---|
| gNATSGO | 0.000 | 0.122 | 0.097 | 0.226 |
| SG2 | 0.122 | 0.000 | 0.180 | 0.320 |
| SPCG | 0.097 | 0.180 | 0.000 | 0.094 |
| PSP | 0.226 | 0.320 | 0.094 | 0.000 |

**Table 5.** Jensen-Shannon distance beween co-occurence vectors; 0–5 cm (top); 30–60 cm (bottom)

### 2.1.6 Landscape metrics

Table 4 shows the statistics from the landscape metrics calculations.

The mean fractal dimensions are almost identical. Otherwise the results are inconsistent; all we can say is that the map patterns vary considerably among products.

Table 5 shows the Jensen-Shannon distance beween co-occurence vectors of the four products. The co-occurence patterns of SG is somewhat similar to that PSP and SPCG, but less similar to gNATSGO, which is quite different from SPCG and PSP, although in the subsoil SPCG is similar to gNATSGO.

### 2.2 Local spatial patterns

The interest here is to see how well DSM methods at relatively fine resolution reproduce known relations at the local geomorphic level, e.g., hillslopes, transects across valleys with multiple terrace levels, and within farms. It has been claimed that DSM at 30 m resolution is sufficient for management of, or even within, individual farm fields. The only DSM product which predicts at this resolution is PSP.

We examine this first qualitatively, i.e., by visual inspection, and then quantitatively, mostly following the methods of the regional assessment.

#### 2.2.1 Qualitative assessment

Fig. 21 shows the silt concentration of the 0–5 cm layer for (top) the gridded SSURGO overlain on the original polygons from which it was derived, and (bottom) the disaggregated PSP grid cells in a hilly landscape near Caroline, NY. Red colours are low silt, in this window alluvial fans (the `C*` map units). Pale grey colours are organic soils (the `Hk, Hl` map units). Light colours are high-silt surface soils (the `L*, V*, B*, M*` map units), from thin glacial till developed on shale and mudstone bedrock.

The gSSURGO product follows the SSURGO lines exactly. Some of the sharp boundary lines do correspond with abrupt transitions on the ground, for example where the steep hillsides are buried by fan alluvium. But others are not, for example on the hilltops. These differences are because the predicted silt concentrations are taken from the official series descriptions. PSP follows the map unit lines fairly well, but is much finer-grained; each 30 m pixel is separately predicted. This results in some smoothing of the abrupt boundary lines from gSSURGO on the hilltops. However within some SSURGO map units PSP predicts quite some differences in topsoil silt concentration. These are map units with contrasting components, which PSP attempts to disaggregate according to their correlation with covariates. For the most part these do not seem to be related to terrain or land use. For example, Fig. 22 shows detail of the Holly-Papakting map unit within this PSP window. This map unit has two contrasting soils in similar proportions: a mineral alluvial soil (Holly series) and an organic soil (Papakting series); the second has much lower silt concentration. It is difficult to see the reason for the pattern within this map unit. PSP has placed the component series in their proper proportions but not according to any landscape feature.

Fig. 23 shows the predicted silt concentration within $\approx 3$ ha field and some adjacent woodland, all within the Chenango series alluvial fan, south of the intersection of Robinson Hollow Road and NY State Route 79 in Tioga County. Values range from 37% (darkest red) to 55% (lightest red), a range with significant management implications. These values come from the constituents listed for this map unit. The named series Chenango is assigned 75% of the area, with a surface soil of 39.7% silt concentration. The other five inclusions have different predicted silt concentrations. However, in this field, there seems to be no justification to map any of these inclusions. For example, the Tioga series inclusion (5%) is found on higher positions of flood plains, and the Middlebury series inclusion (5%) is found in recent alluvium, but this field is all on the alluvial fan terrace. This disaggregation is clearly not based on land use, and there is no terrain or parent material differentiation in this almost flat

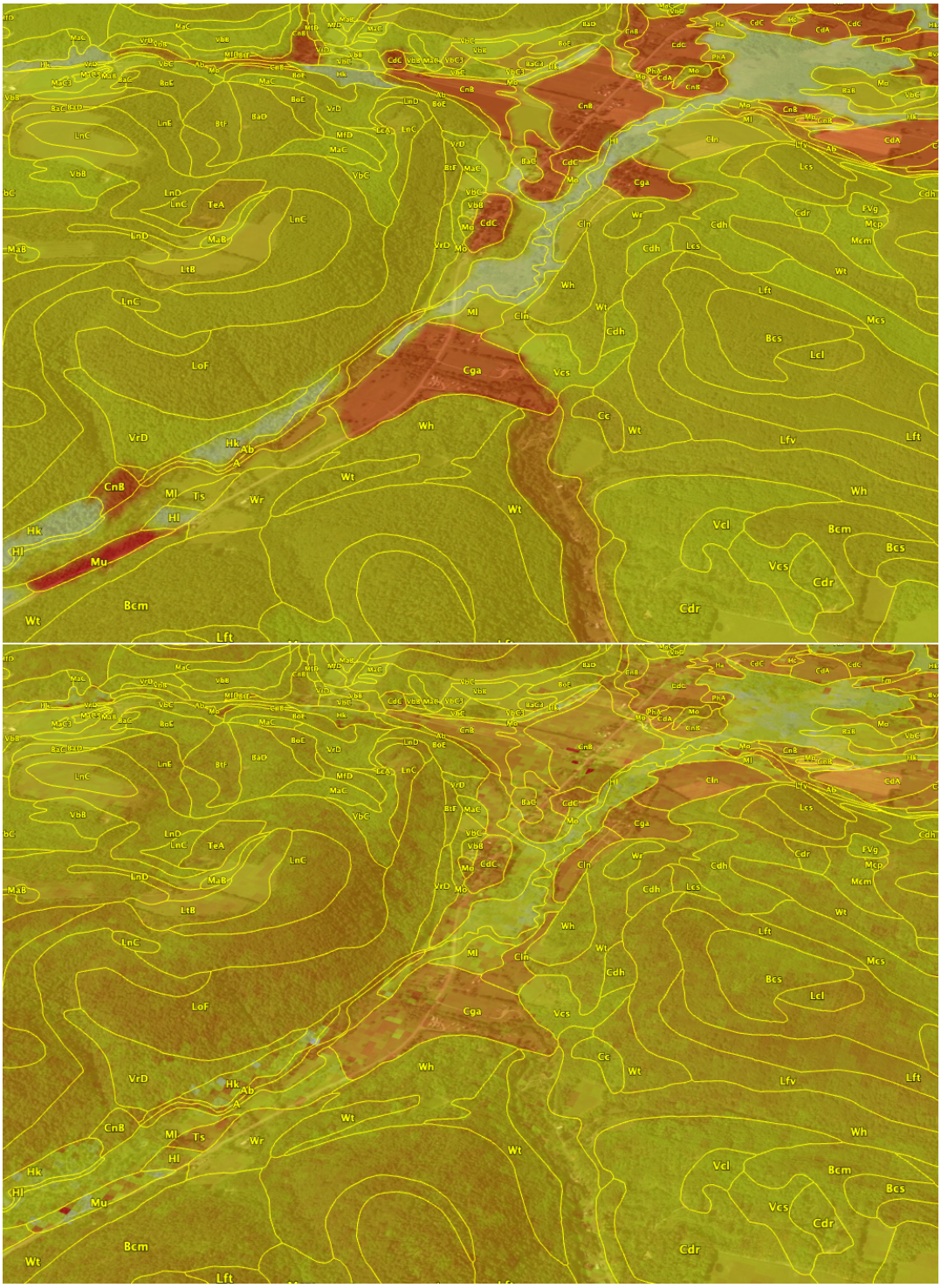


**Figure 21.** Ground overlay from gSSURGO (top) and PSP (bottom), silt % 0–5 cm, with SSURGO polygons from SoilWeb. Centre of image $-76°16'25"\mathrm{E}, 42°22'53"N$; view azimuth 247°

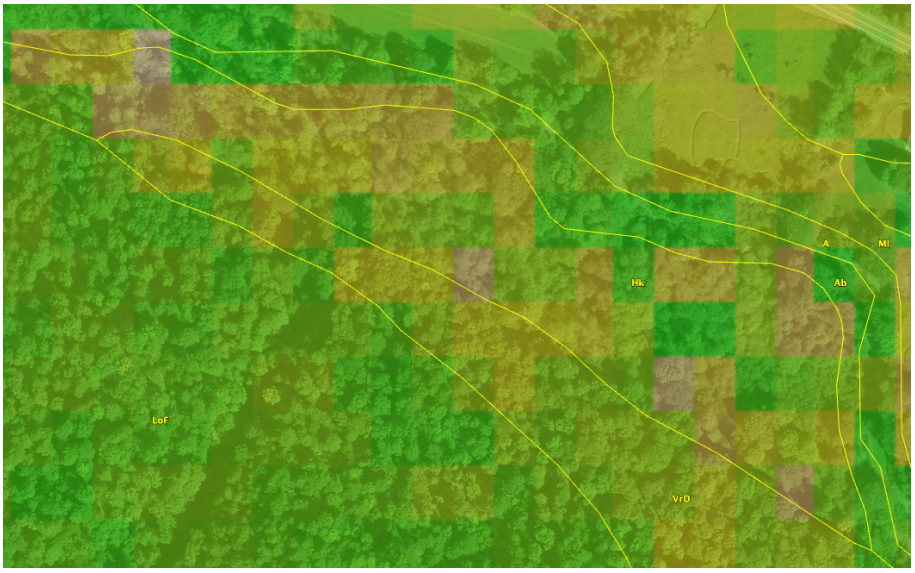


**Figure 22.** Ground overlay from PSP in the Holly-Papakting map unit, silt % 0–5 cm. Centre of image $-76°16'03"\mathrm{E}, 42°22'30"N$

field. There would be no basis for differential management of each $\approx 700\ m^2$ grid cell, as is implied by the fine resolution and strong differentiation within the field.

**Figure 23.** Ground overlay from PSP in the Chenango gravelly loam map unit, silt % 0–5 cm. Centre of image $-76°17'03"\mathrm{E}, 42°22'40"N$

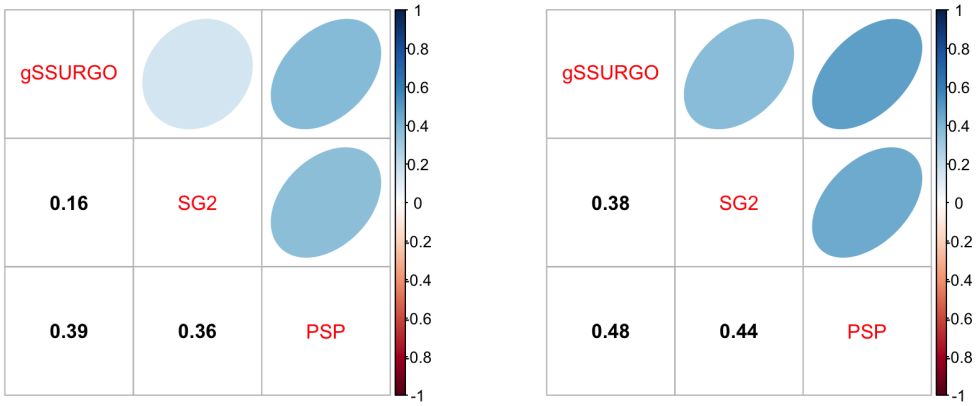


**Figure 24.** Pearson correlations between local products, pHx10, 0–5 cm (left), 30–60 cm (right)

### 2.2.2 Quantitative assessment

To see the fine differences at this high resolution, we concentrate on a $0.15 \times 0.15°$ subtile in an area near Freeville, NY with lower-right corner $(-76.30°\mathrm{E}, 42.45°\mathrm{N})$ and evaluate pH, as in the regional assessment (§2.1). The southern part of the map is northern limit of the Appalachian plateau, ending in the SSW-NNE trending Portage escarpment. The northern part is the
235 southern limit of the Lake Ontario upland till plain, and in the centre are glacial valleys.

Table 6 shows the statistical differences between gSSURGO (reference) and the DSM products, along with the predictions of pH in the two depth intervals. Fig. 24 shows the pairwise Pearson correlations between the maps. These results are comparable to those for the full tile at regional resolution: both SG2 and PSP under-predict pH by from about 0.35–0.45 pH. Correlations are fairly strong between PSP and gSSURGO, and between SG2 and PSP, but weak between SG2 and gSSURGO.

| DSM_product | MD | RMSD | RMSD.Adjusted | DSM_product | MD | RMSD | RMSD.Adjusted |
|---|---|---|---|---|---|---|---|
| SG2 | 4.436 | 6.758 | 5.097 | SG2 | 1.444 | 4.688 | 4.46 |
| PSP | 3.462 | 5.625 | 4.433 | PSP | 3.751 | 5.9 | 4.554 |

**Table 6.** Statistical differences between gSSURGO and DSM products, pHx10, 0–5 cm. Centre of map $-76°30'30"\mathrm{E}, 42°52'30"N$

240 Figs. 25 and 26 show gSSURGO (reference) along with the predictions of pH in the two depth intervals of the PSP products. Figs. 27 and 28 show these as difference maps. Clearly, gSSURGO has overall higher values than the other two products, and despite the fine resolution, has in general large areas of identical values. The differentiation between map units follows

sharp boundaries even within a single landscape (e.g., the plateau), and this is likely an artefact of relying on the representative profiles in the official series descriptions for property values. PSP has a finer pattern, due to disaggregation, and shows a more realistic local pattern by smoothing out the sharp boundaries between map units within a landscape. PSP shows large areas of low pH ($< 5$), especially in the subsoil. SG2 does not well follow the landscape lines, especially the sharp boundaries between uplands and valleys, and predicts very low pH ($\approx 4.5$) on the plateau. It is difficult to recognize local landscape units in this global product.

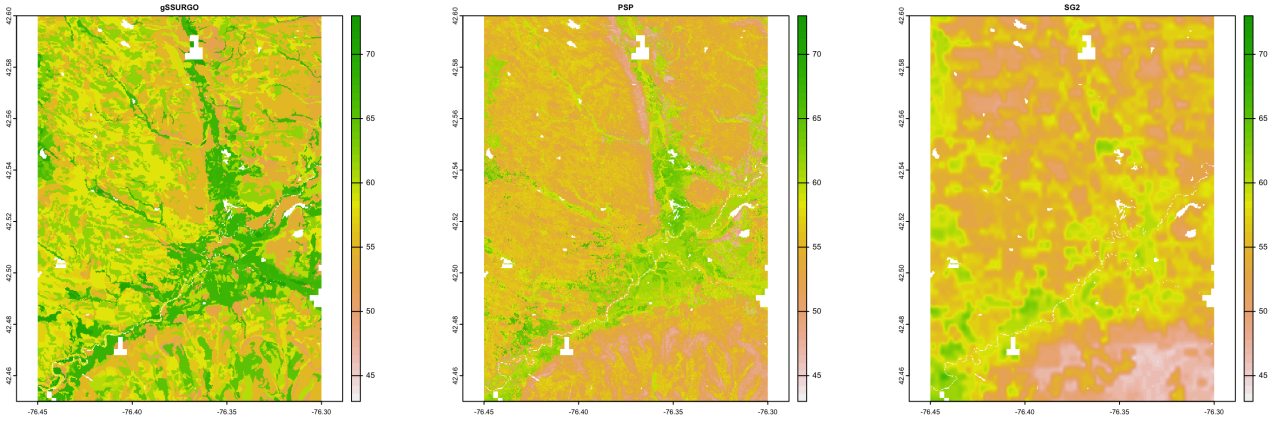


**Figure 25.** Topsoil (0-5 cm) pHx10, according to gSSURGO and DSM products

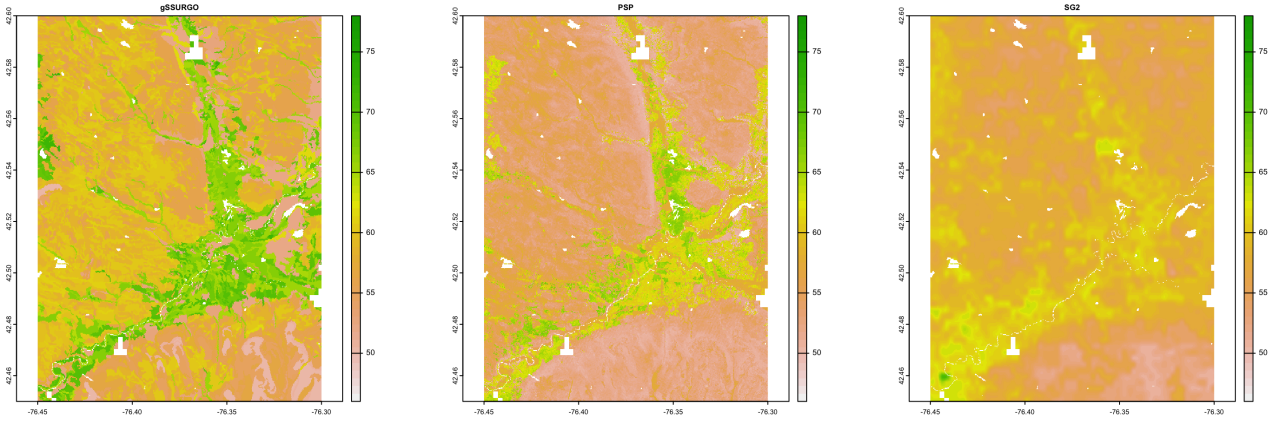


**Figure 26.** Subsoil (30-60 cm) pHx10, according to gSSURGO and DSM products

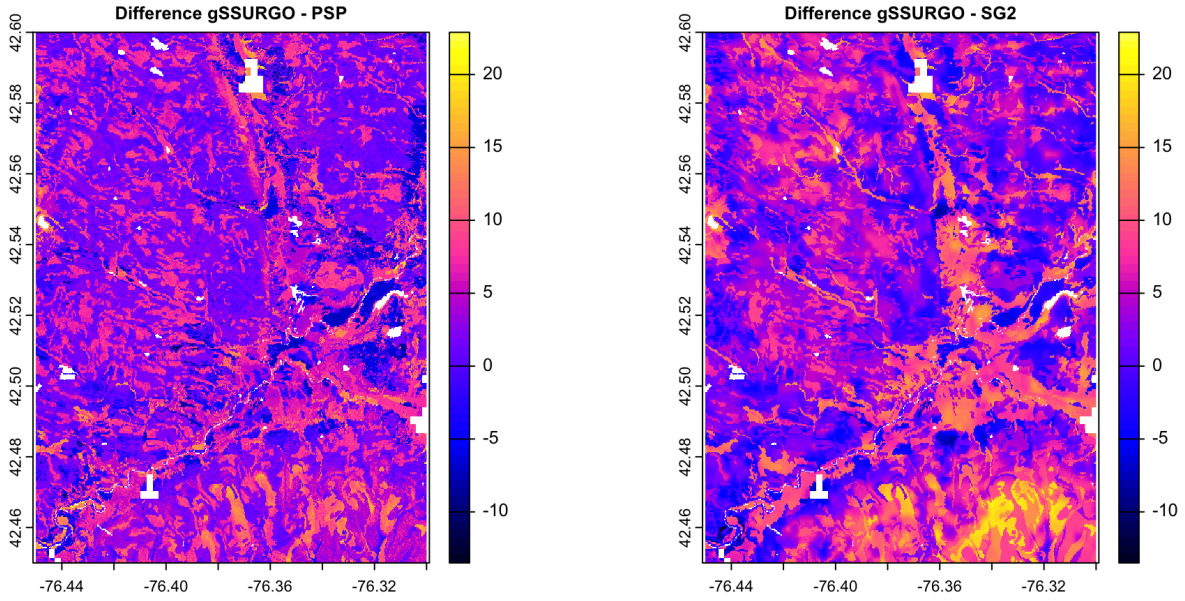


**Figure 27.** Difference between gSSURGO and DSM products, pHx10, 0–5 cm

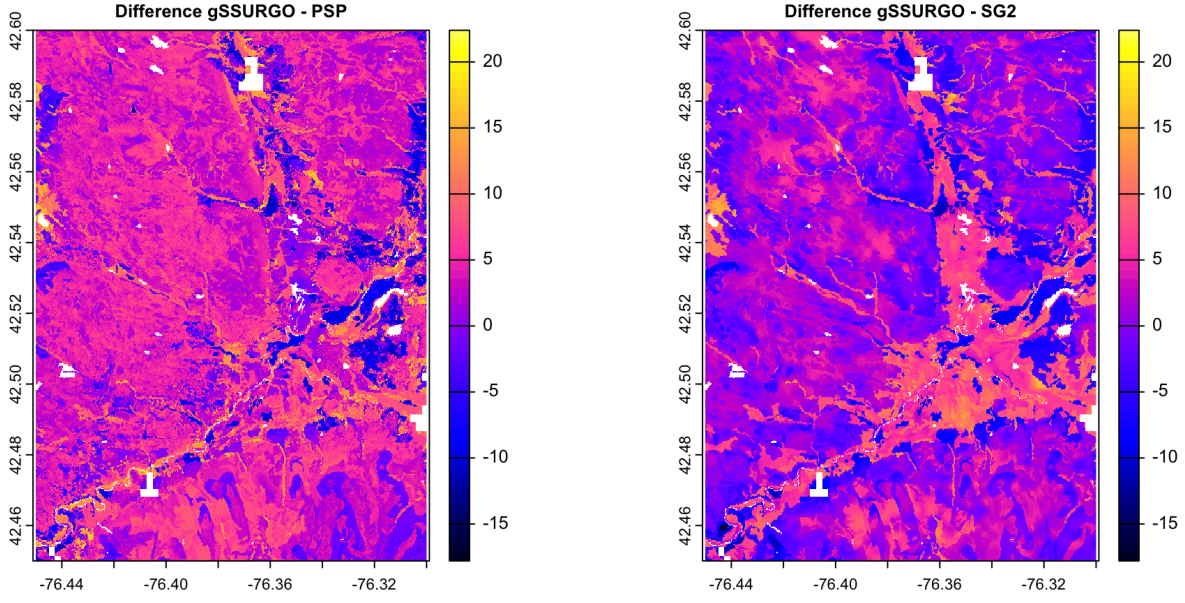


**Figure 28.** Difference between gSSURGO and DSM products, pHx10, 30–60 cm

### 2.2.3 Class maps

Fig. 29 shows the topsoil and subsoil pH, respectively, classified into eight histogram-equalized classes. Class limits for the surface soil in this area are approximately 5.30, 5.44, 5.55, 5.61, 5.74, 5.89, and 6.15 pH, with the extreme values of 4.44 and 7.00 pH, and for the subsoil are approximately 5.28, 5.47, 5.59, 5.72, 5.83, 6.00, and 6.23, with the extreme values of 4.76 and 7.21 pH.

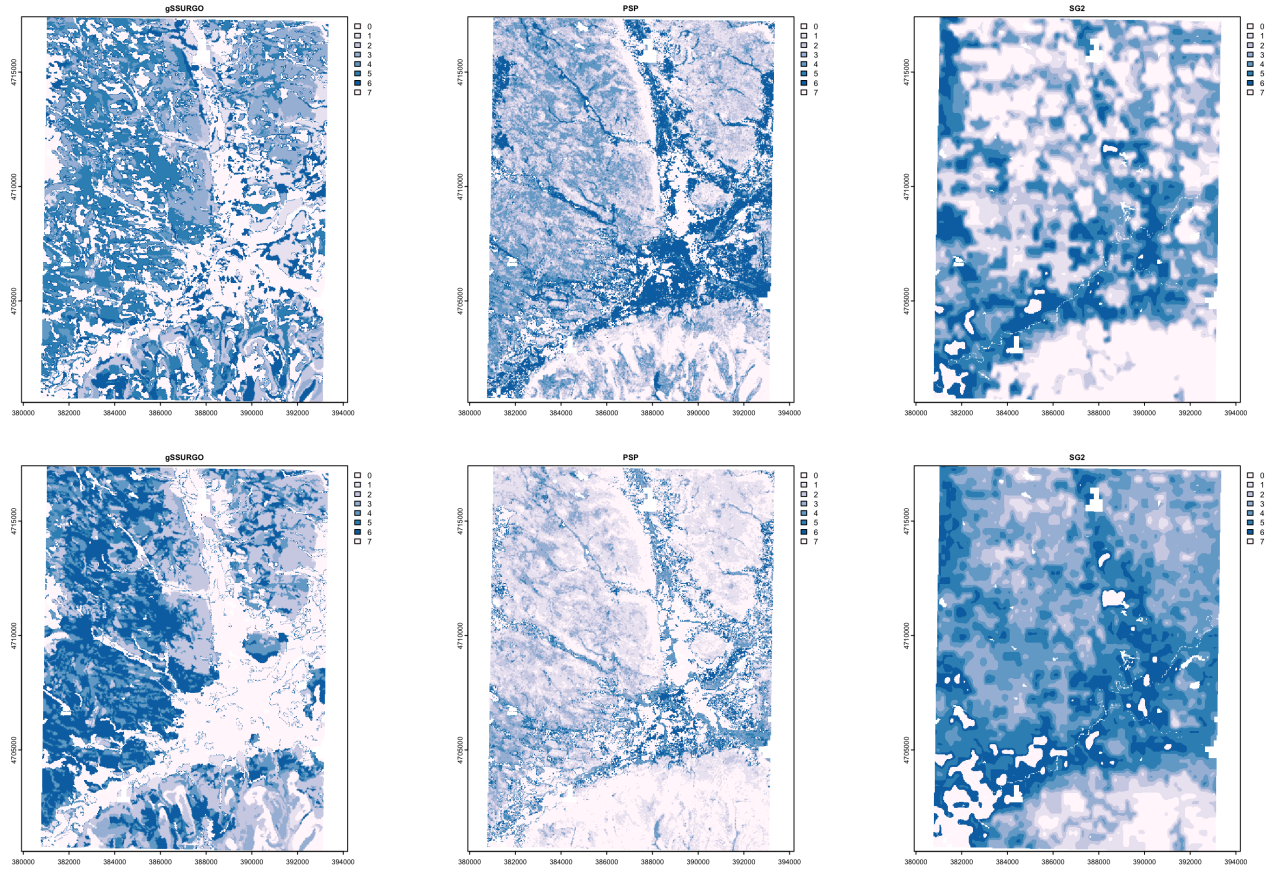


**Figure 29.** pH classes, 0–5 cm (top), 30–60 cm (bottom), central NY, detail. Coordinates are UTM 18N meters

Clearly, SG2 misses the landscape details, even at 250 m resolution. PSP shows details but the classes, even allowing for the bias, do not match well with gSSURGO.

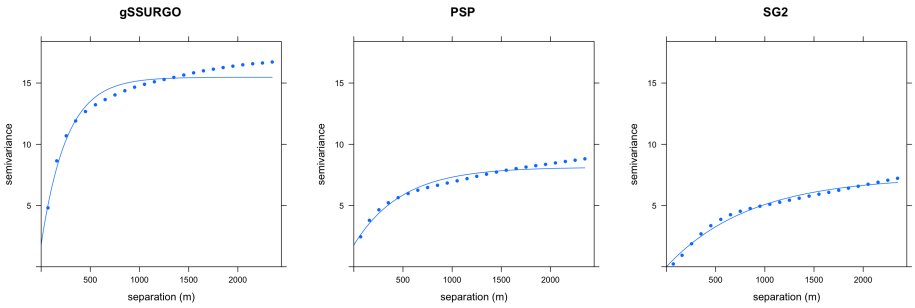


**Figure 30.** Fitted variograms, pH 0–5 cm (top), 30–60 cm (bottom), central NY. Semivariance units $(\mathrm{pH}x10)^2$

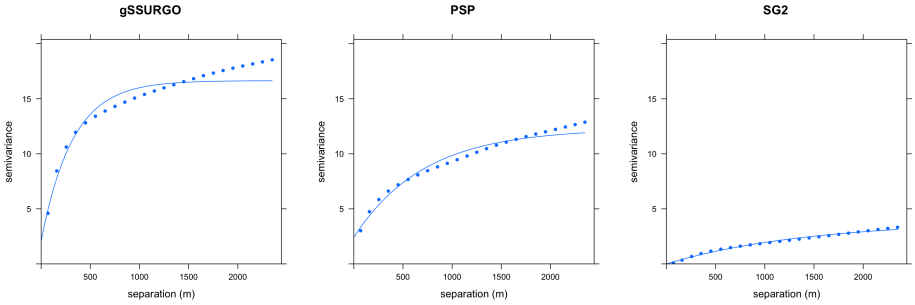


**Figure 31.** Fitted variograms, pH 0–5 cm (top), 30–60 cm (bottom), central NY. Semivariance units $(\mathrm{pH}x10)^2$

### 2.2.4 Local spatial autocorrelation

The local variograms and their fitted exponential models are shown in Figs. 30 and 31. Table 7 shows their statistics. gSSURGO has the shortest effective range and highest sill for both topsoil and subsoil pH. PSP has a longer range and low sill, due to the harmonization from DSMART that removes some of the overall variability. SG2 has no nugget variance, a low sill, and long range, consistent with its regional scale.

### 2.2.5 Landscape metrics

Table 8 shows the statistics from the landscape metrics calculations.

The mean fractal dimensions are almost identical. Otherwise the results are inconsistent; all we can say is that the map patterns vary considerably among products.

Table 9 shows the Jensen-Shannon distance beween co-occurence vectors of the four products. The co-occurence patterns of SoilGrids is somewhat similar to that PSP but quite different from gSSURGO.

| Product | Effective range | Structural Sill | Proportional Nugget |
|---|---|---|---|
| gSSURGO | 774.00 | 13.67 | 0.12 |
| SG2 | 2550.00 | 7.34 | 0.00 |
| PSP | 1455.00 | 6.36 | 0.22 |

| Product | Effective range | Structural Sill | Proportional Nugget |
|---|---|---|---|
| gSSURGO | 963.00 | 14.56 | 0.13 |
| SG2 | 4335.00 | 3.89 | 0.00 |
| PSP | 2139.00 | 9.87 | 0.20 |

**Table 7.** Fitted variogram parameters, pH 0–5 cm (top), 30–60 cm (bottom). Effective range in $\mathrm{m}$; structural sill in $(\mathrm{pH}x10)^2$, proportional nugget on $[0 \dots 1]$

| product | ai | frac_mn | lsi | shdi | shei |
|---|---|---|---|---|---|
| gSSURGO | 73.658 | 1.049 | 71.395 | 1.845 | 0.887 |
| SG2 | 87.647 | 1.106 | 34.978 | 1.941 | 0.934 |
| PSP | 56.376 | 1.045 | 116.476 | 2.006 | 0.965 |

| product | ai | frac_mn | lsi | shdi | shei |
|---|---|---|---|---|---|
| gSSURGO | 76.398 | 1.047 | 64.258 | 1.938 | 0.932 |
| SG2 | 92.156 | 1.063 | 23.221 | 1.874 | 0.901 |
| PSP | 65.826 | 1.039 | 91.746 | 1.829 | 0.880 |

**Table 8.** Landscape metrics statistics, pH 0–5 cm (top); 30–60 cm (bottom). `frac_mn`: Mean Fractal Dimension; `lsi`: Landscape Shape Index; `shdi`: Shannon Diversity; `shei`: Shannon Evenness; `ai`: Aggregation Index

| | gSSURGO | SG2 | PSP |
|---|---|---|---|
| gSSURGO | 0.000 | 0.218 | 0.168 |
| SG2 | 0.218 | 0.000 | 0.112 |
| PSP | 0.168 | 0.112 | 0.000 |

| | gSSURGO | SG2 | PSP |
|---|---|---|---|
| gSSURGO | 0.000 | 0.156 | 0.181 |
| SG2 | 0.156 | 0.000 | 0.294 |
| PSP | 0.181 | 0.294 | 0.000 |

**Table 9.** Jensen-Shannon distance beween co-occurence vectors; 0–5 cm (top); 30–60 cm (bottom)

### 2.3 Summary (Central NY)

In both the 0–5 cm and 30–60 cm layers the spatial patterns and uncertainty estimates, as well as the predicted values, differ substantially among DSM products, and between these and the digitized field surveys. There is little difference between the globally-calibrated models of SG2 and the USA-specific models of SPCG. Both show soil-environmental relations that, according to field survey, are not realistic, although the overall pattern does find the main soil landscape features. For the selected soil property (pH) there is not much difference in these results between top- and subsoil. Since pH is often the property best-predicted by DSM, these results are worrying.


**Figure 32.** 1° tile of the North Carolina coastal plain study area, (-78 – -77° E, 35–36° N).

## 3 North Carolina coastal plain

This area, bounding box (-78 – -77° E, 35–36° N), with Rocky Mount on the NW edge and New Bern on the SE edge (Fig. 32), was selected because of its clear pattern of soils related to sedimentary facies.

The coastal plain has several levels of Pliocene, Pleistocene and Holocene terraces, from very young, including swamps with organic soils and poorly-drained sandy soils, to quite old (in pedogenetic terms), including soils with plinthite. The plain is

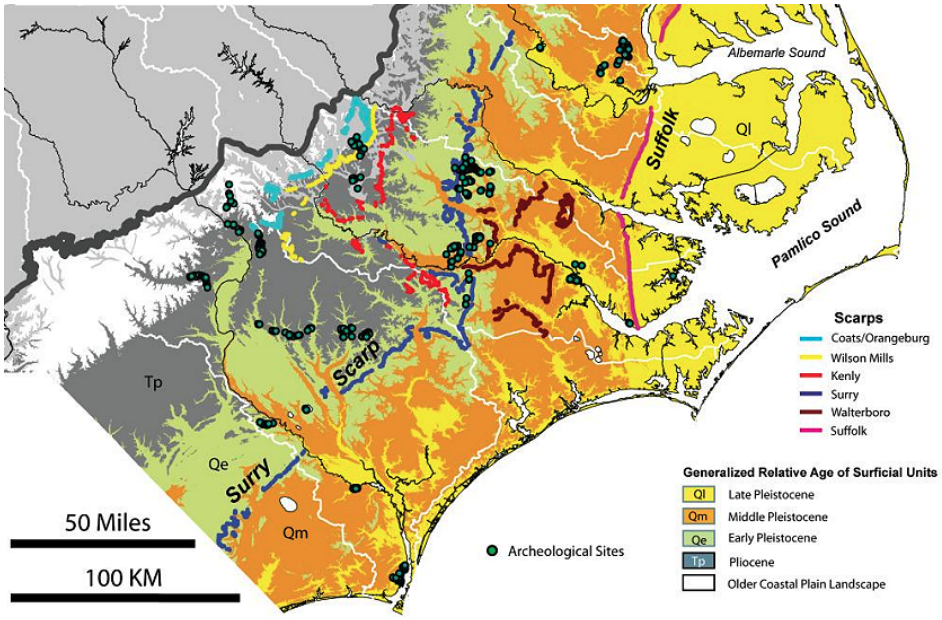


**Figure 33.** Generalized map of the surficial units of the coastal plain. Source: (Abbott Jr. et al., 2011), Fig. 2-5. Used by permission.

dissected by several broad rivers (in this tile the Tar and Neuse) and their tributary streams, with alluvial soils. The Piedmont soils are residual on crystalline rocks. The soil geomorphology of this area is described by Daniels et al. (1999). Fig. 33 shows the sequence of coastal plain terraces on the interfluves between rivers, and the clear separating scarps.

The $0.2 \times 0.2°$ subtile for pattern analysis is (-77.8 – -77.6° E, 35.2–35.4° N), centred a few km NW of Kinston, NC (Fig. 34). This figure shows the general soil associations, overlain on Google Earth by the Soil Web network link (https://casoilresource.lawr.ucdavis.edu/soilweb-apps/). This area includes the N-S trending Surry scarp, separating the Wicomico (14–30 m.a.s.l) from the Sunderland (30–45 m.a.s.l.) terraces. Association `s4680` (Candor-Autryville) are more developed soils (Grossarenic Paleudults and Arenic Kandiudults) on the Sunderland terrace; association `s4768` (Rains-Lynchburg-Goldsboro-Coxville) are less-developed soils (Typic and Aeric Paleaqults, Aquic Paleaqults) on the Wicomico terrace. The Sunderland terrace soils have thick E and Bt horizons, the Wicomico terrace soils have thinner horizons and (in this area) are more poorly drained. At the southern edge of this area is association `s4658`, (Wehadkee-Meggett-Chewacla), Fluvaquentic Dystrudepts along the Neuse River.

A critical factor in land use of this region is particle-size distribution (PSD). The dominant World Reference Base for Soil Resources (WRB) (IUSS Working Group WRB, 2015) Reference Soil Group is *Acrisols*, here equivalent to USDA Soil Taxonomy (Soil Survey Division Staff, 2014) *Ultisols*. These are texture-contrast soils. The surface soil PSD is especially important for tillage and development of sweet potatoes and peanuts; the subsoil PSD is especially important for the soil functions water-holding capacity and thus drought resistance. The Soil Taxonomy families in this area are mainly separated by the particle-size class of the control section, roughly equivalent to the upper subsoil. The area also has soils from deep

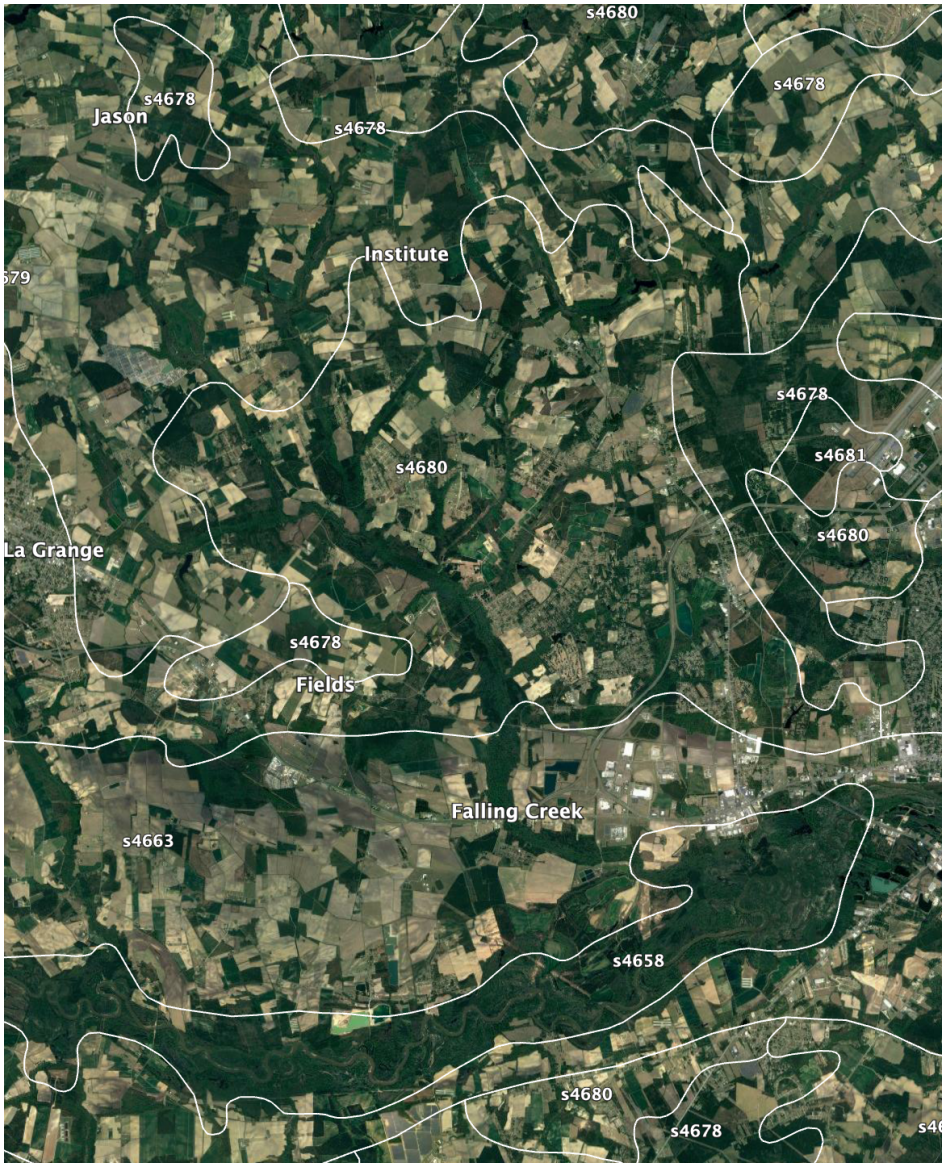


**Figure 34.** 0.2° sub-tile of the North Carolina coastal plain study area, (-77.8 – -77.6° E, 35.2–35.4° N), Kinston NC at the E edge

sands and clayey alluvium. As an approach to these soil functions, we present an analysis of clay concentration in the 0–5 and 30–60 cm layers. This allows us to compare the success of various DSM methods in the surface and subsoils.

| Product | MD | RMSD | RMSD.Adjusted |
|---|---|---|---|
| SG2 | -47.423 | 70.867 | 52.661 |
| PSP | -1.754 | 51.713 | 51.683 |
| SPCG | 9.362 | 51.414 | 50.554 |

| Product | MD | RMSD | RMSD.Adjusted |
|---|---|---|---|
| SG2 | -37.637 | 129.124 | 123.517 |
| PSP | 30.828 | 77.006 | 70.566 |
| SPCG | -14.882 | 117.958 | 117.015 |

**Table 10.** Statistical differences between NATSGO and the other DSM products, clay %% 0–5 cm (top), 30–60 cm (bottom)

### 3.1 Regional spatial patterns

#### 3.1.1 Regional maps

Figs. 35 and 36 show gNATSGO (reference) along with the predictions of clay concentration in the two depth intervals (0-5 cm, 30–60 cm, respectively) of the other products. Figs. 37 and 38 shows their histograms, and Fig. 39 the pairwise Pearson correlations between all maps. Figs. 40 and 41 show the differences as maps. Table 10 shows the statistical differences.

Mean differences are substantial for SG2, an over-prediction of about 4.7% (surface) and 3.7% (subsoil). SPCG under-predicts the surface by about 1% and over-predicts the subsoil by about 1.4% PSP under-predicts the subsoil by about 3.2% but is almost unbiased for the surface soil. However, the RMSD are much higher, from 4.5–7% topsoil and 7.5–12.9% subsoil. This latter is particularly problematic because of the role of clay in water and nutrient retention, hydraulic conductivity, and nutrient supply.

The products are not well-correlated, except for gNATSGO and PSP in the subsoil. SG2 is almost uncorrelated with gNATSGO and PSP in the subsoil, and only weakly correlated in the topsoil. This means that their spatial patterns are substantially different. The relation between SG2 and SPCG is better, likely because they use the same methodology. Thus SG2 performs quite poorly for this area and property, even after accounting for bias.

The spatial patterns are wildly different, especially for the subsoil. gNATSGO and the other products derived from gSSURGO clearly shows the heavy soils of the lowest level of the coastal plain, surrounding Albemarle and Pamlico sounds. Low clay subsoils are also clear on the river bottoms and backswamps leading to the sounds. In the middle coastal plain, in a band from SW to NE there is a complex pattern due to sedimentary facies. The lower-clay subsoils here have high silt content.

PSP is similar to gNATSGO but does not identify the highest clay concentrations. It also predicts much higher surface clay proportion in some areas not mapped by gNATSGO; these are water bodies which should not have been predicted.

The two products using SoilGrids methodology are quite poor, especially SG2 for the subsoil. The presented pattern has no relation to reality. SPCG is quite different but still unrealistic, and shows an unusual feature in the southeast of the tile, especially visible in the subsoil. This likely comes from the use of a generalized geologic map (North Carolina Geological Survey Section, 1985) which differentiates the central coastal plain sediments in this portion of the map, but not in the undifferentiated northern portion, likely due to a difference in field survey methods. So this is likely not a true lithologic boundary.

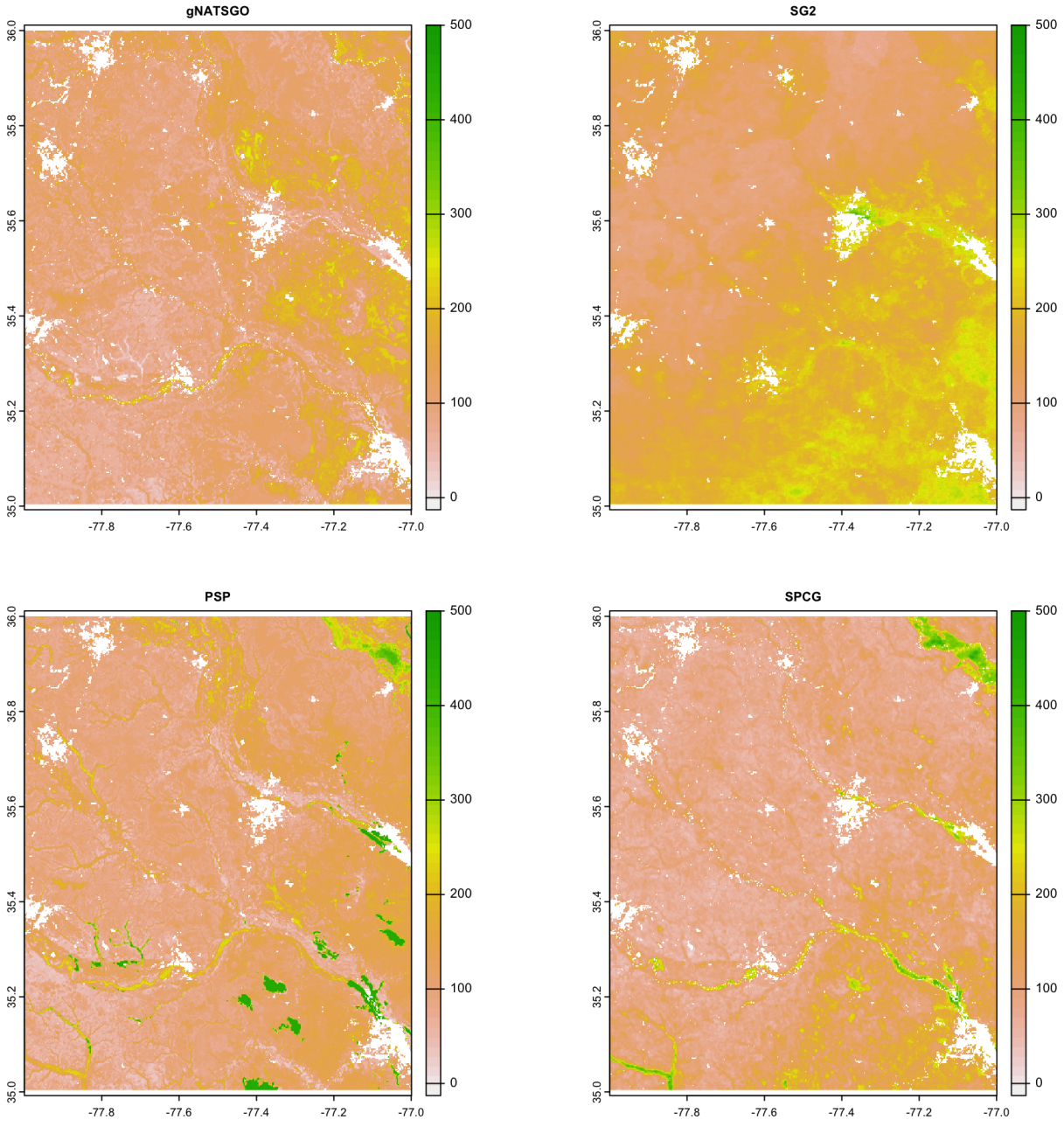


**Figure 35.** 0-5 cm clay %%, according to different DSM products

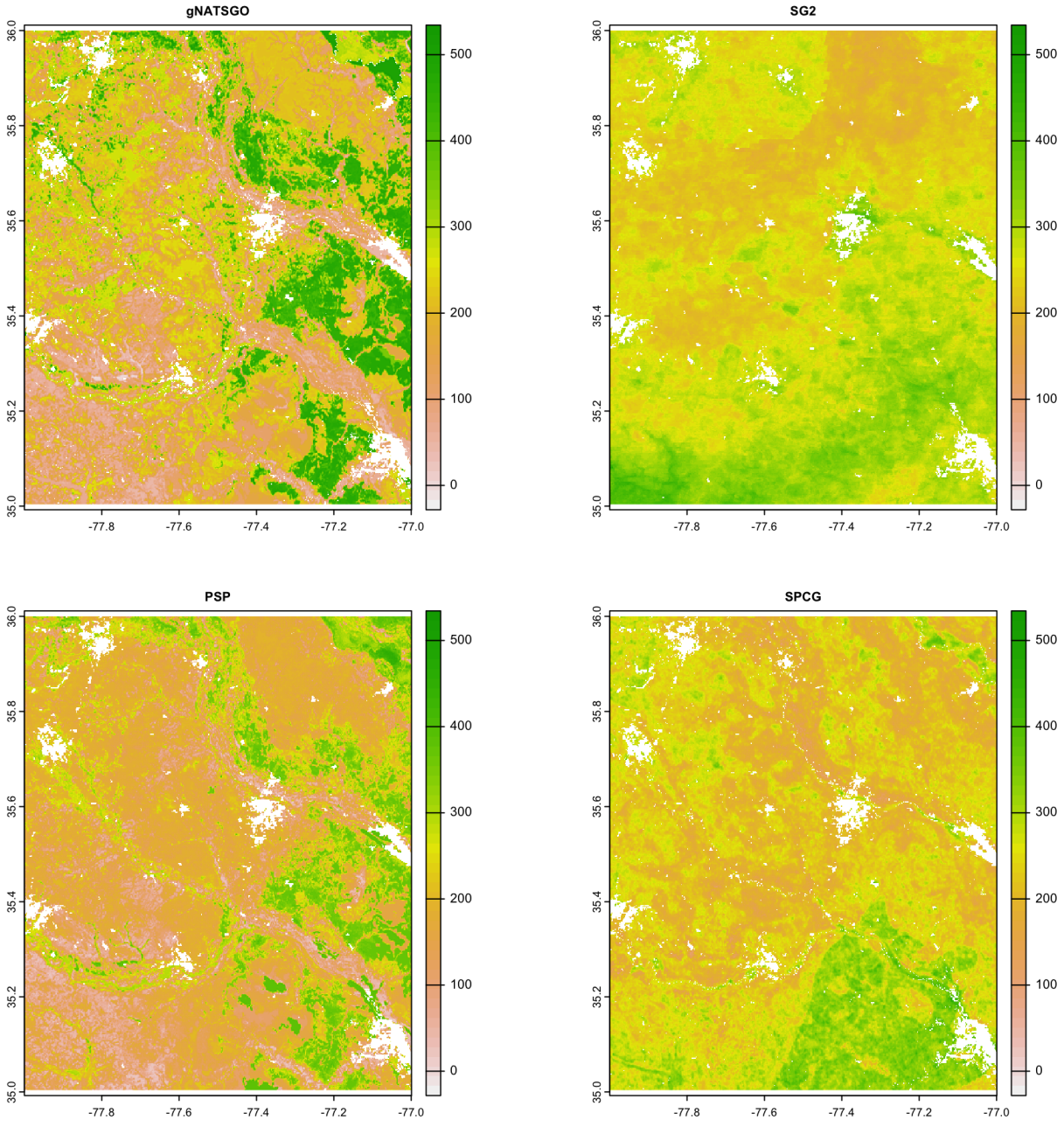


**Figure 36.** 30-60 cm clay %%, according to different DSM products

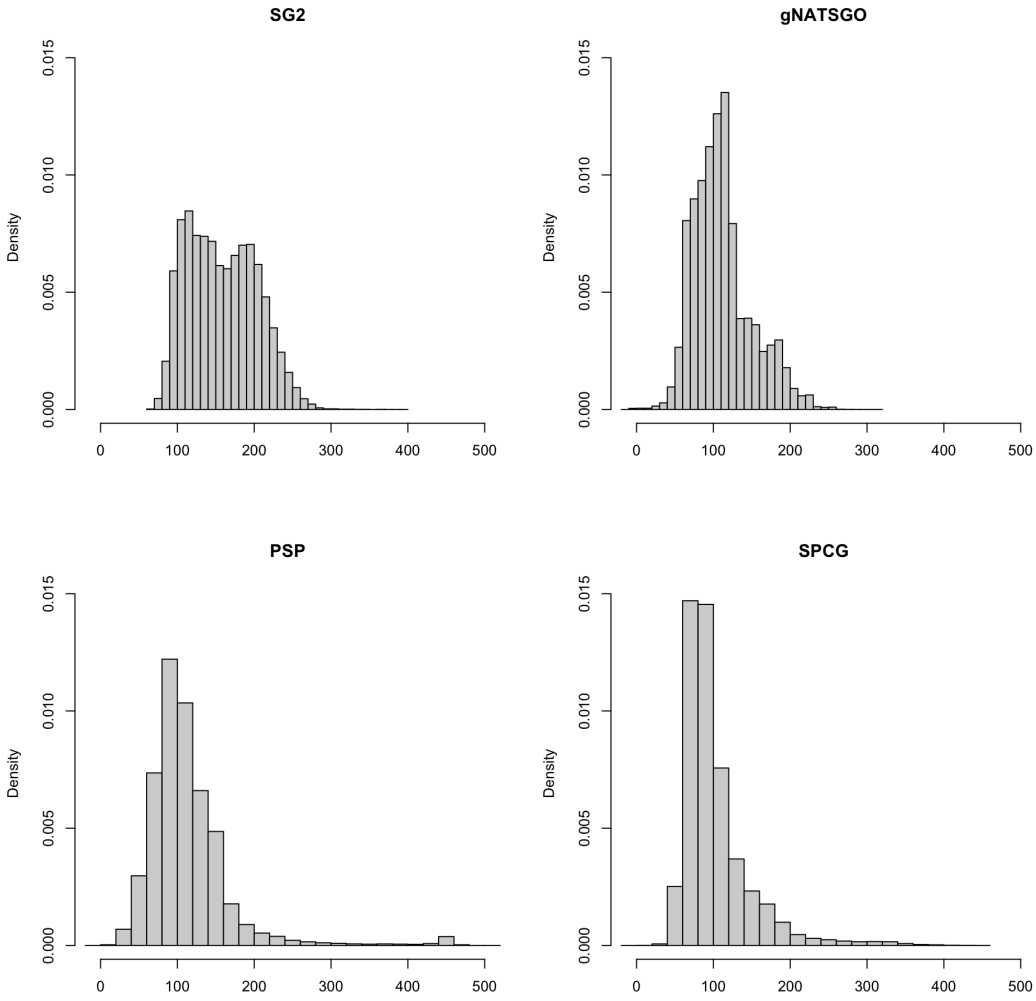


**Figure 37.** Histograms of 0–5 cm clay %%, according to different DSM products

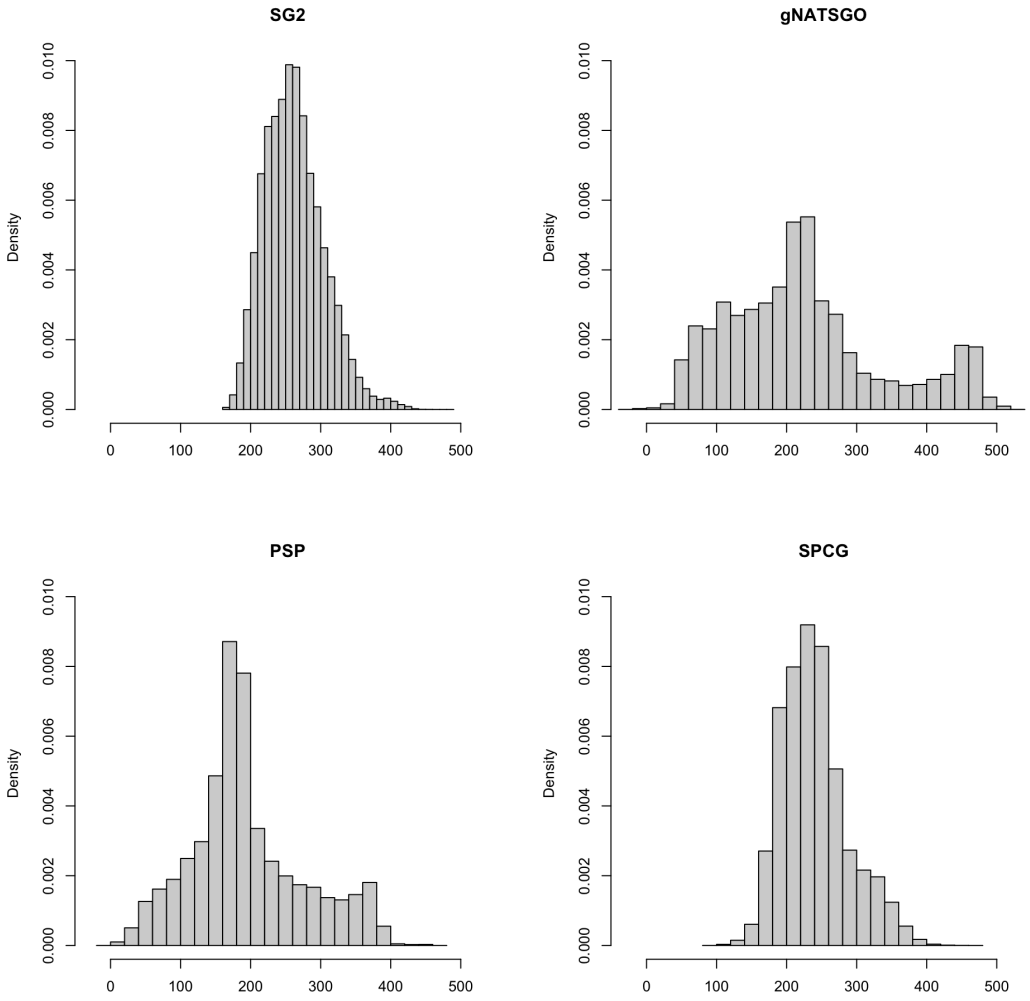


**Figure 38.** Histograms of 30–60 cm clay %%, according to different DSM products

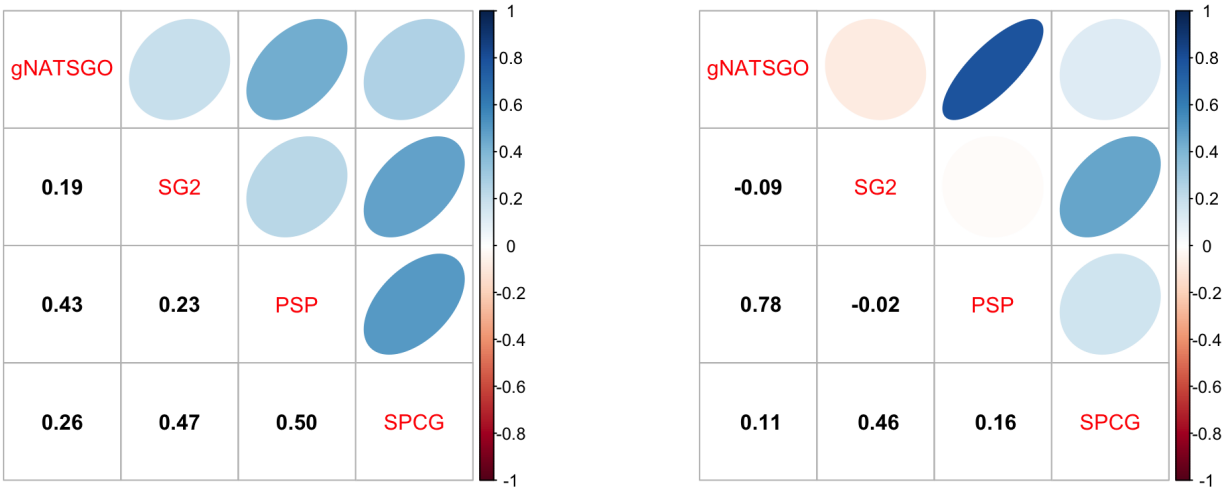


**Figure 39.** Pearson correlations between all products, clay %%, 0–5 cm (left), 30–60 cm (right)

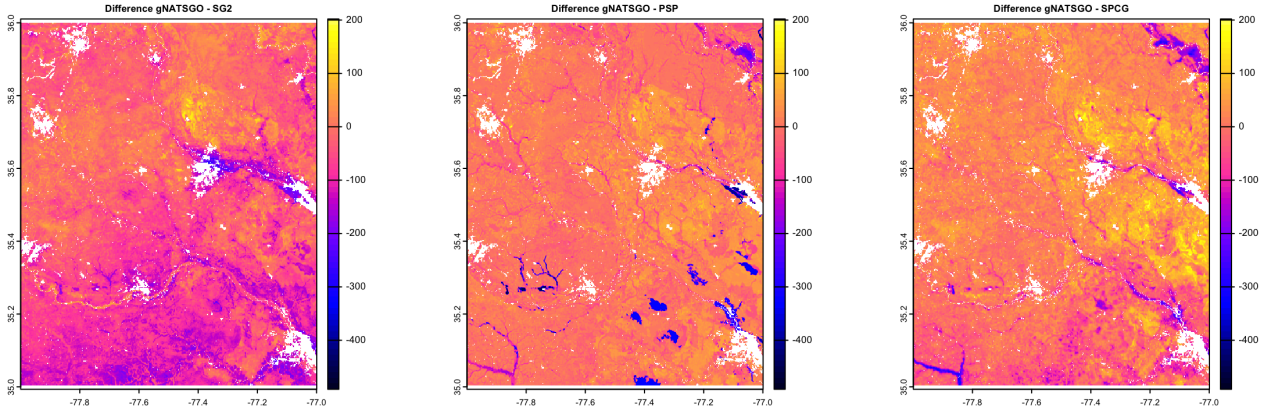


**Figure 40.** Difference between gNATSGO and other DSM products, clay %%, 0–5 cm

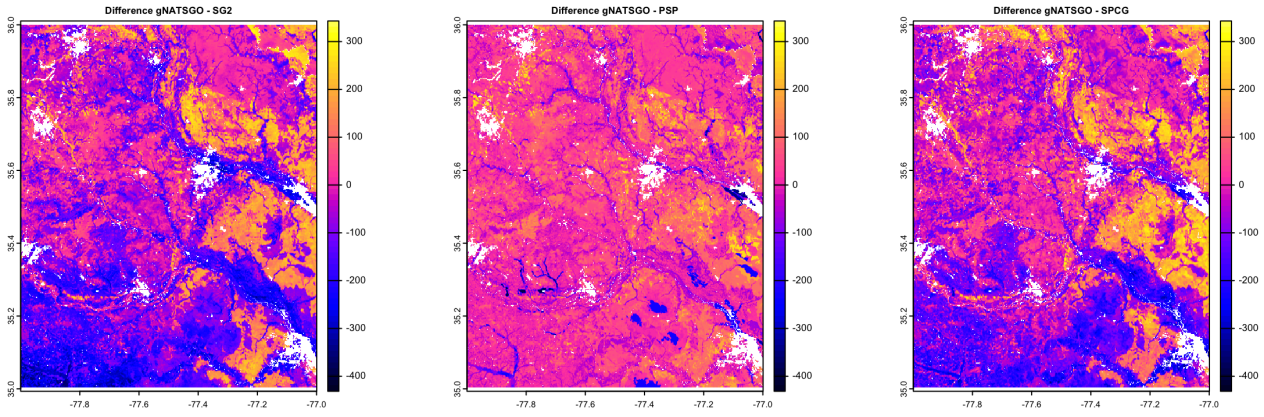


**Figure 41.** Difference between gNATSGO and other DSM products, clay %%, 30–60 cm

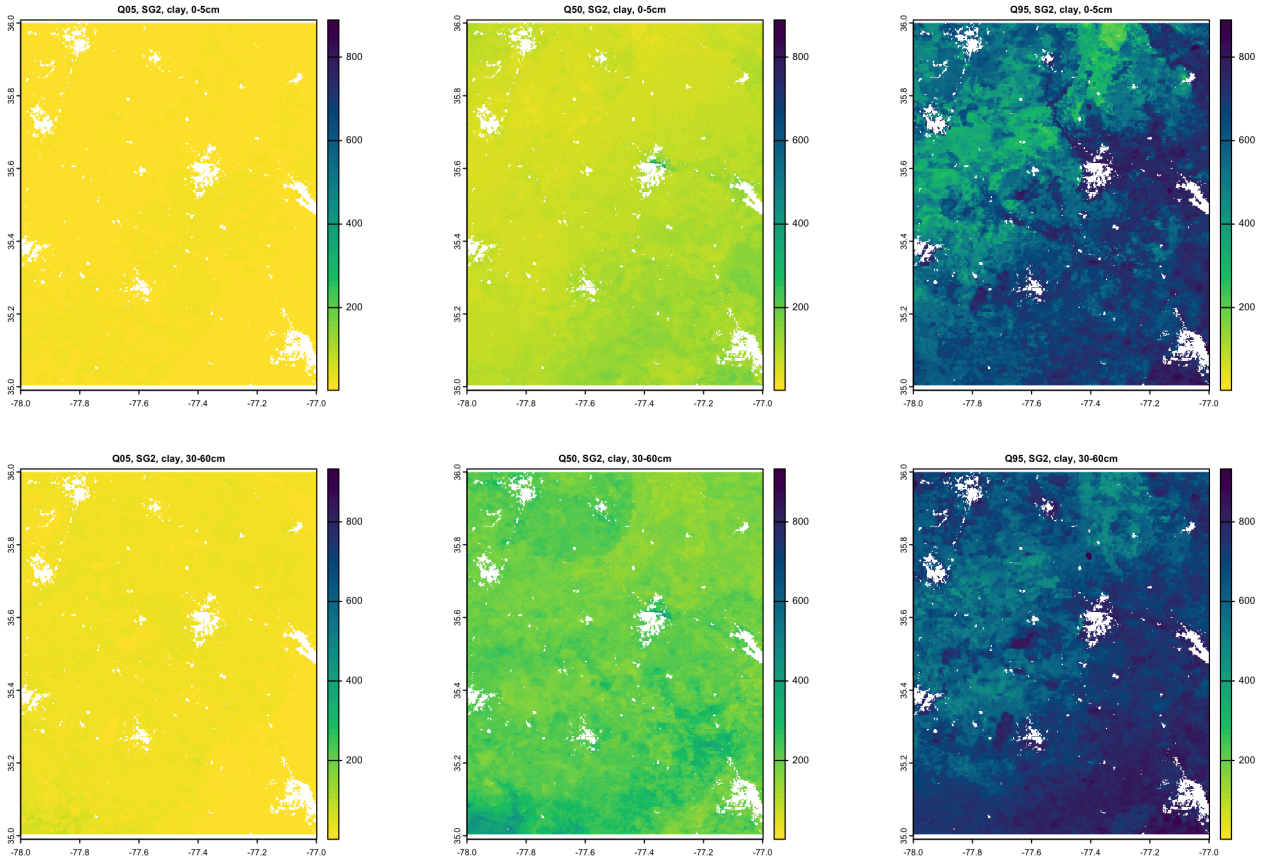


**Figure 42.** Quantiles of the prediction, SG2, clay %x10, 0–5 cm (top), 30–60 cm (bottom)

### 3.1.2 Uncertainty

The 5%, 50%, and 95% prediction quantile maps are shown in Figs. 42 (SG2) and 43 (PSP); each figure has its own stretch. The "low", "representative" and "high" values from gNATSGO are shown in Fig. 44

Fig. 45 shows the inter-quartile range 5–95% (IQR), along with the low-high range for gNATSGO, for the two products at the two depth intervals.

SG2 has a quite wide IQR, mostly from about 30% to 75% clay concentration in the surface soil and somewhat narrower in the subsoil, with more uncertainty in the higher coastal plain terraces. By contrast PSP has a much narrower range, on the order of 20%-30% clay concentration, with the higher uncertainty mostly in the lower coastal plain terraces and river valleys.

Fig. 46 shows the spatial differences between the two IQR. SG2 is everywhere less certain than PSP, mostly by a large margin.

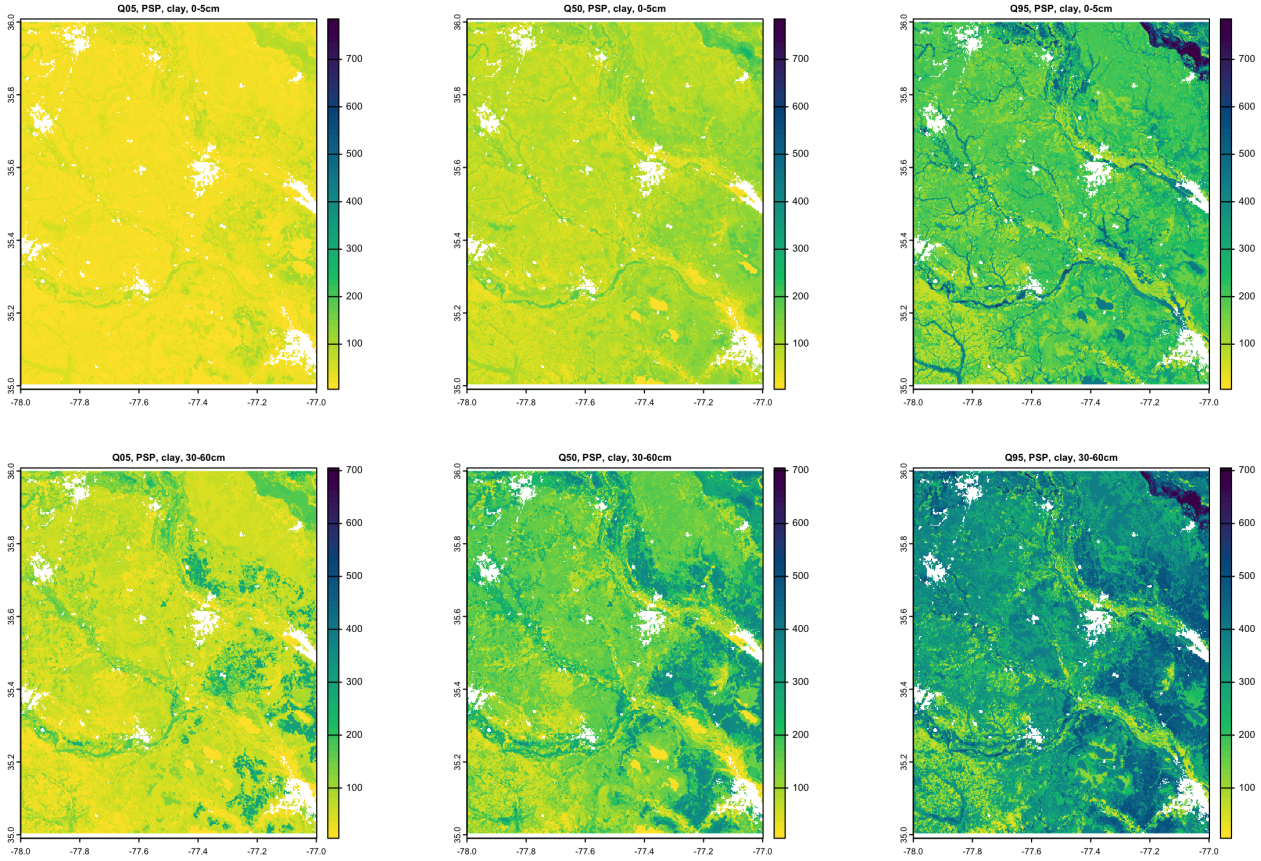


**Figure 43.** Quantiles of the prediction, PSP, clay %x10, 0–5 cm (top), 30–60 cm (bottom)

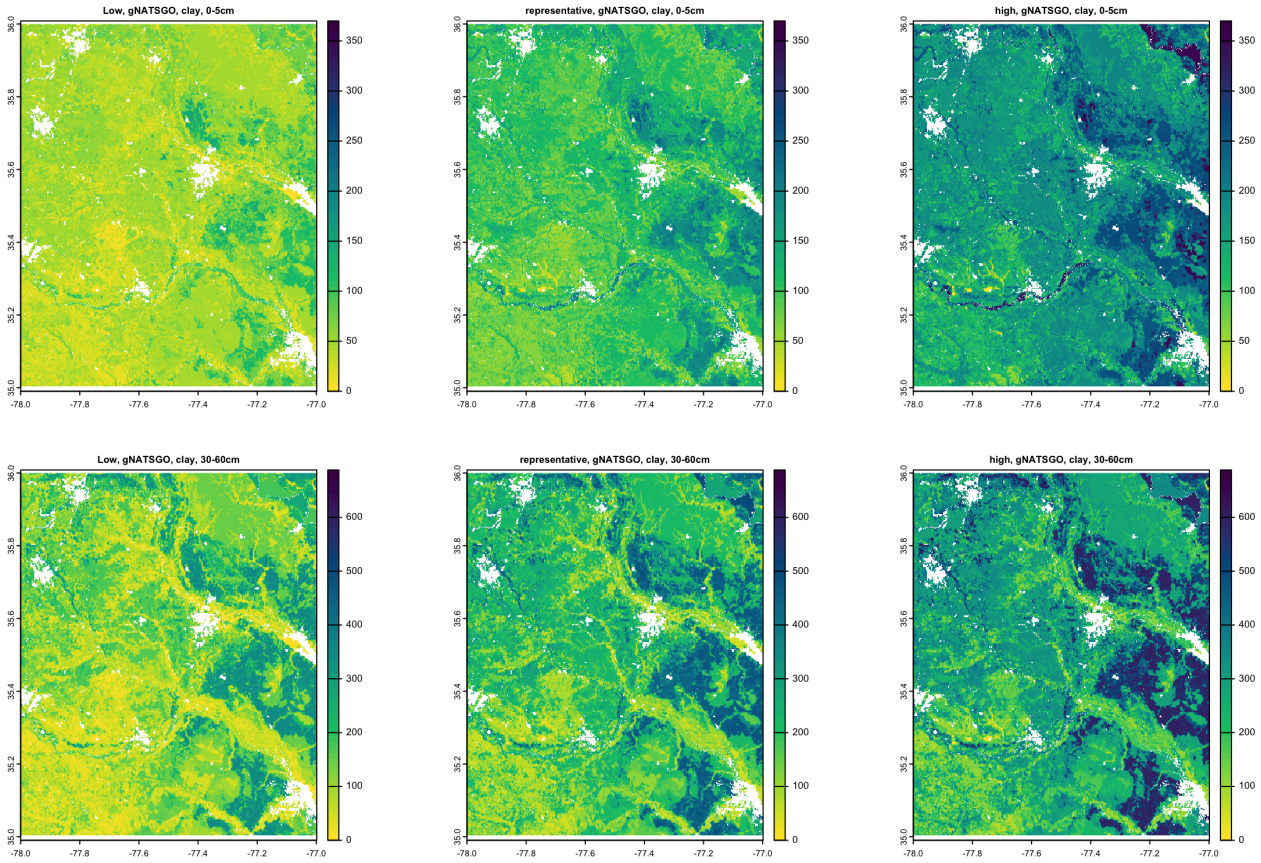


**Figure 44.** Low, representative, high values from gNATSGO, pHx10, 0–5 cm

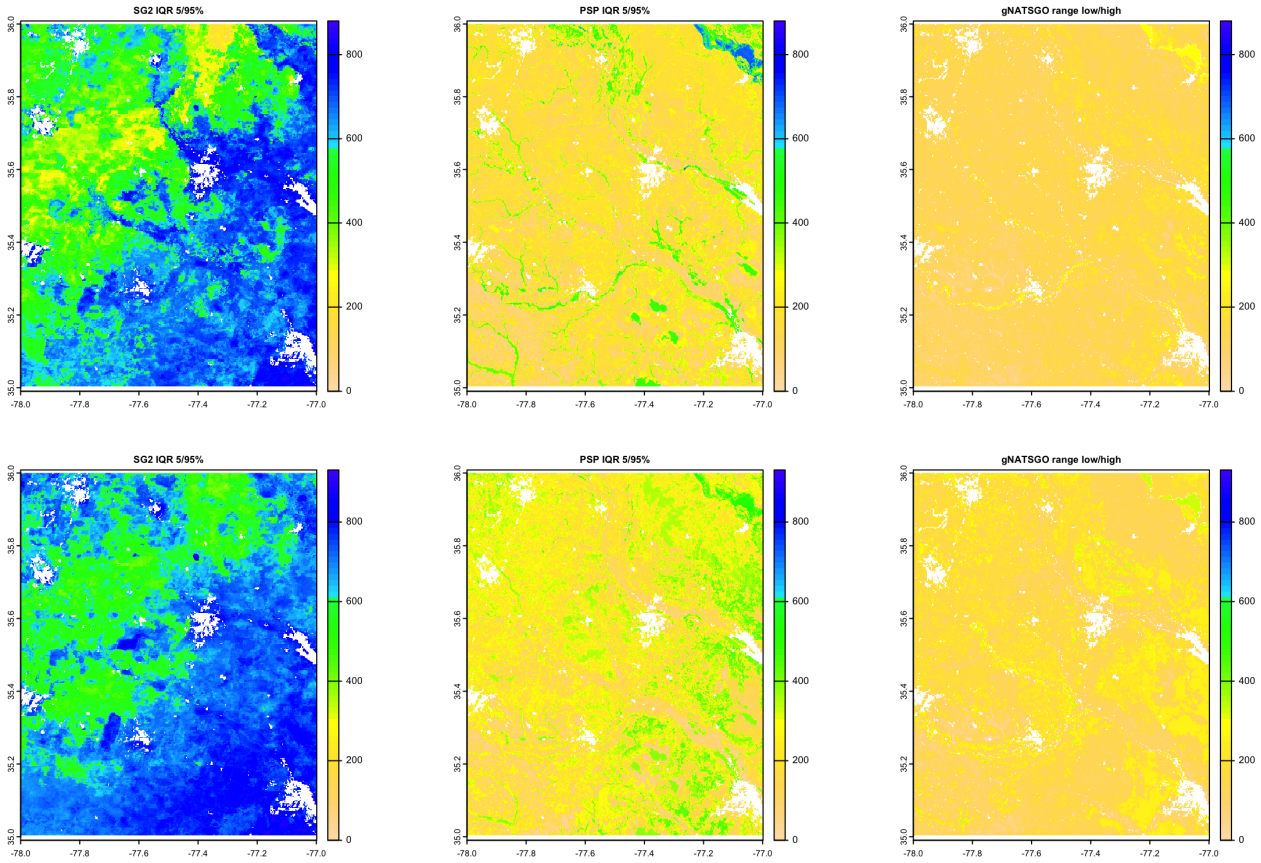


**Figure 45.** Quantiles of the prediction, PSP, clay %x10, 0–5 cm (top), 30–60 cm (bottom)

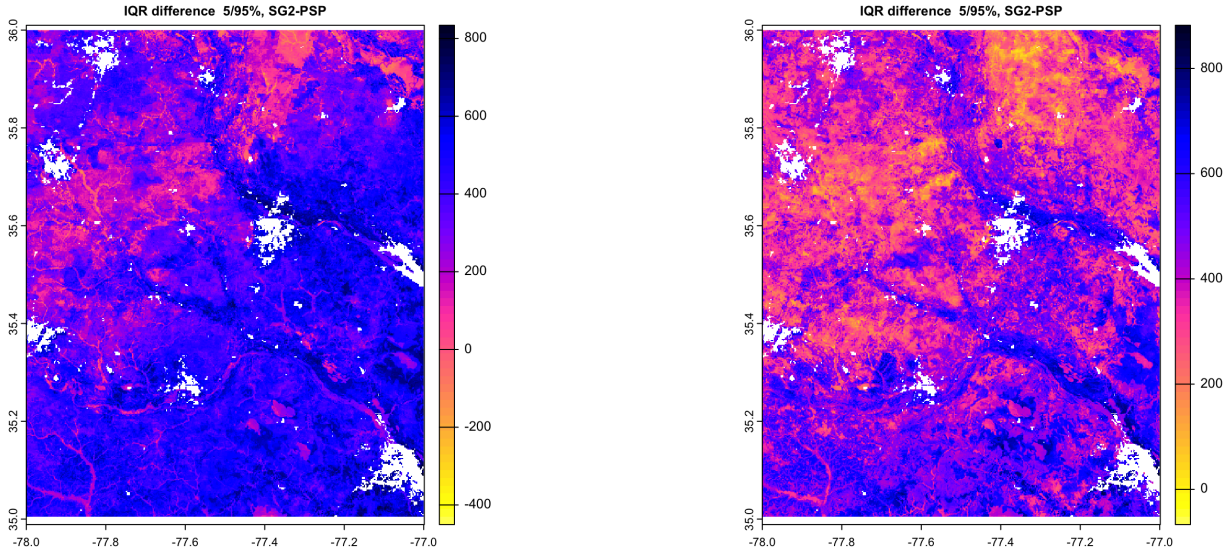


**Figure 46.** Difference between Inter-quantile ranges 0.05–0.95, Δ(clay %x10) 0–5 cm (left), 30–60 cm (right)

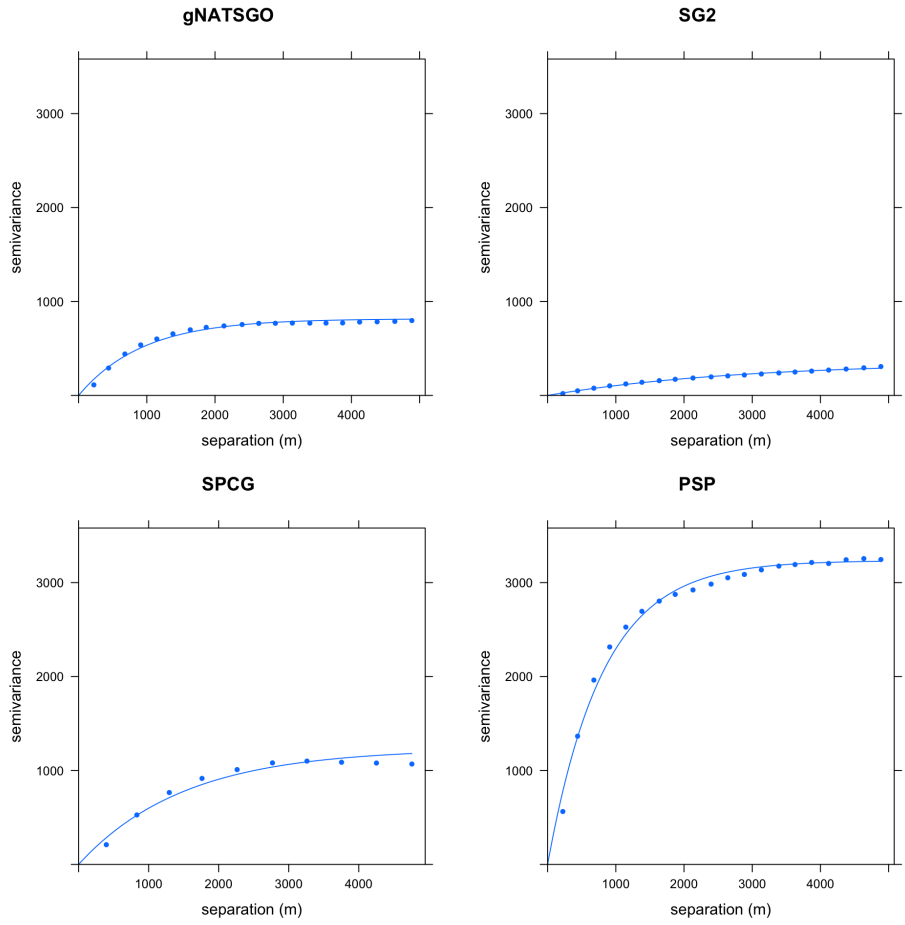


**Figure 47.** Fitted variograms, clay %%, 0–5 cm. Semivariance units $(\text{clay}\%\%)^2$

### 3.1.3 Local spatial autocorrelation

Figs. 47 and 48 show the local variograms and their fitted models, and Tables 11 and 12 show their statistics. These are dramatically different in this small test area. Most notably, SG2 has very little local variability, as shown by the very low sill and long range. SPCG shows a similar but less dramatic result. PSP and gNATSGO have fairly high structural sills and short ranges, i.e., high local variability.

**Classification**: Class limits from histogram equalization for the surface soil are approximately 6.33, 7.25, 8.16, 9.13, 10.67, 13.17, and 16.70%, with the extreme values of 0.00 and 46.00 %; this is a strongly right-skewed distribution. Class limits for the subsoil are approximately 10.55, 15.00, 17.96, 20.56, 22.38, 24.40, and 26.93%, with the extreme values of 0.00 and 47.00 %; this distribution is moderately left-skewed. The texture contrast is obvious.

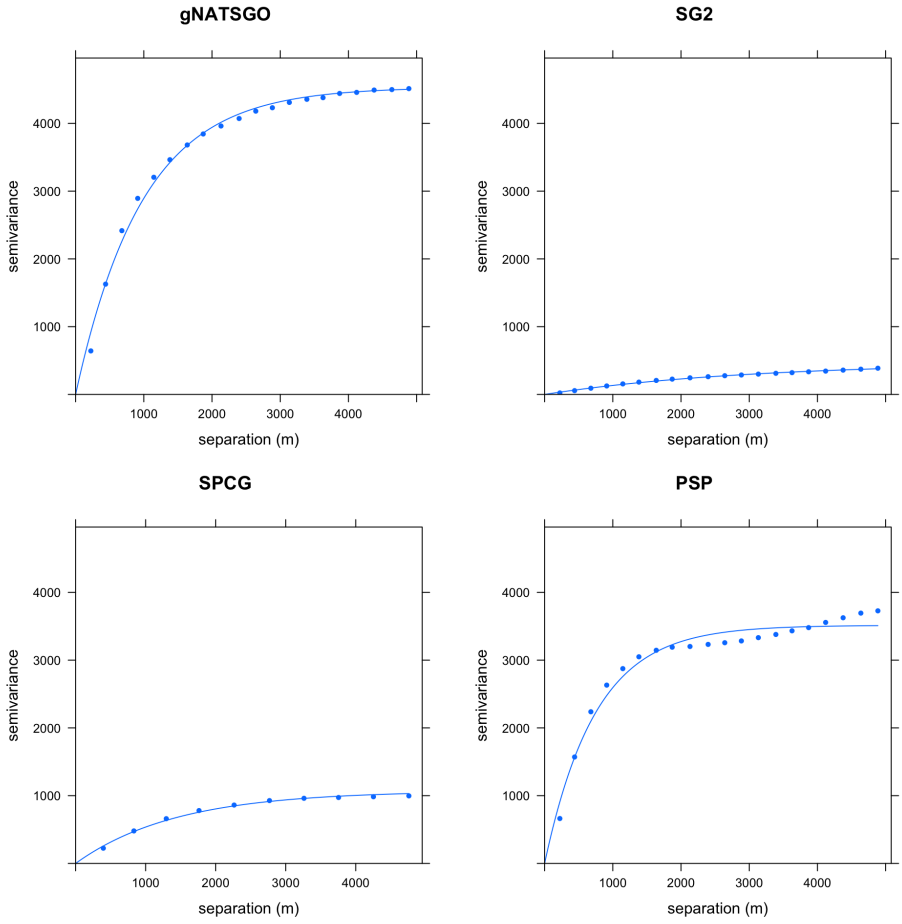


**Figure 48.** Fitted variograms, clay %%, 30–60 cm. Semivariance units $(\text{clay}\%\%)^2$

| Product | Effective range | Structural Sill | Proportional Nugget |
|---|---|---|---|
| gNATSGO | 2823.00 | 816.41 | 0.00 |
| SG2 | 8565.00 | 354.01 | 0.00 |
| SPCG | 4518.00 | 1232.98 | 0.00 |
| PSP | 2427.00 | 3234.89 | 0.00 |

**Table 11.** Fitted variogram parameters, clay %%, 0–5 cm. Range in $\text{m}$; structural sill in $(\text{clay}\%\%)^2$, proportional nugget on $[0 \dots 1]$

| Product | Effective range | Structural Sill | Proportional Nugget |
|---|---|---|---|
| gNATSGO | 2952.00 | 4534.76 | 0.00 |
| SG2 | 9105.00 | 473.32 | 0.00 |
| SPCG | 4308.00 | 1069.98 | 0.00 |
| PSP | 2238.00 | 3513.92 | 0.00 |

**Table 12.** Fitted variogram parameters, clay %%, 30–60 cm. Range in $\mathrm{m}$; structural sill in $(\mathrm{clay}\%\%)^2$, proportional nugget on $[0 \dots 1]$

| DSM_products | V_measure | Homogeneity | Completeness |
|---|---|---|---|
| gNATSGO vs. SG2 | 0.0293 | 0.0237 | 0.0385 |
| gNATSGO vs. SPCG | 0.1012 | 0.0992 | 0.1032 |
| gNATSGO vs. PSP | 0.2085 | 0.2128 | 0.2044 |
| SPCG vs. SG2 | 0.0486 | 0.0399 | 0.0623 |

**Table 13.** V-measure statistics, clay %%, 0–5 cm

| DSM_products | V_measure | Homogeneity | Completeness |
|---|---|---|---|
| gNATSGO vs. SG2 | 0.0151 | 0.0133 | 0.0174 |
| gNATSGO vs. SPCG | 0.0351 | 0.0337 | 0.0366 |
| gNATSGO vs. PSP | 0.2554 | 0.2494 | 0.2616 |
| SPCG vs. SG2 | 0.0074 | 0.0068 | 0.0082 |

**Table 14.** V-measure statistics, clay %%, 30–60 cm

Figs. 49 and 50 show, respectively, the topsoil and subsoil clay, classified into eight histogram-equalized classes in a small 0.2 x 0.2° sub-area, with limits $(-77.11 \cdots -76.91)°$ E, $(35.70 \cdots 35.90)°$ N, centred about 8 km SE of Williamson, NC (the unmapped area). Note that each depth interval has a separate histogram equalization. The high-clay Neuse River floodplain runs generally E-W towards the bottom of the map. A scarp separating two coastal plain levels runs N-S through this area. The higher clay proportions are shown in the darker blue. There is an obvious overall difference in class distribution. The classified PSP map shows the landscape pattern somewhat more clearly than gNATSGO on which it is based. The classified SG2 map completely fails to capture the magnitude and the pattern of the clay concentration classes.

### 3.1.4 V-measure

Tables 13 and 14 show the statistics from the V-measure calculations. Unlike the case for central New York State topsoil pH, here the two DSM products based on SoilGrids methodology (SG2 and SPCG) are quite dissimilar

Figs. 51 and 52 show the computed homogeneity and completeness of the SG2 surface and subsoil clay class maps, with respect to gNATSGO.

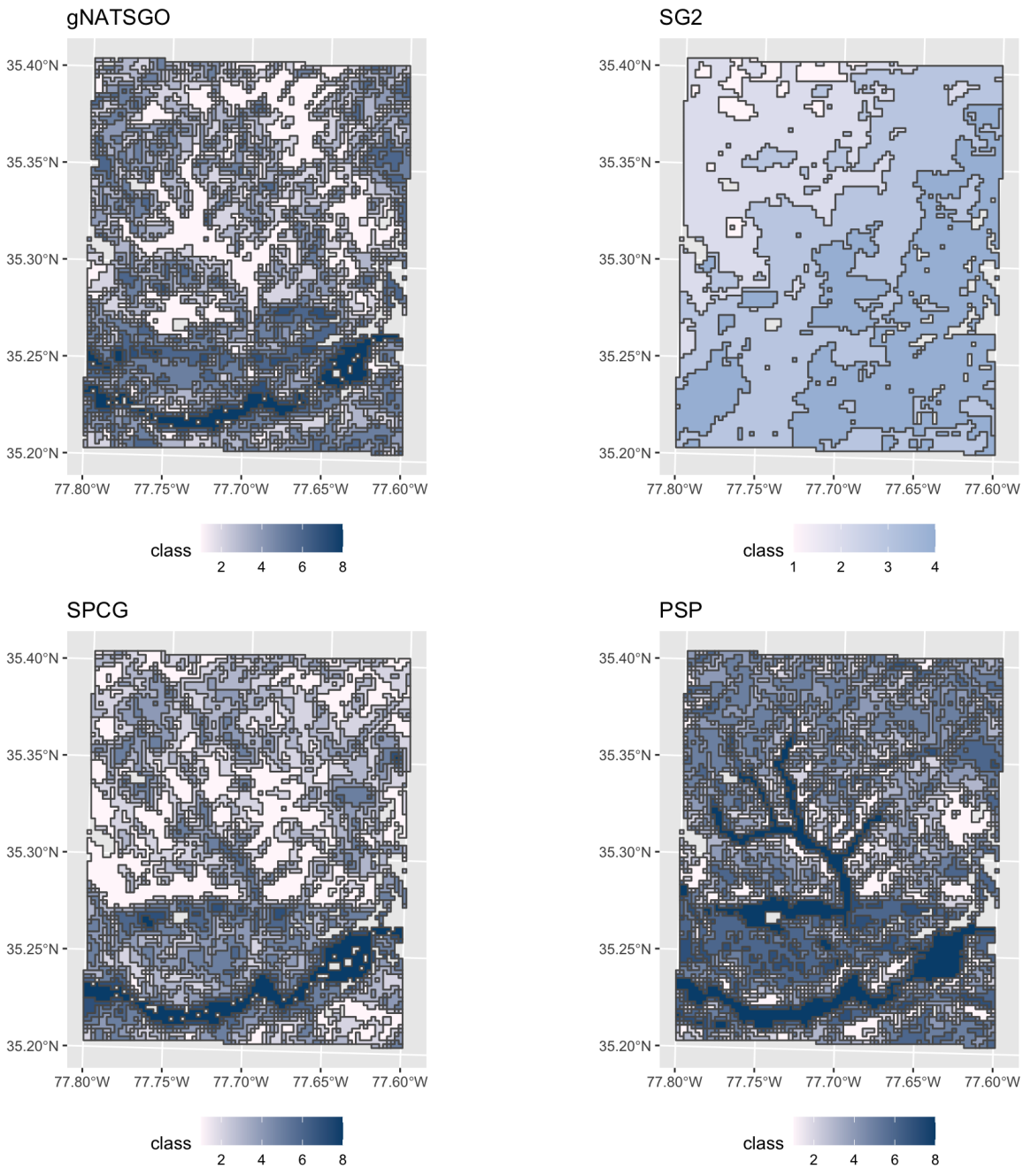


**Figure 49.** clay %% classes, 0–5 cm, coastal plain NC, detail

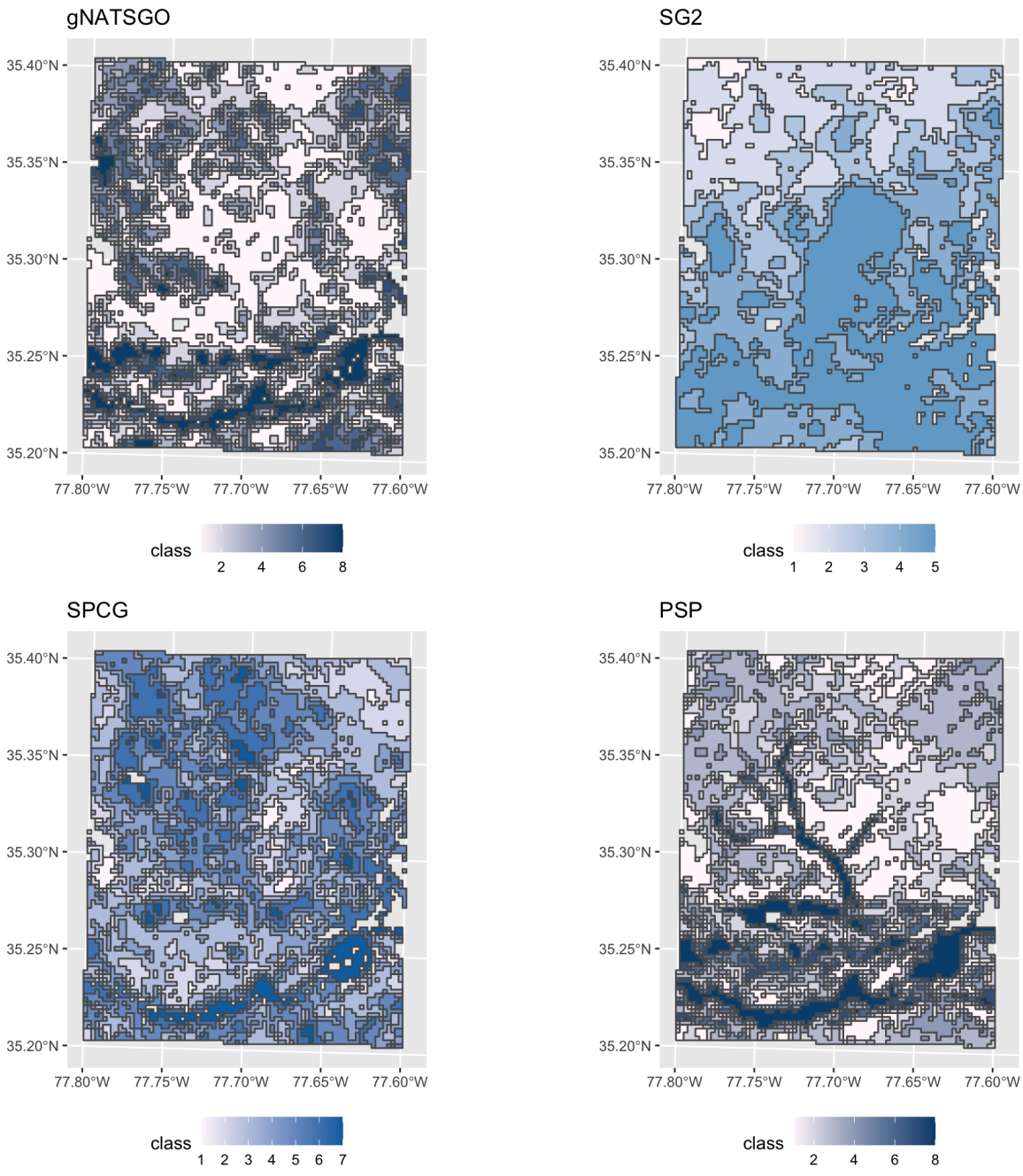


**Figure 50.** clay %% classes, 30–60 cm, coastal plain NC, detail

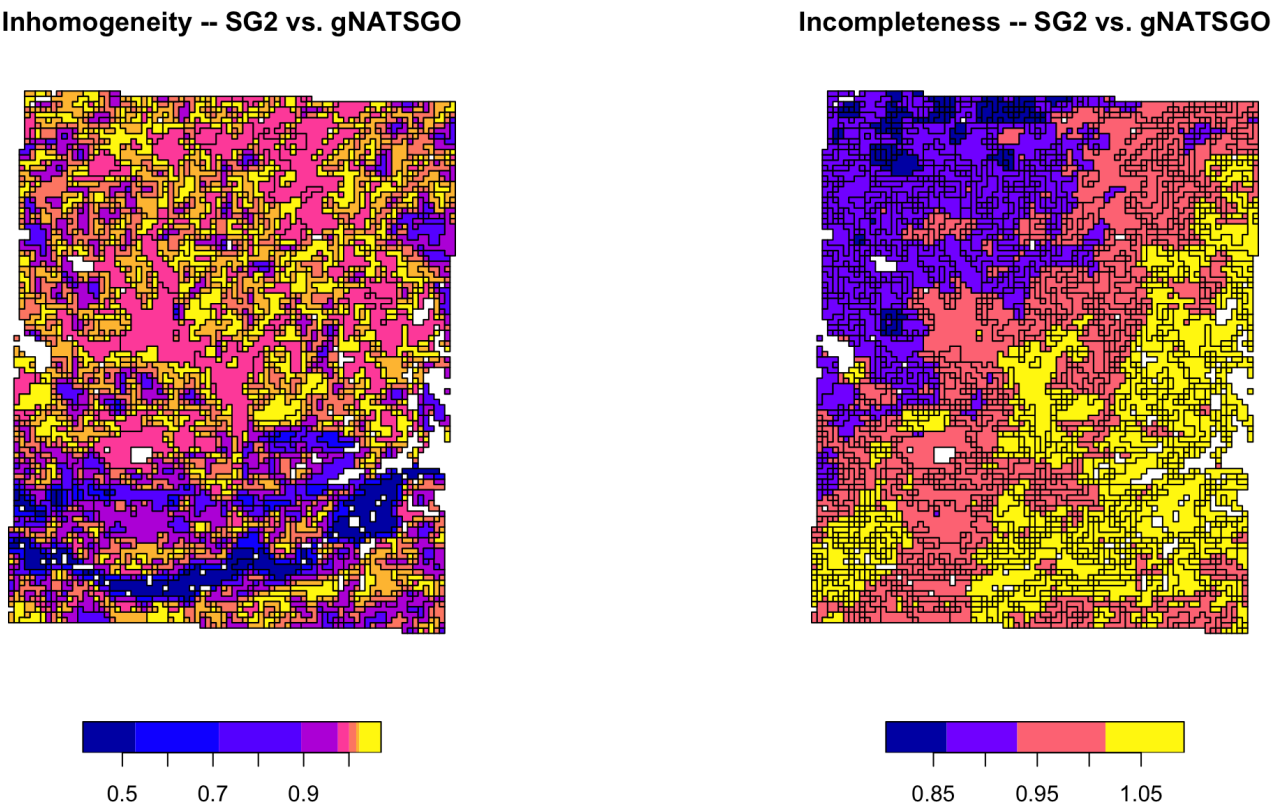


**Figure 51.** Homogeneity (left) and Completeness (right) of the SG2 surface soil clay class map, with respect to GSM map

| product | ai | frac_mn | lsi | shdi | shei |
|---|---|---|---|---|---|
| gNATSGO | 47.051 | 1.039 | 25.359 | 1.917 | 0.922 |
| SG2 | 87.535 | 1.032 | 7.357 | 1.177 | 0.849 |
| SPCG | 54.513 | 1.043 | 22.147 | 1.842 | 0.886 |
| PSP | 44.583 | 1.029 | 26.205 | 1.998 | 0.961 |

| product | ai | frac_mn | lsi | shdi | shei |
|---|---|---|---|---|---|
| gNATSGO | 50.548 | 1.031 | 23.805 | 1.874 | 0.901 |
| SG2 | 82.077 | 1.034 | 9.823 | 1.433 | 0.891 |
| SPCG | 59.04 | 1.045 | 20.184 | 1.726 | 0.887 |
| PSP | 55.1 | 1.028 | 21.59 | 1.791 | 0.861 |

**Table 15.** Landscape metrics statistics, clay %%, 0–5 cm (top), 30–60 cm (bottom). `frac_mn`: Mean Fractal Dimension; `lsi`: Landscape Shape Index; `shdi`: Shannon Diversity; `shei`: Shannon Evenness

### 3.1.5 Landscape metrics

Table 15 shows the statistics from the landscape metrics calculations.

There is almost no difference in the mean fractal dimension and Shannon evenness. However, SG2 has a much lower landscape shape index and Shannon diversity. This is clear from the SG2 class maps shown in Figs. 49 and 50.

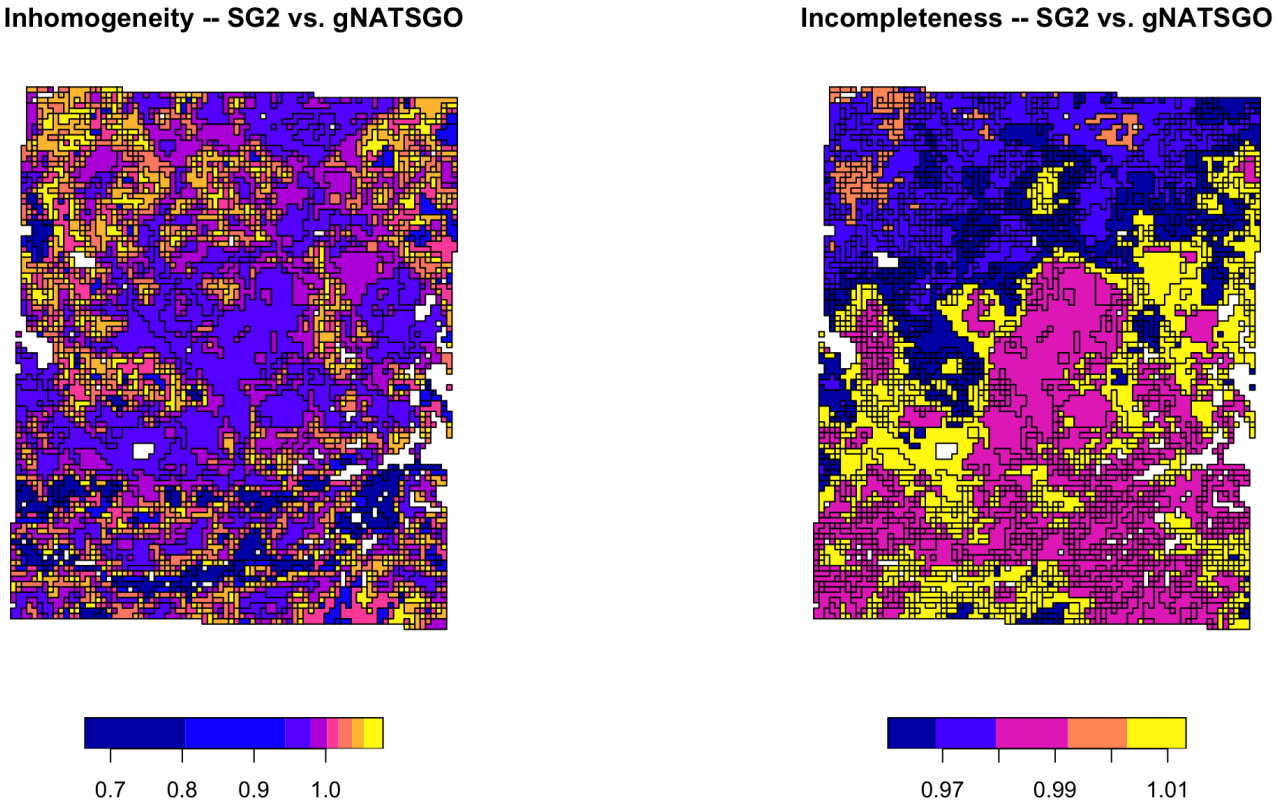


**Figure 52.** Homogeneity (left) and Completeness (right) of the SG2 subsoil clay class map, with respect to GSM map

### 3.2 Local spatial patterns

We examine this first qualitatively, i.e., by visual inspection, and then quantitatively, mostly following the methods of the regional assessment.

#### 3.2.1 Qualitative assessment

For this assessment we examine the 0–5 cm layer soil organic carbon (SOC), since this is expected to have a strong relation with land use. Fig. 53 shows the concentration of the 0–5 cm layer for (top) SOC of gSSURGO overlain on the original polygons from which it was derived, and (bottom) the soil organic matter of the disaggregated PSP grid cells along the Tar River at Old Sparta, NC. Note that these are different properties but related by a multiplicative factor, so the relative colours are indicative. Red colours are low, in this window relict sand bars (the `Ta*` map units). Light colours are high-organic matter surface soils (the `Ba, Pu` map units), from relict backswamps. Intermediate colours are upland Acrisols developed in loamy coastal plain sediments (e.g., the drainage sequence `No*, Go*, Ly*, Ra*`, with the more poorly drained series somewhat higher in organic matter.

The gSSURGO product follows the SSURGO lines exactly, and show a narrow range of predicted SOC concentration. Some of the sharp boundary lines do correspond with abrupt transitions on the ground, for example between the relict excessively drained sand bars and the poorly-drained backswamps. But others are not, for example on the upland coastal plain the sharp transition between the Goldsboro `Go*` series and the other series in its drainage sequence. These differences are because the predicted concentrations are taken from the official series descriptions. PSP follows the map unit lines fairly well, but is much finer-grained; each 30 m pixel is separately predicted. This results in some smoothing of the abrupt boundary lines from gSSURGO on the upland coastal plain. However within some SSURGO map units PSP predicts quite some differences in topsoil silt concentration, for example in the `TaB` polygon at Old Sparta. This is because PSP predicts each grid cell separately, and some cells better match series other than the mapped one. In this case the map unit description only has one series, but PSP predicts some others, as shown in Fig. 54. It is difficult to see any relation between these differences and terrain or land use.

#### 3.2.2 Quantitative assessment

To see the fine differences at this high resolution, we concentrate on a $0.15 \times 0.15°$ subtile with lower-right corner (-77.34° E, 35.70° N) and evaluate clay concentration, as in the regional assessment (§3.1). The Tar River runs approximately N-S on the W edge of this area, transgressing westward into the Sunderland marine terrace (Pliocene-Early Pleistocene) of the upper coastal plain. This transgression has left a series of sand bars and swales in the centre. This abandoned river plain is limited on the E by the younger Wicomico marine terrace (Medial Pleistocene) of the lower coastal plain, about 16 m lower than the older Sunderland terrace (Daniels et al., 1978). The town of Bethel is the unmapped spot towards the NE of the subtile.

Table 16 shows the statistical differences between gSSURGO (reference) and the DSM products. Fig. 55 shows the pairwise Pearson correlations between the maps. Both SG2 and PSP substantially under-predict clay concentration, by from about 2.5–3.8% in the surface soil and 6.6-8.2% in the subsoil. RMSD is around 5% for the surface and 11-15% for the subsurface. PSP

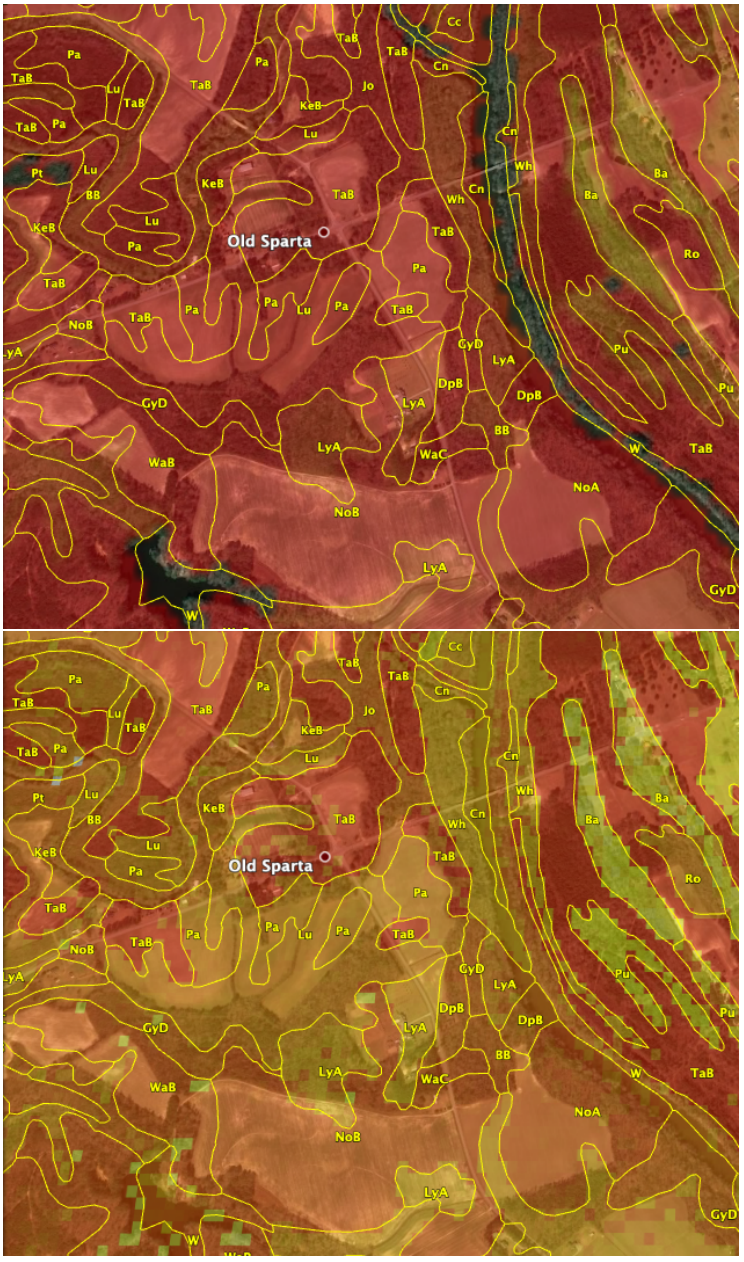


**Figure 53.** Ground overlay from gSSURGO (top) and PSP (bottom), organic C or matter % 0–5 cm, with SSURGO polygons from SoilWeb. Centre of image $-77°32'36"\mathrm{E}, 35°47'09"N$

**Figure 54.** Detail of PSP organic matter % 0–5 cm. Crossroads at $-77°33'17"\mathrm{E}, 35°47'20"N$

is somewhat closer to gSSURGO than SG2, which is not surprising since PSP is based on gSSURGO. Correlations are fairly strong between PSP and gSSURGO but weak between SG2 and the other products.

| DSM_product | MD | RMSD | RMSD.Adjusted |
|---|---|---|---|
| SG2 | 30.747 | 57.985 | 49.162 |
| PSP | 25.458 | 55.131 | 48.901 |

| DSM_product | MD | RMSD | RMSD.Adjusted |
|---|---|---|---|
| SG2 | 81.638 | 168.964 | 147.932 |
| PSP | 62.565 | 124.914 | 108.116 |

**Table 16.** Statistical differences between gSSURGO and DSM products, clay %%, 0–5 cm. Centre of map $-77.395°\mathrm{E}, 35.755°\mathrm{N}$

Figs. 56 and 57 show gSSURGO (reference) along with the predictions of clay concentration in the two depth intervals of the PSP products. Figs. 58 and 59 show these as difference maps.

The contrast between landscape units is fairly clear in the gSSURGO map. However, a clear artefact can be seen in the NE corner: a small portion of Martin County, here mapped as the Coxville series (*Fine, kaolinitic, thermic Typic Paleaquults*) was not correlated across the boundary of Pitt County, where the Exum series (*Fine-silty, siliceous, subactive, thermic Aquic Paleudults*) was mapped. So there is sharp transition from lower to higher clay concentration, based on the respective official series descriptions. PSP has smoothed out this boundary, by selecting most probable soil series for this landscape position. PSP also shows a fine spatial pattern, due to disaggregation by DSMART. However the resulting fine pattern does not seem to correspond to actual landscape features. SG2 hardly shows any differentiation, and does not seem related in any way to the details shown by gSSURGO.

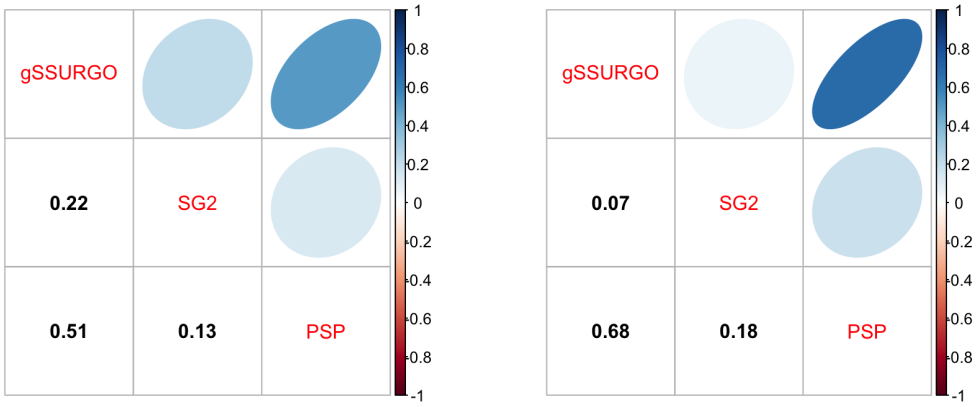


**Figure 55.** Pearson correlations between local products, clay %%, 0–5 cm (left), 30–60 cm (right)

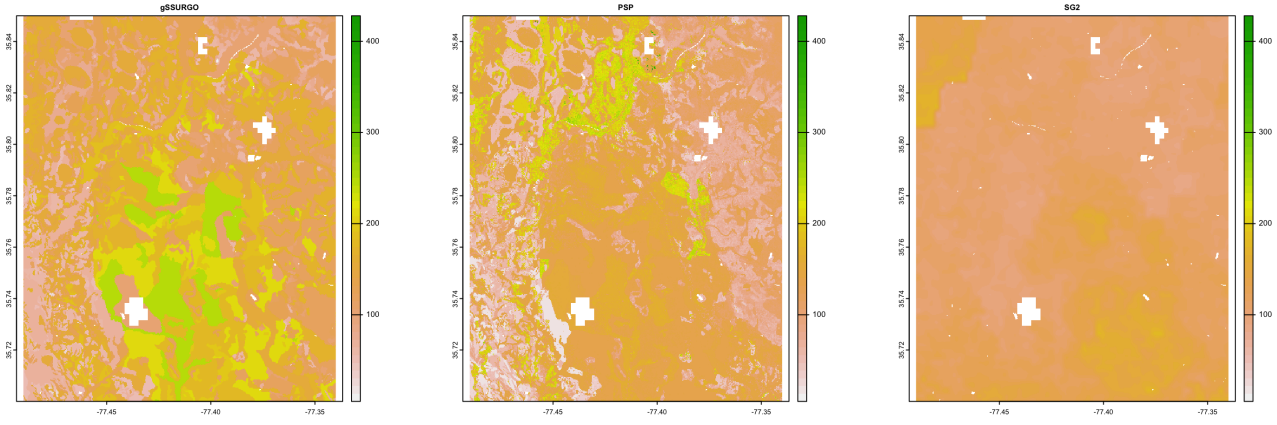


**Figure 56.** Topsoil (0-5 cm) clay %%, according to gSSURGO and DSM products

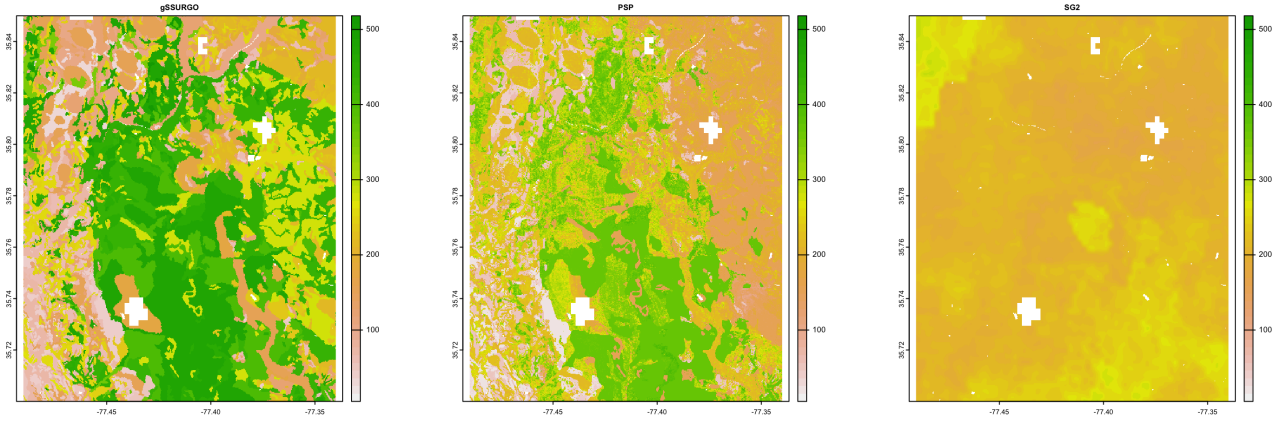


**Figure 57.** Subsoil (30-60 cm) clay %%, according to gSSURGO and DSM products

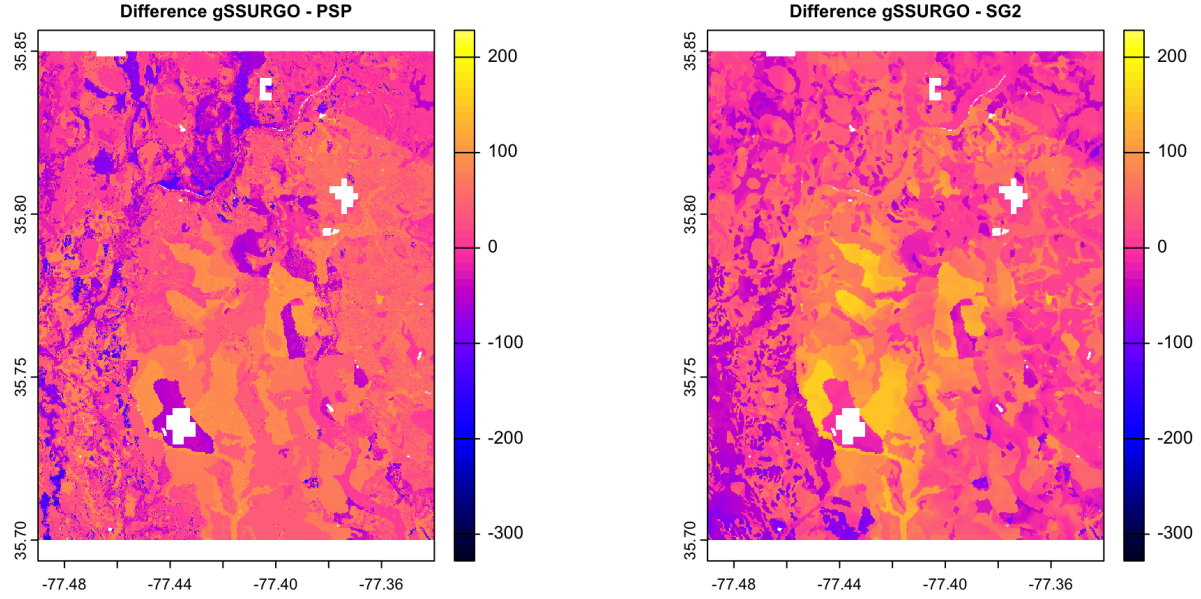


**Figure 58.** Difference between gSSURGO and DSM products, clay %%, 0–5 cm

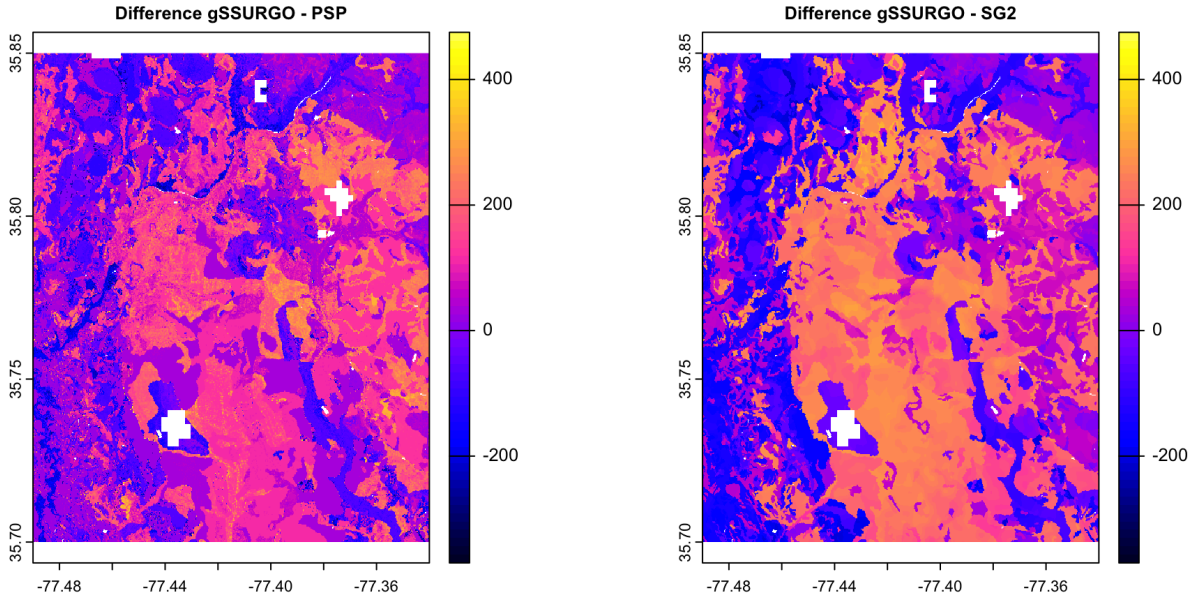


**Figure 59.** Difference between gSSURGO and DSM products, clay %%, 30–60 cm

### 3.2.3 Class maps

Fig. 60 shows the topsoil and subsoil clay concentration, respectively, classified into eight histogram-equalized classes. Class limits for the surface soil in this area are approximately 8.70, 10.33, 11.34, 12.29, 13.79, 15.00, and 17.00%, with the extreme values of 0.50 and 39.06%, and for the subsoil are approximately 15.39, 19.33, 20.288, 22.19, 24.80, 30.64, and 40.20% , with the extreme values of 0.50 and 51.82%

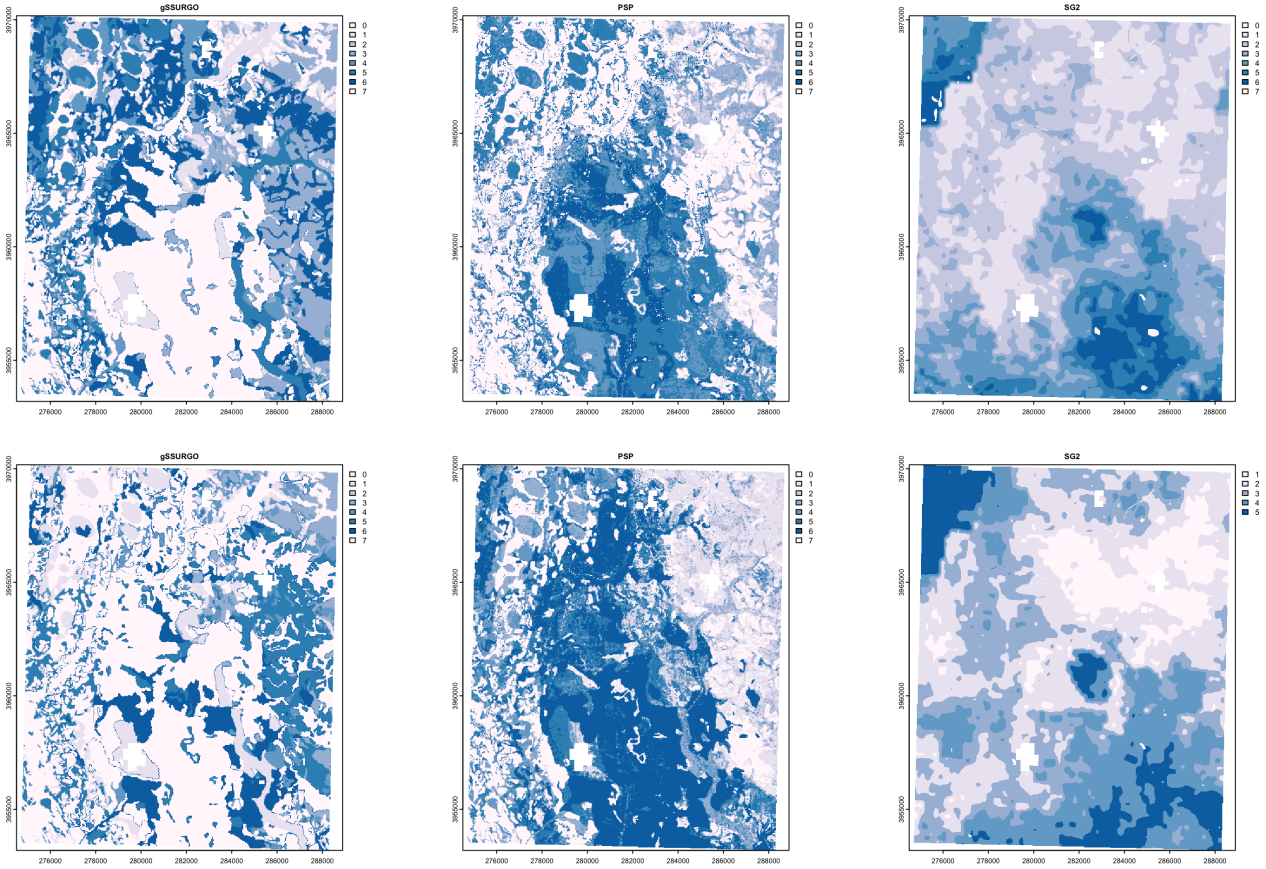


**Figure 60.** clay concentration classes, 0–5 cm (top), 30–60 cm (bottom), central NY, detail. Coordinates are UTM 18N meters

Again, PSP shows fine detail and SG2 is largely unrelated to the actual spatial pattern.

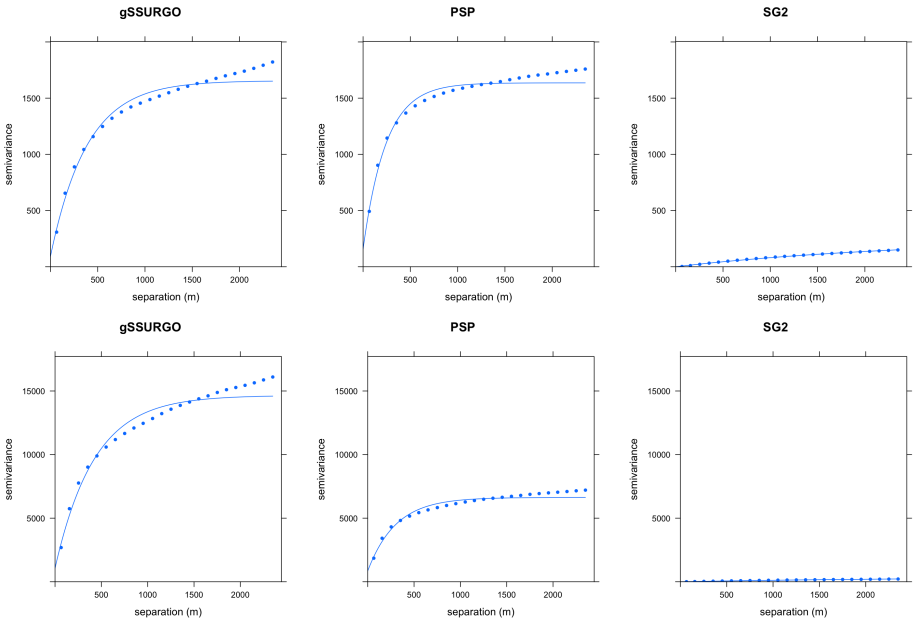


**Figure 61.** Fitted variograms, clay concentration 0–5 cm (top), 30–60 cm (bottom), central NY. Semivariance units $\%\%^2$

| Product | Effective range | Structural Sill | Proportional Nugget |
|---|---|---|---|
| gSSURGO | 1158.00 | 1564.03 | 0.05 |
| SG2 | 7878.00 | 254.82 | 0.00 |
| PSP | 723.00 | 1478.39 | 0.10 |
| **Product** | **Effective range** | **Structural Sill** | **Proportional Nugget** |
| gSSURGO | 1269.00 | 13583.20 | 0.07 |
| SG2 | 8322.00 | 382.64 | 0.00 |
| PSP | 909.00 | 5781.93 | 0.13 |

**Table 17.** Fitted variogram parameters, clay concentration 0–5 cm (top), 30–60 cm (bottom). Effective range in $\mathrm{m}$; structural sill in $\%\%^2$, proportional nugget on $[0 \ldots 1]$

### 3.2.4 Local spatial autocorrelation

The local variograms and their fitted exponential models are shown in Fig. 61. Table 17 shows their statistics.

As in the regional assessment, SG2 has very low sill and long range, i.e., very little local spatial variation. This is only partly due to the lower resolution of SG2. PSP has a shorter range, due to the disaggregation and resulting fine structure, but a lower structural sill, due to the selection of most probable series, rather than the full range of series in gSSURGO.

| product | ai | frac_mn | lsi | shdi | shei |
|---|---|---|---|---|---|
| gSSURGO | 83.524 | 1.039 | 45.685 | 1.914 | 0.920 |
| SG2 | 95.299 | 1.058 | 14.484 | 1.671 | 0.804 |
| PSP | 68.181 | 1.038 | 86.242 | 1.944 | 0.935 |

| product | ai | frac_mn | lsi | shdi | shei |
|---|---|---|---|---|---|
| gSSURGO | 84.501 | 1.039 | 43.053 | 1.779 | 0.855 |
| SG2 | 96.187 | 1.052 | 12.027 | 1.525 | 0.947 |
| PSP | 68.580 | 1.040 | 85.129 | 1.828 | 0.879 |

**Table 18.** Landscape metrics statistics, clay %% 0–5 cm (top); 30–60 cm (bottom). `frac_mn`: Mean Fractal Dimension; `lsi`: Landscape Shape Index; `shdi`: Shannon Diversity; `shei`: Shannon Evenness; `ai`: Aggregation Index

| | gSSURGO | SG2 | PSP |
|---|---|---|---|
| gSSURGO | 0.000 | 0.303 | 0.083 |
| SG2 | 0.303 | 0.000 | 0.325 |
| PSP | 0.083 | 0.325 | 0.000 |

| | gSSURGO | SG2 | PSP |
|---|---|---|---|
| gSSURGO | 0.000 | 1.039 | 0.184 |
| SG2 | 1.039 | 0.000 | 1.011 |
| PSP | 0.184 | 1.011 | 0.000 |

**Table 19.** Jensen-Shannon distance beween co-occurence vectors; 0–5 cm (top); 30–60 cm (bottom)

### 3.2.5 Landscape metrics

Table 18 shows the statistics from the landscape metrics calculations.

The main differences are in the Landscape Shape Index and (to a lesser extent) the Shannon diversities, where SG2 is much simpler than gSSURGO, as expected due to its coarser resolution. PSP is much more complex than gSSURGO due to the disaggregation; whether this is realistic is questionable.

Table 19 shows the Jensen-Shannon distance beween co-occurence vectors of the four products. There is substantial difference between products, especially in the subsoil. The co-occurence patterns of SG2 is somewhat similar to that PSP but quite different from gSSURGO.

## 3.3 Summary (Coastal plain NC)

This property and area are more poorly mapped by DSM than the property and area in the main text. It appears that the covariates used by SG2 and SPCG do not well represent the sedimentary facies that are the main control of particle-size distribution in the coastal plain. Since PSP is based on gSSURGO, it is much closer to gSSURGO, but identifies fine-scale variability that may not be realistic.

## 4 Southwestern Indiana

This area, bounding box (-87 – -86° E), (38–39° N), with Newberry IN (SW of Bloomington) on the NW edge and Brandenburg KY (SW of Louisville) on the SE edge, was selected because of the its interesting combination of geology, physiography, land use and soil characteristics (Fig. 56). The non-soil area near the middle of the tile is Patoka Lake. Fig. 62 shows some features of this area.

The area is dominated by Major Land and Resource Areas (MLRAs) (Natural Resources Conservation Service, 2006) 120B on the west and 122 on the east, with small areas of MLRA 120C and 114B on the north east corner (Reference). The area is in the Highland Rim Section of the Interior Low Plateaus Province of the Interior Plains physiographic region. The boundary between Crawford Upland on the west and Mitchell Karst Plateau on the east divides approximately these two MLRAs. There is an Escarpment Section transitioning between Crawford Upland and Mitchell Karst Plateau. Early and Middle Pennsylvanian and Late Mississippian sedimentary rocks underlie loess, which is typically less than a meter thick. The rocks consist mainly of flat-lying, interbedded sandstone, shale, coal, and siltstone for MLRA 120 and mainly limestone and dolomite for MLRA 122. Bedrock outcrops are exposed along major streams on steep slopes situated between well-defined broad or narrow ridges and floodplains. The major Soil Taxonomy soil orders are *Alfisols*, *Ultisols*, and *Inceptisols* formed on loess, residuum, and alluvial deposits. Alfisols are associated mostly with loess caps occurring on summits, ridges and upper slopes, while Ultisols occur on eroded steep slopes and footslopes where residuum is exposed. Inceptisols occur mostly on floodplains. The land use reflects the broad soil order divisions with pasture occurring on ridges and summits, forest on steep slopes and foot slopes and corn/soybean on floodplains. The dissected landscape with average distances between ridges and floodplains at about 100 to 150 meters combined with the relationships between soil and slope position and land use make this area unique with regard to capturing and modeling soil-landscape and soil property-landscape relationships.

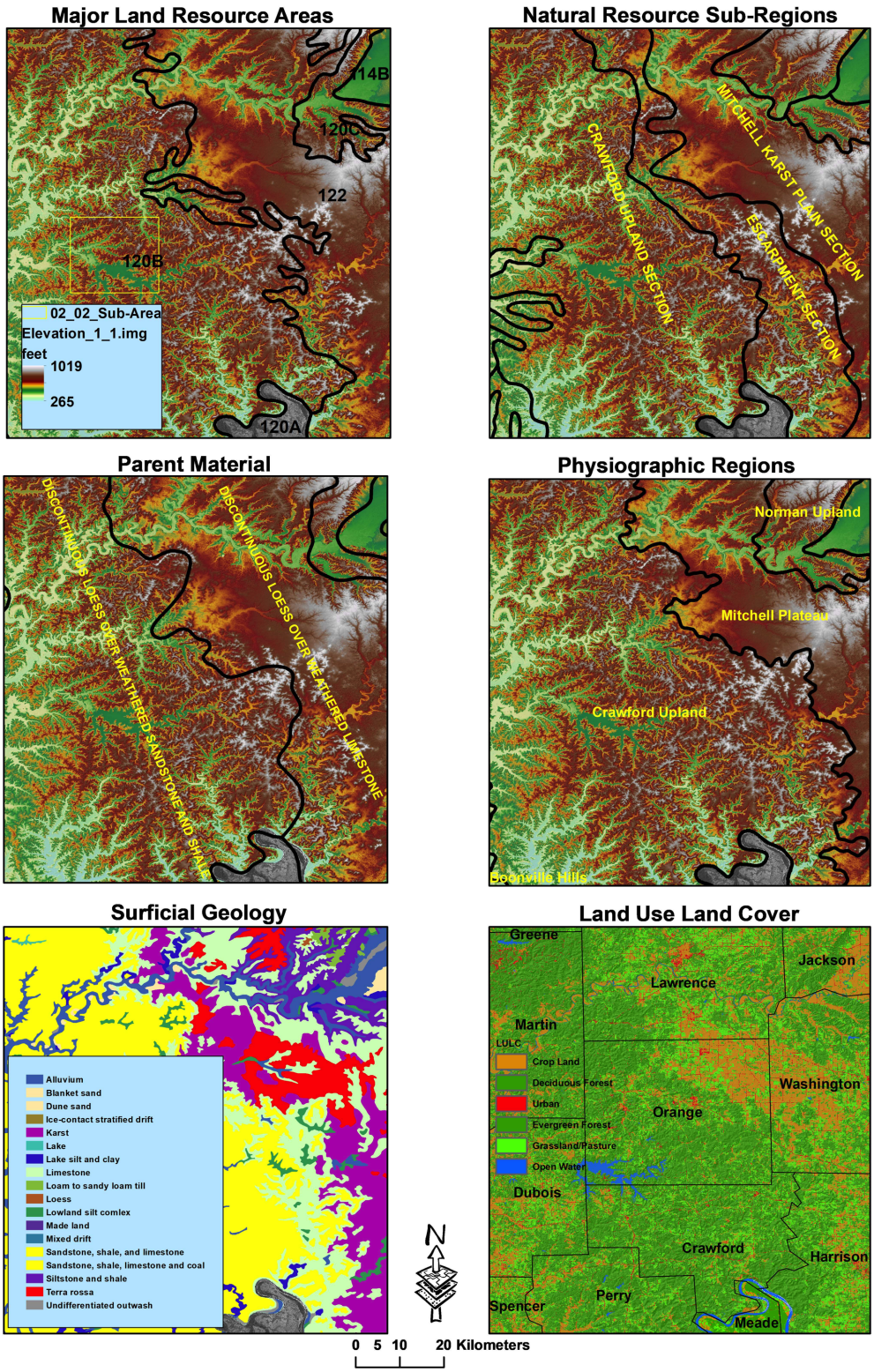


**Figure 62.** Context of the southwest Indiana case study

The property chosen for analysis is soil organic Carbon (SOC) in the two upper GlobalSoilMap layers, namely 0–5 and 5–15 cm, where the great majority of the SOC is concentrated. This property and depths were selected due to their strong relationship with soils, slope position, and land use.

## 4.1 Regional spatial patterns

### 4.1.1 Regional maps

Figs. 63 and 64 show gNATSGO (reference) along with the predictions of SOC concentration in the two depth intervals (0-5 cm, 5–15 cm, respectively) of the other products and figure 65 the pairwise Pearson correlations between all maps. Figs. 66 and 67 shows their histograms, and Fig. 65 the pairwise Pearson correlations between all maps. Figs. 69 and 70 show the differences as maps. Table 20 shows the statistical differences.

| Product | MD | RMSD | RMSD.Adjusted |
|---|---|---|---|
| SG2 | 920.013 | 1021.28 | 443.384 |
| PSP | 363.077 | 602.922 | 481.343 |
| SPCG | 532.275 | 698.439 | 452.217 |

| Product | MD | RMSD | RMSD.Adjusted |
|---|---|---|---|
| SG2 | 1081.177 | 1144.251 | 374.656 |
| PSP | 382.131 | 542.429 | 384.975 |
| SPCG | 1038.522 | 1103.95 | 374.403 |

**Table 20.** Statistical differences between DSM products, SOC %, 0–5 cm (left), 5–15 cm (right)

The DSM products under-predict the SOC compared to gSSURGO on average by 6% and 8.3% for 0–5 cm and 5–15 cm depth increments. SG2 under-predicts the most for both depths with 9.2% and 10.1%, while PSP the least with 3.6% and 3.8%. Similar trends are observed for RMSD, however, the adjusted RMSD decreases to 4.6% and 3.8% for the 0–5 cm and 5–15 cm depth increments, and all DSM products have similar differences with gSSURGO.

The histograms corroborate the observed statistical differences. The DSM shows narrower distribution of SOC values and higher counts of cells with SOC values between 2.0% and 3.5% (SG2) and between 5 and 15% (SPCG and PSP) compared to gSSURGO with SOC values between 8% and 25%. Similar trends are observed for 0-15 cm depth, however the distribution of values for DSM products in comparison to gSSURGO is narrower than for 0–5 cm depth.

The DSM products are poorly correlated with gSSURGO. The highest correlation is observed between gSSURGO and SG2 for 0–5 cm depth increment (r <0.5) and the lowest between gSSURGO and PSP for 5–15 cm depth increment ($r < 0.1$). Also, the DSM products are poorly correlated with each other with correlations of less than 0.1 for SG2 vs PSP (0-5 cm) and close to 0.3 for SG2 vs SPCG (5-15 cm).

The spatial distribution of SOC shows substantial differences between all products for both soil depth increments. gSSURGO shows finer spatial details compared to DSM products. The difference in spatial patterns is in line with the observed histogram distribution which showed narrower ranges in SOC and with statistical metrics which shows DSM under predicting the SOC compared to gSSURGO.

The SOC patterns for DSM under predict the SOC especially for the western portion of the area. SG2 and to a lesser degree SPCG shows somewhat similar pattern distribution with gSSURGO, especially for the 0–5 cm depth increment, while for PSP the pattern appears to be random. The observed pattern for gSSURGO can be related to the Major Land Resources Areas (MLRAs) as shown in Figs. 63 and 64 . The MLRAs are generally differentiated by multiple criteria such as physiography, geology, climate and subsequently soils. The two major MLRA in the area are 120B and 122. Major soils in MLRA 120B are

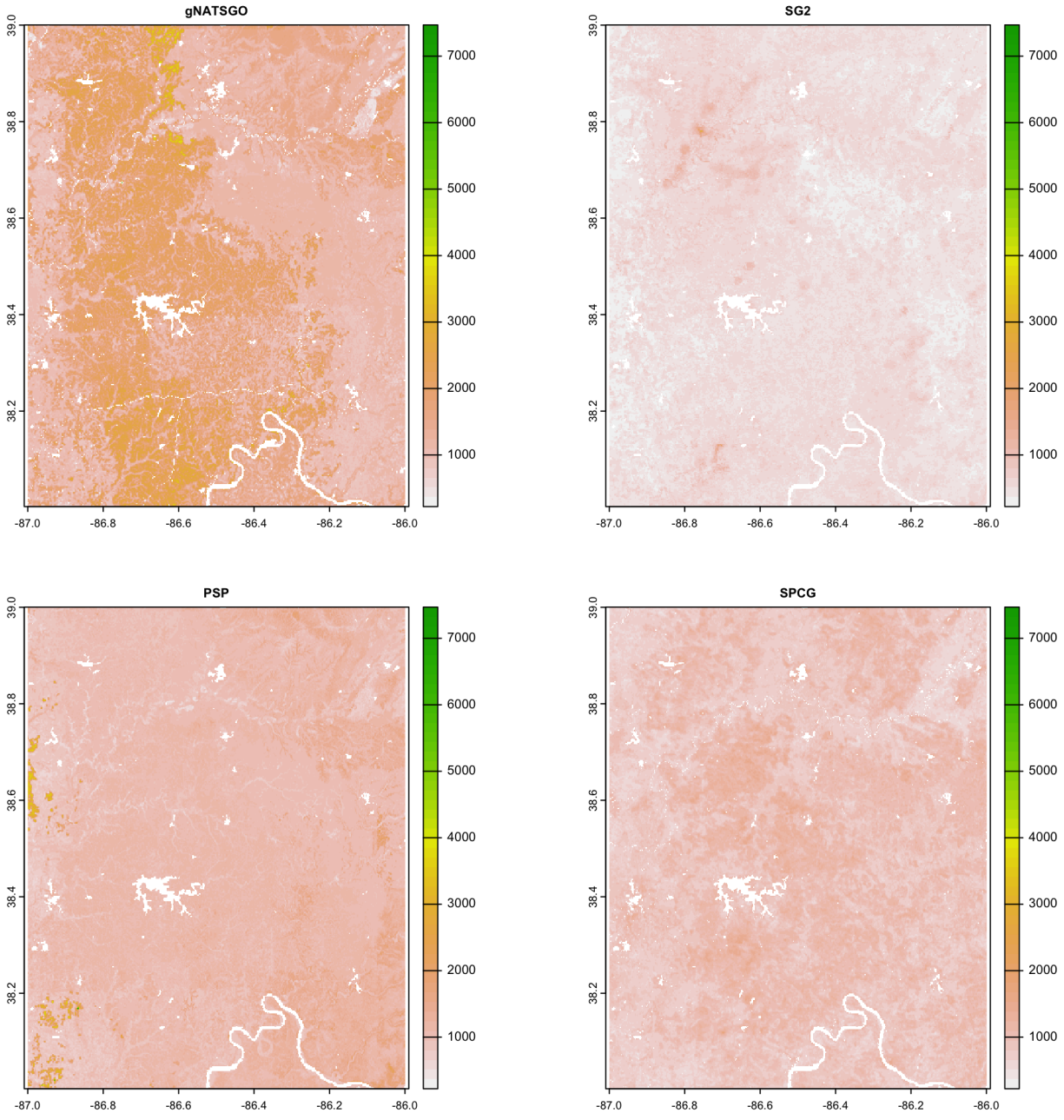


**Figure 63.** 0-5 cm SOC %, according to different DSM products

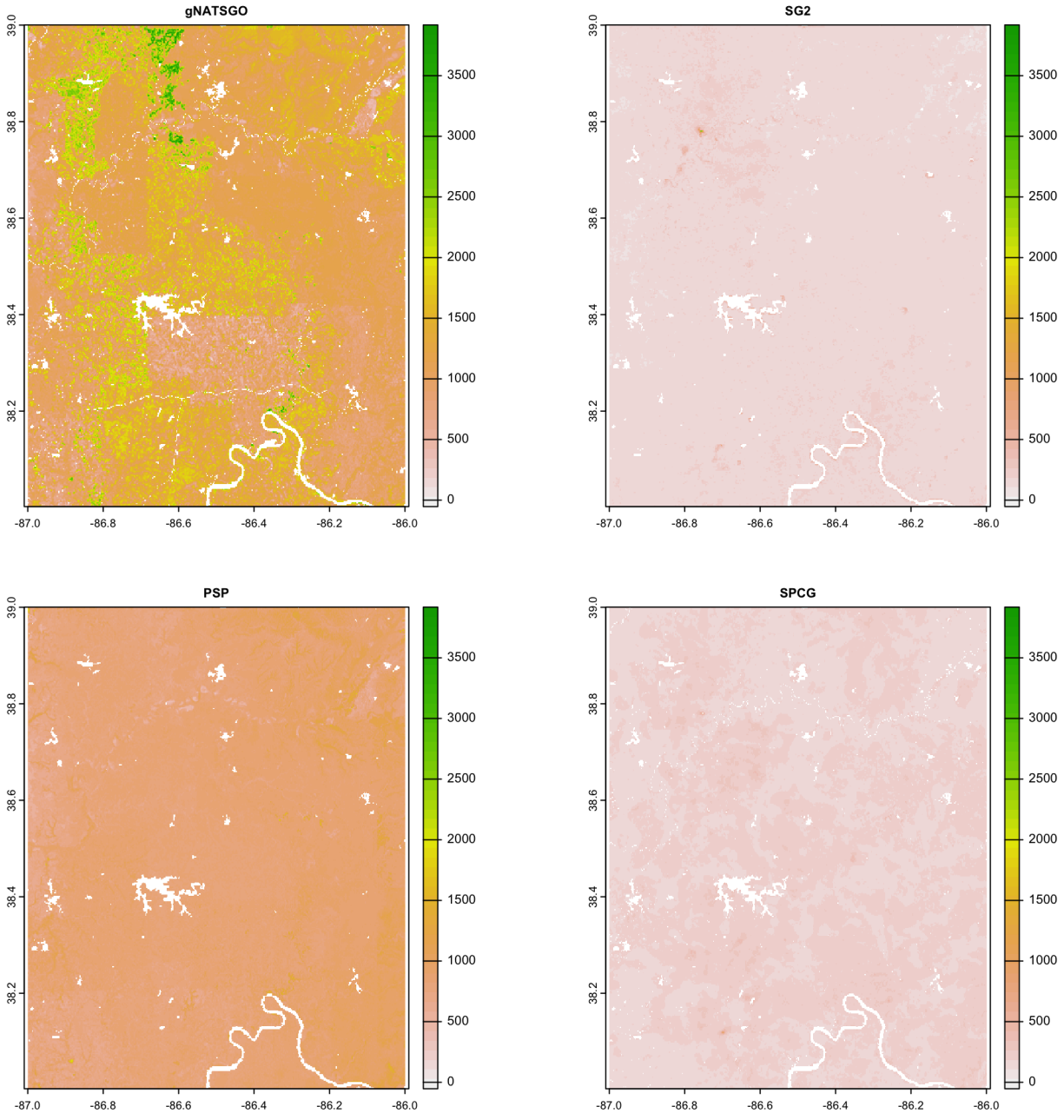


**Figure 64.** 0-15 cm SOC %, according to different DSM products

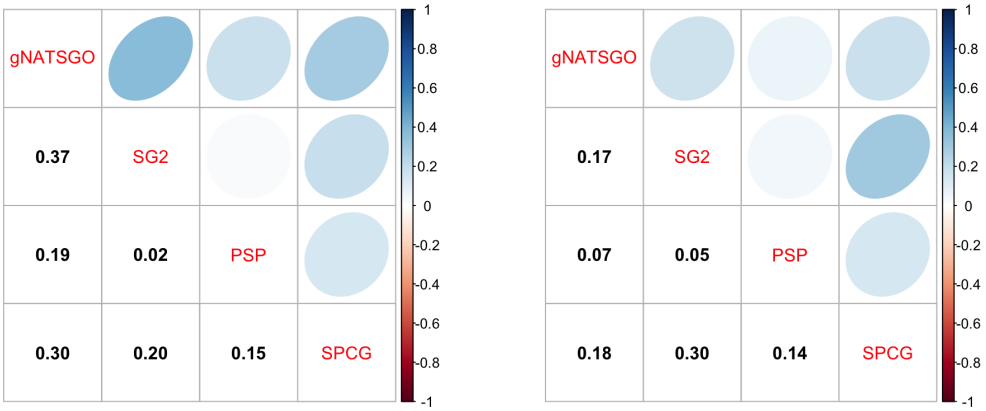


**Figure 65.** Pearson correlations between DSM products, SOC %, 0–5 cm (left), 5–15 cm (right)

formed on discontinuous loess over weathered sandstone and shale. In MLRA 122 soils are formed on loess over limestone or on limestone residuum. Also, the gSSURGO spatial pattern is in line with major land use characteristics of the area, with higher SOC for forested areas for both depth increments. However, for the 5–15 cm depth increment none of the DSM products shows any pattern, while gSSURGO shows artifact related to county administrative boundaries.

The SOC distribution pattern difference between gSSURGO and DSM products reflect the MLRA boundaries and land use for 0–5 cm. depth increment (Fig. 63). However, for 5–15 cm depth increment (Fig. 64), the differences are due to administrative boundaries, i.e., soil surveys of different vintages and with different standards, in addition to land use and MLRA boundaries.

### 4.1.2 Uncertainty

The 5%, 50%, and 95% prediction quantile maps are shown in Figs. 71 (SG2) and 72 (PSP); each figure has its own stretch. The "low", "representative" and "high" values from gNATSGO are shown in Fig. 73

Fig. 74 shows the inter-quartile range 5–95% (IQR), along with the low-high range for gNATSGO, for the two products at the two depth intervals.

The inter-quartile range 5-95% (IQR), an expression of confidence intervals, for SG2 and PSP for both depth increments are relatively homogeneous except for PSP (5-15 cm). The IQR for 0–5 cm is wider for the major part of the area from about 20 to 60% SOC compared to 5–15 cm depth increment from about 3 to 35% SOC. SG2 and PSP for 0–5 cm depth increment is relatively uniform and slightly higher for MLRA 120B, especially for forested areas. PSP IQR for 5–15 cm depth increment

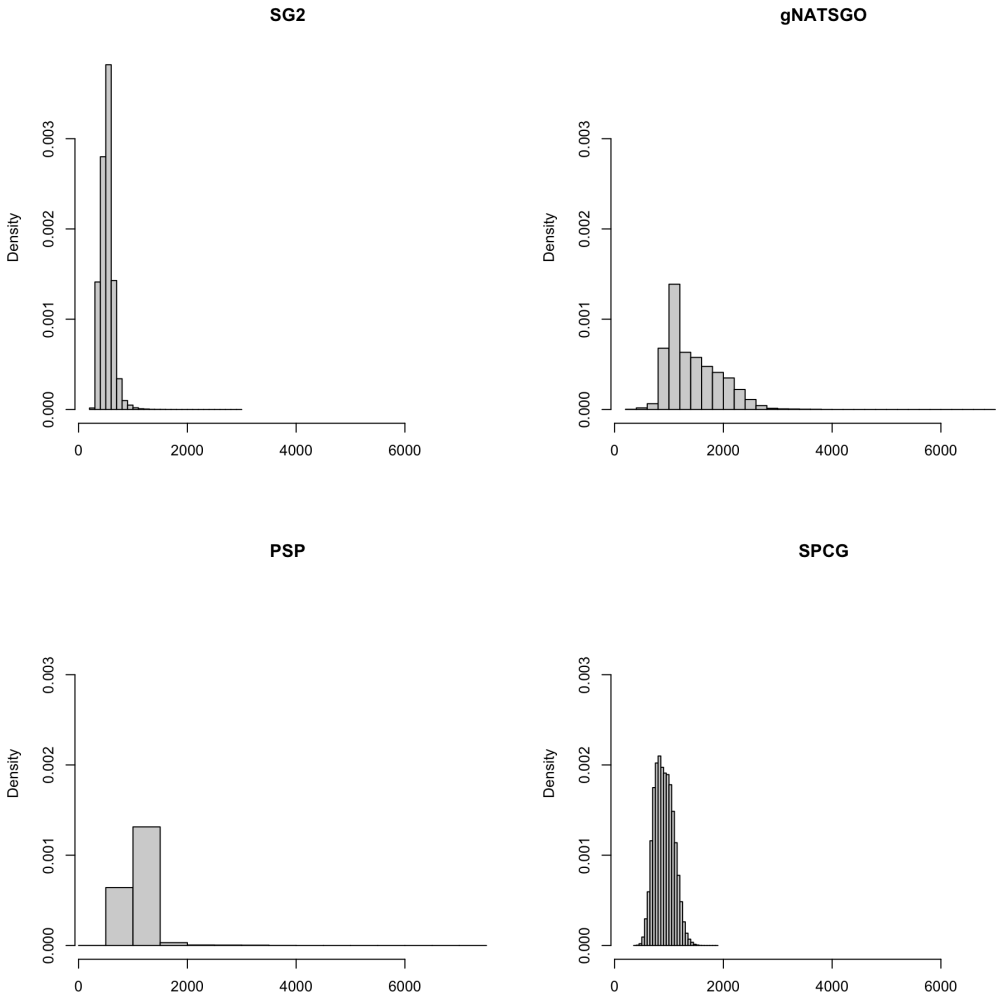


**Figure 66.** Histograms of 0–5 cm SOC %, according to different DSM products

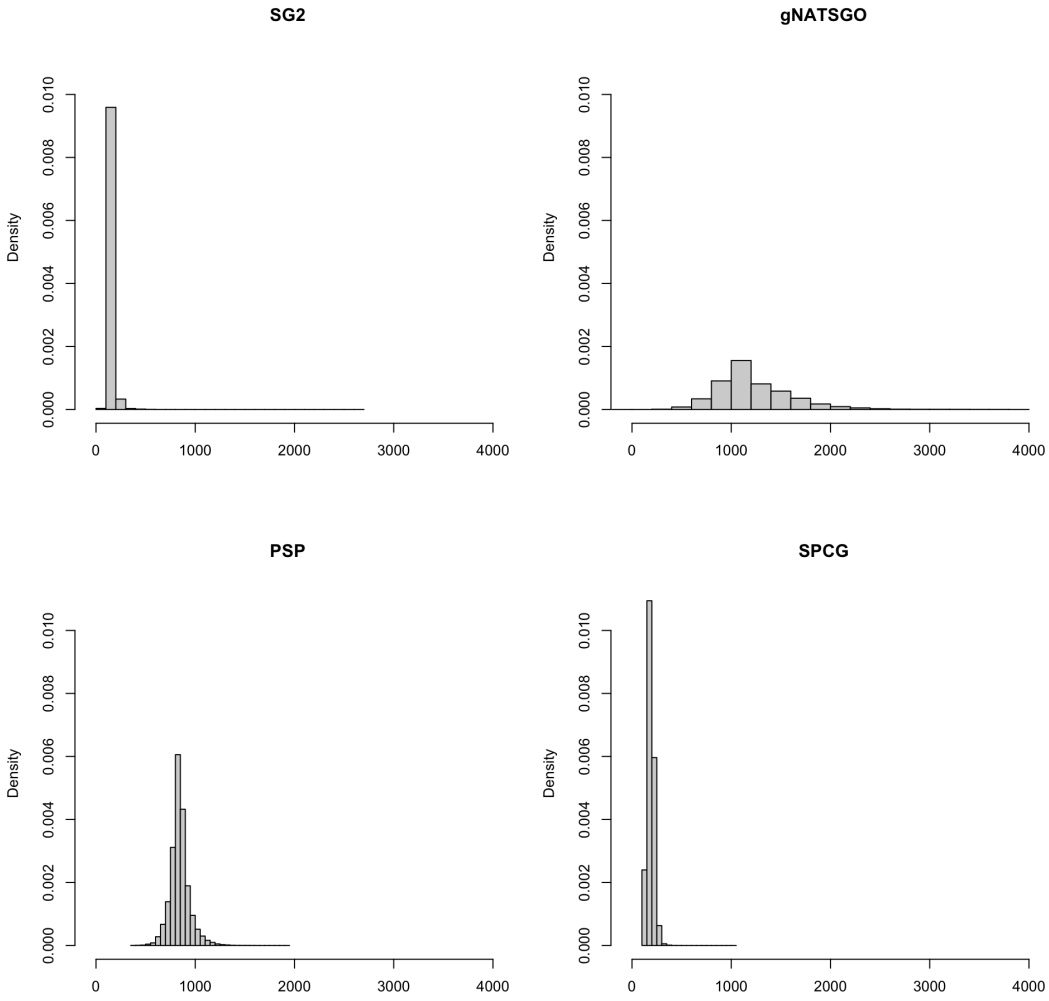


**Figure 67.** Histograms of 5–15 cm SOC %, according to different DSM products

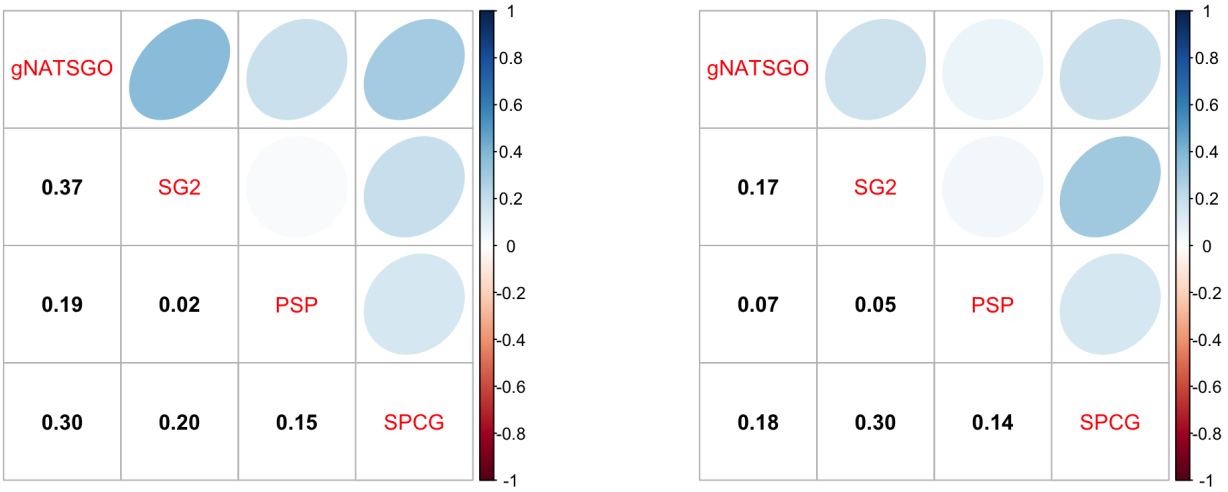


**Figure 68.** Pearson correlations between all products, SOC %%, 0–5 cm (left), 5–15 cm (right)

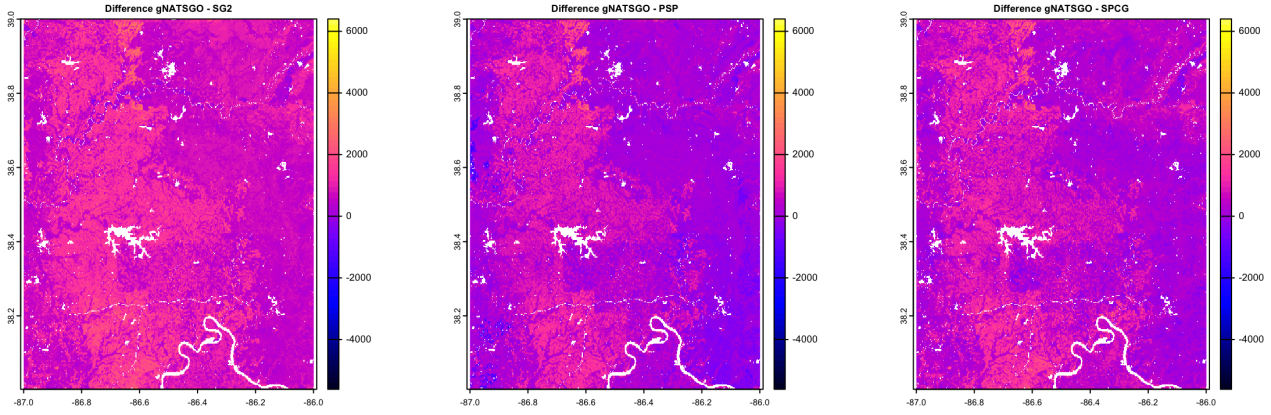


**Figure 69.** Difference between gSSURGO and other DSM products, SOC %, 0–5 cm

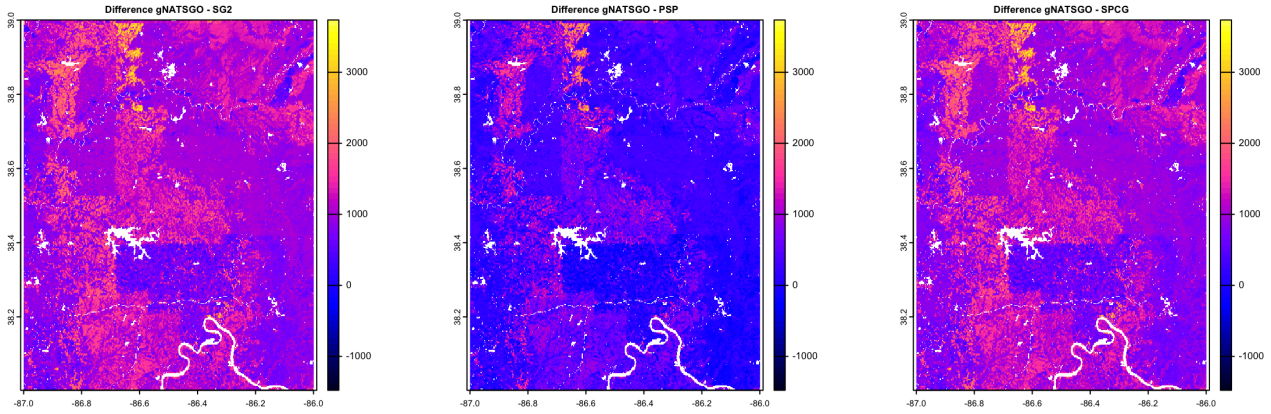


**Figure 70.** Difference between gSSURGO and other DSM products, SOC %, 5–15 cm

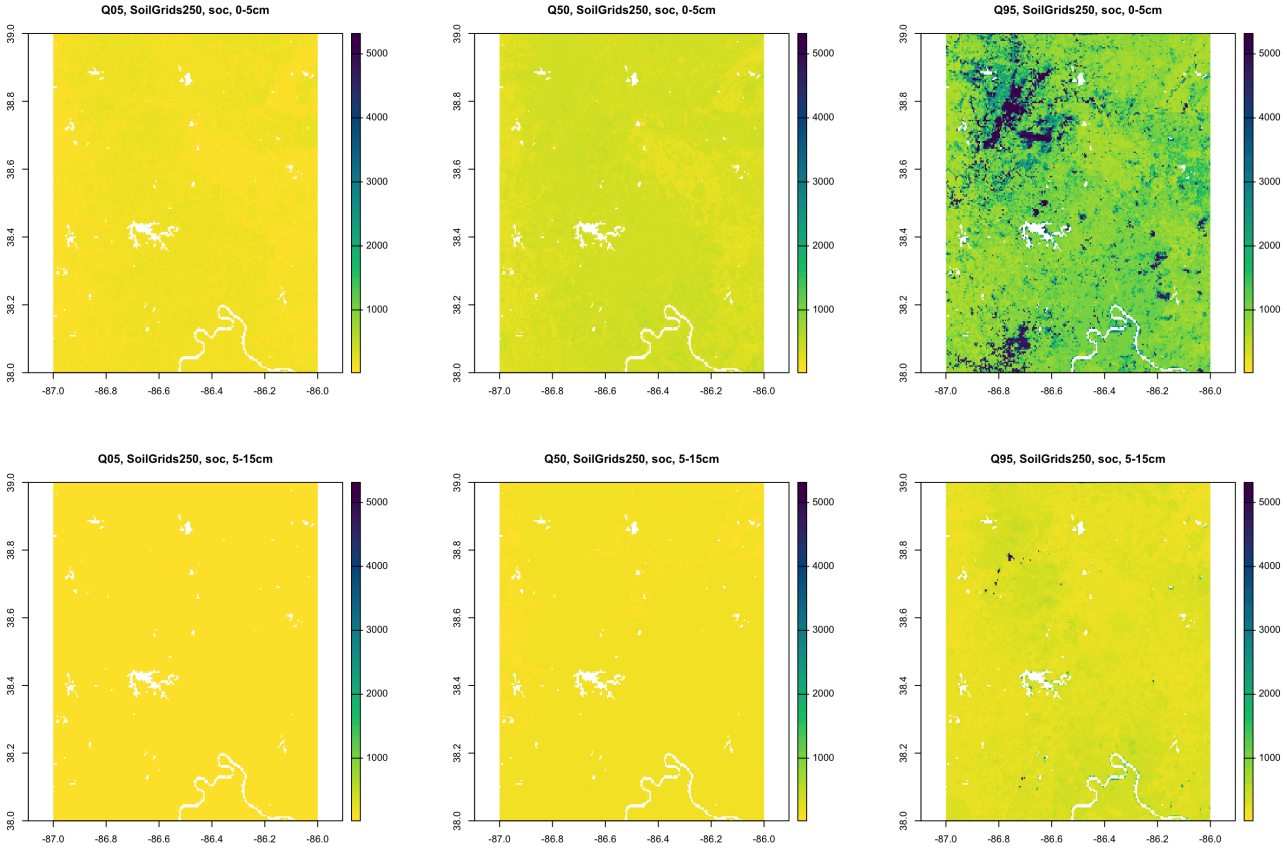


**Figure 71.** Quantiles of the prediction, SG2, SOC %, 0–5 cm (top), 5–15 cm (bottom)

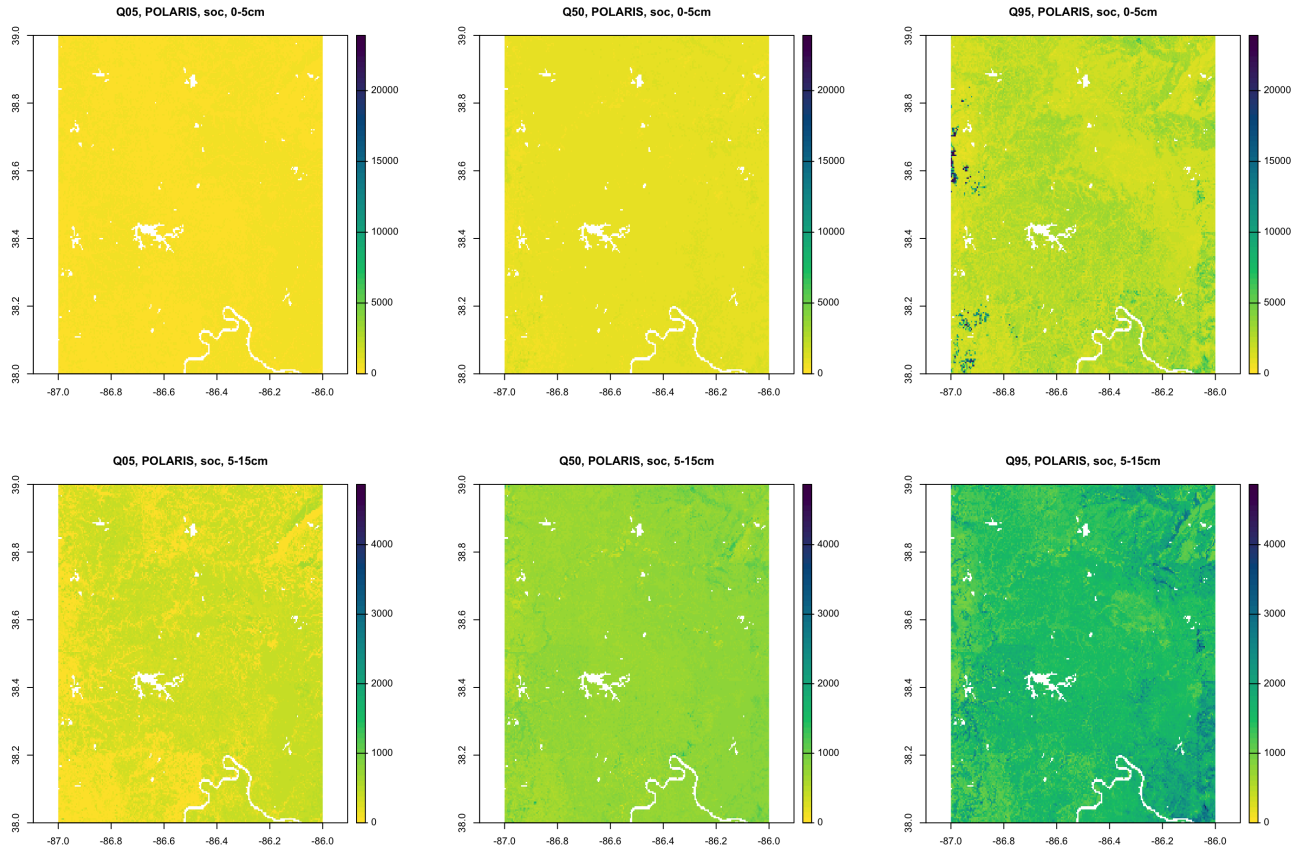


**Figure 72.** Quantiles of the prediction, PSP, SOC %, 0–5 cm (top), 5–15 cm (bottom)

shows more variability and is higher for the easter portion of the area (southern portion of MLRA 122 and southeast portion of MLRA 120C and 114B).

The spatial difference between the IQR from SG2 and PSP for both depth increments shows relatively little variation over the area. However, for 0–5 cm depth increment, the spatial difference is less for small isolated areas on the northwest part compared with the rest. The spatial difference for 5–15 cm depth increment is more variable compared to 0–5 cm, but relatively narrower overall. The relatively narrow distribution of predicted SOC for DSM compared to gSSURGO for both depths, the poor correlations between DSM and gSSURGO and among DSM, and the differences in IQR (SG2 and PSP) point to high uncertainties and different results from all models.

### 4.1.3 Local spatial autocorrelation

The local variograms and their fitted exponential models are shown in Fig. 75. Table 21 shows their statistics.

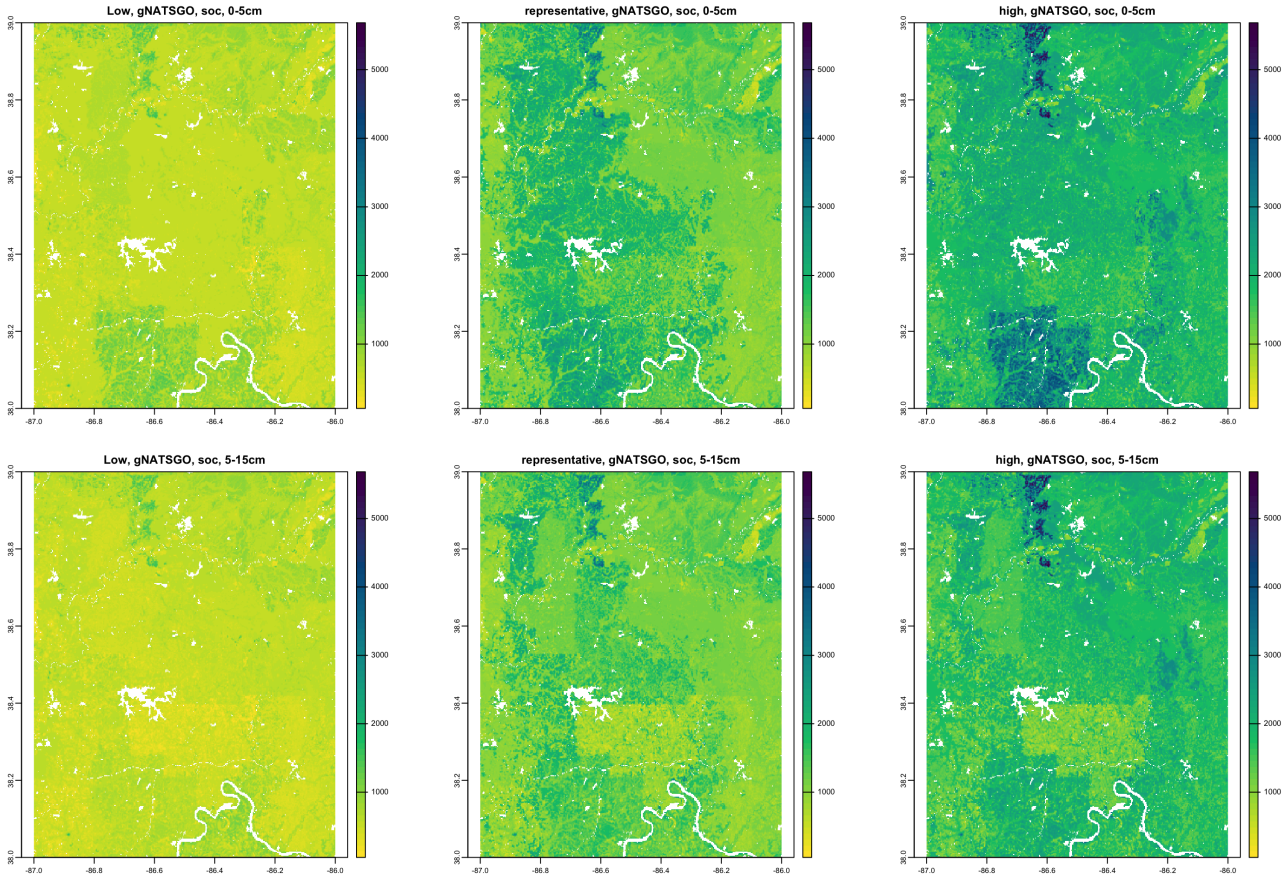


**Figure 73.** Low, representative, high values from gNATSGO, pHx10, 0–5 cm

gSSURGO has the shortest effective range for both topsoil (1611 m) and subsoil (1644 m) SOC indicating a fine-scale structure even at 250 m resolution compared to DSM products. Among DSM products the SPCG has the largest range between 4272 m (0-5 cm) and 5934 (5-15 cm) and PSP the shortest 2046 m for both depth increments showing that the DSM models in general do not capture well the fine-scale variation compared to gSSURGO. The sill for DSM products is particularly small by orders of magnitude compared to gSSURGO. The long range and very low sill indicate a severe smoothing effect, likely due to spatial continuity in the covariates. Another potential explanation is the scale mismatches at the landscape scale between gSSURGO and DSM products regarding the physical and geomorphic principles or processes as represented by soil landscape or covariates. The low proportional nuggets are due to the relatively coarse resolution.

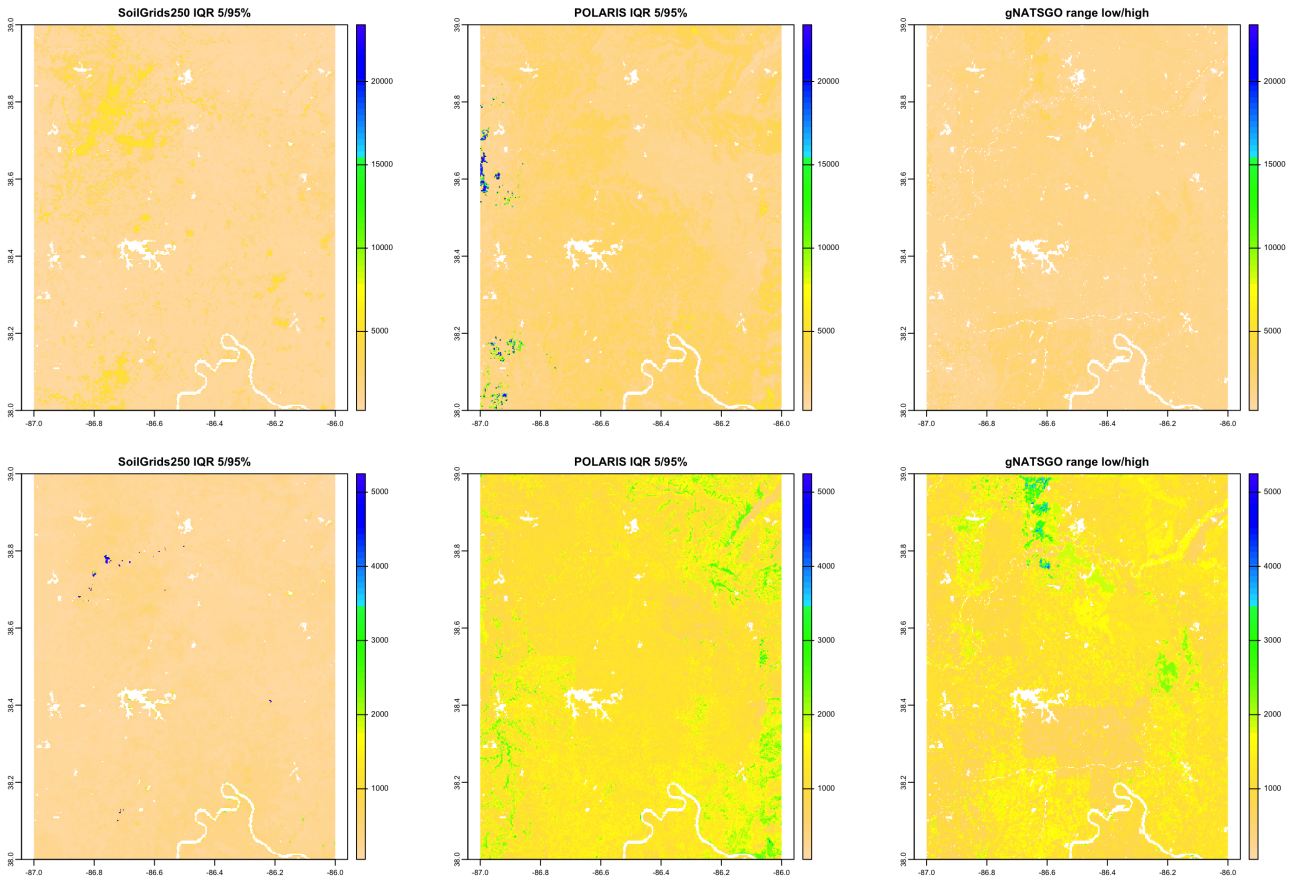


**Figure 74.** Quantiles of the prediction, PSP, SOC %, 0–5 cm (top), 5–15 cm (bottom)

### 4.1.4 Classification

Figs. 76 and 77 shows the topsoil and subsoil SOC, respectively, classified into eight histogram-equalized classes in a 0.2 x 0.2° sub-area, with limits $(-86.8 \cdots -86.7)^\circ$ E, $(34.45 \cdots 38.65)^\circ$ N, located on the west central portion of the study area. The higher SOC are shown in the darker blue. Class limits for the surface soil are approximately 5.5, 7.0, 9.5, 10.5, 11.0, 12.5, and 19.0%, with the extreme values of 3.7 and 25.0%, and for the subsoil are approximately 0.1, 0.7, 1.0, 2.5, 8.0, 9.0, and 12.5%, with the extreme values of 0.0 and 24.0% SOC. The surface layer (0-5 cm) has more SOC compared to the subsurface layer (5-15 cm). The differences in distribution of classes between gSSURGO and other DSM products for both depth increments are obvious. gSSURGO shows more areas in the highest SOC class than the PSP products for both depth increments. Also, gSSURGO shows more details compared to SPCG but is relatively comparable in the level of details with SPCG and PSP. For the subsurface layer, gSSURGO, SPCG and PSP show larger homogeneous areas compared to SG2. However, gSSURGO

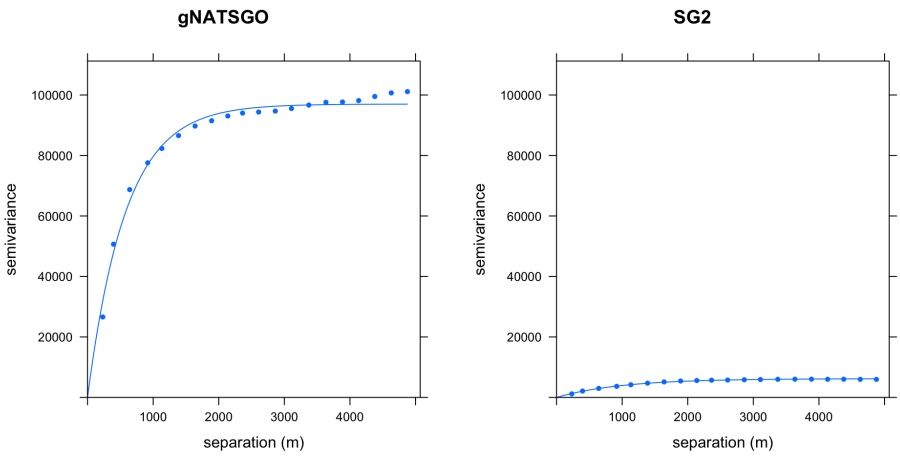
gNATSGO
SG2
semivariance
separation (m)
100000
80000
60000
40000
20000
1000
2000
3000
4000

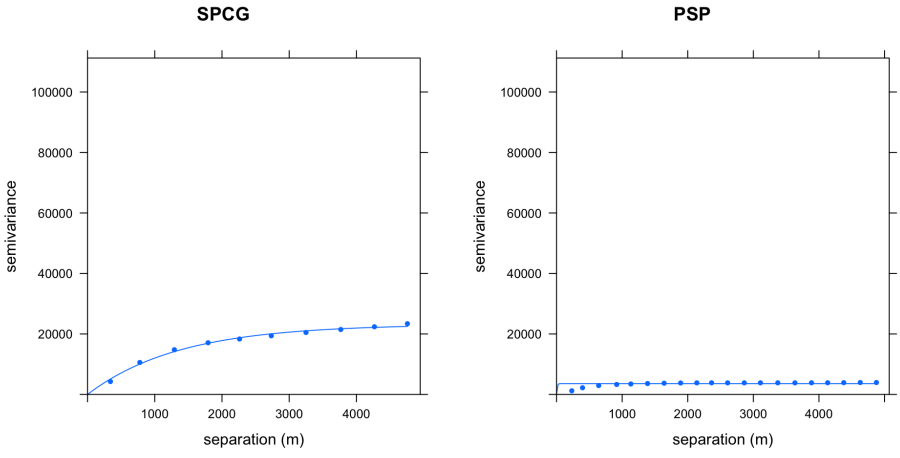
SPCG
PSP
semivariance
separation (m)
100000
80000
60000
40000
20000
1000
2000
3000
4000

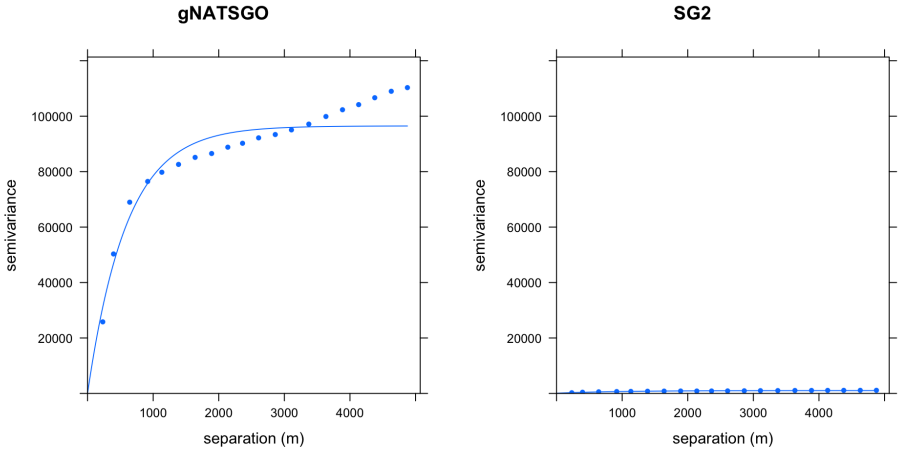
gNATSGO
SG2
semivariance
separation (m)
100000
80000
60000
40000
20000
1000
2000
3000
4000

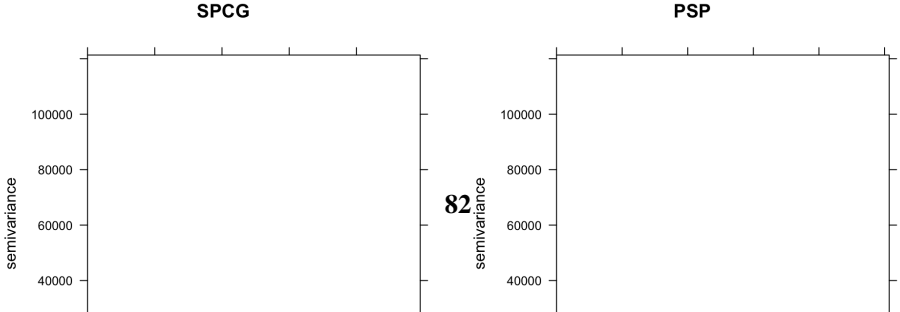
SPCG
PSP
semivariance
separation (m)
100000
80000
60000
40000
1000
2000
3000
4000

| Product | Effective range | Structural Sill | Proportional Nugget |
|---|---|---|---|
| gNATSGO | 1743.00 | 96993.34 | 0.00 |
| SG2 | 2967.00 | 6204.06 | 0.00 |
| SPCG | 4113.00 | 23197.96 | 0.00 |
| PSP | 24.00 | 3516.06 | 0.01 |

| Product | Effective range | Structural Sill | Proportional Nugget |
|---|---|---|---|
| gNATSGO | 1788.00 | 96488.92 | 0.00 |
| SG2 | 2901.00 | 964.91 | 0.07 |
| SPCG | 8505.00 | 1089.67 | 0.00 |
| PSP | 1776.00 | 1125.74 | 0.00 |

**Table 21.** Fitted variogram parameters, SOC concentration 0–5 cm (top), 5–15 cm (bottom). Effective range in $\mathrm{m}$; structural sill in $\%^2$, proportional nugget on $[0 \ldots 1]$

| DSM_products | V_measure | Homogeneity | Completeness |
|---|---|---|---|
| gNATSGO vs. SG2 | 0.0241 | 0.0225 | 0.0258 |
| gNATSGO vs. SPCG | 0.046 | 0.0592 | 0.0376 |
| gNATSGO vs. PSP | 0.1337 | 0.1547 | 0.1178 |
| SPCG vs. SG2 | 0.0227 | 0.0177 | 0.0318 |

| DSM_products | V_measure | Homogeneity | Completeness |
|---|---|---|---|
| gNATSGO vs. SG2 | 0.0036 | 0.0039 | 0.0033 |
| gNATSGO vs. SPCG | 0.0225 | 0.0237 | 0.0214 |
| gNATSGO vs. PSP | 0.0096 | 0.0094 | 0.0098 |
| SPCG vs. SG2 | 0.0124 | 0.0128 | 0.012 |

**Table 22.** V-measure statistics, SOC 0–5 cm (top), 5–15 cm (bottom)

shows also homogeneous areas and classes that are divided based on administrative boundaries as shown on the upper left corner of the area.

### 4.1.5 V-measure

Table 22 shows the statistics from several V-measure comparisons, based on the histogram-equalized class maps. There is no spatial association between the maps with all V-values ranging from 0.0036 (gSSURGO vs SG2; 5–15 cm) to 0.13 gSSURGO vs PSP; 0–5 cm).

Figs. 78 (0-5 cm) and 79 (5-15 cm) show the computed homogeneity and completeness of the SG2 SOC class map, with respect to the gSSURGO SOC class map. Yellow areas in the homogeneity map to the left for 0–5 cm shows that one class

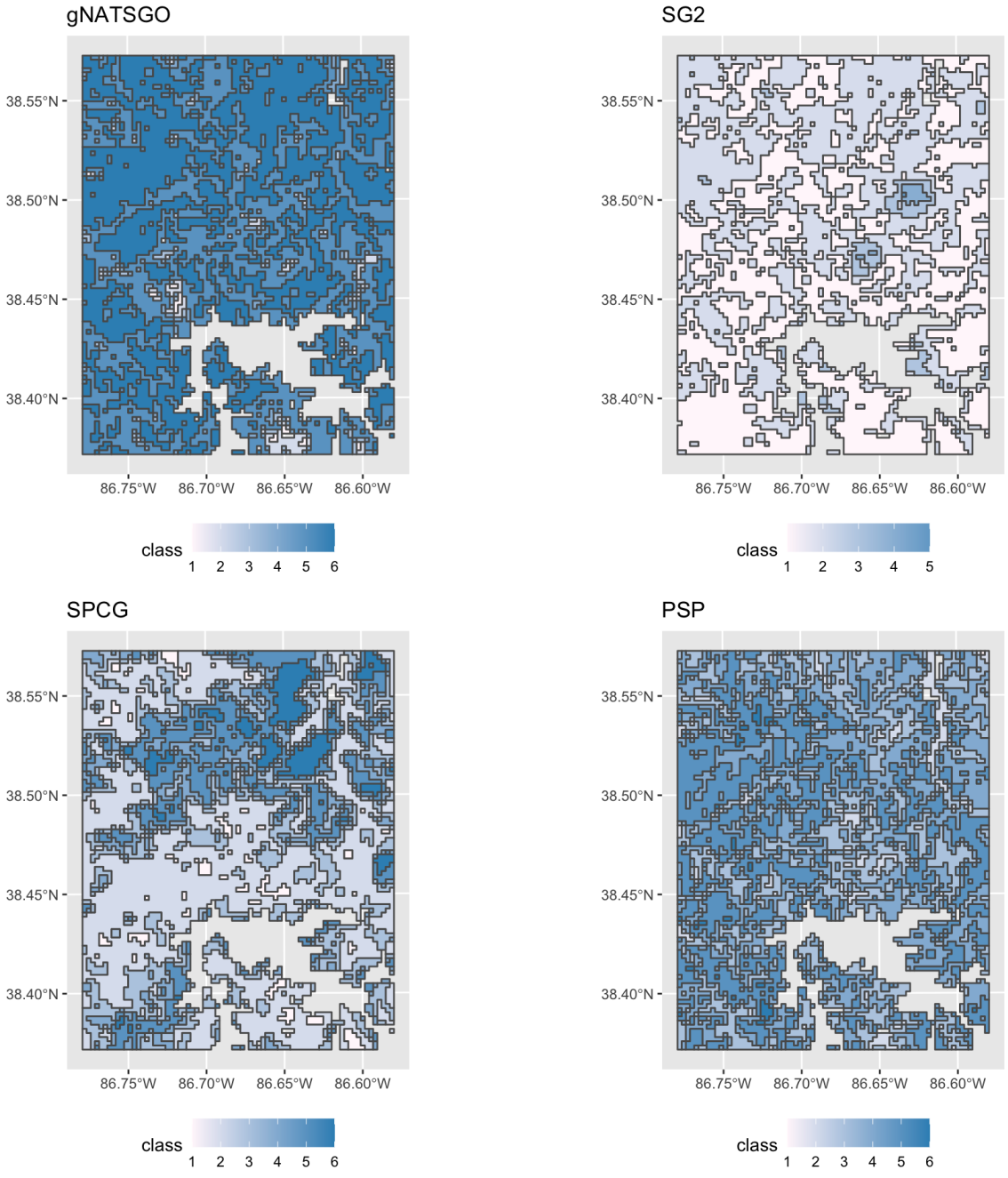


**Figure 76.** SOC classes, 0–5 cm, SW Indiana, detail

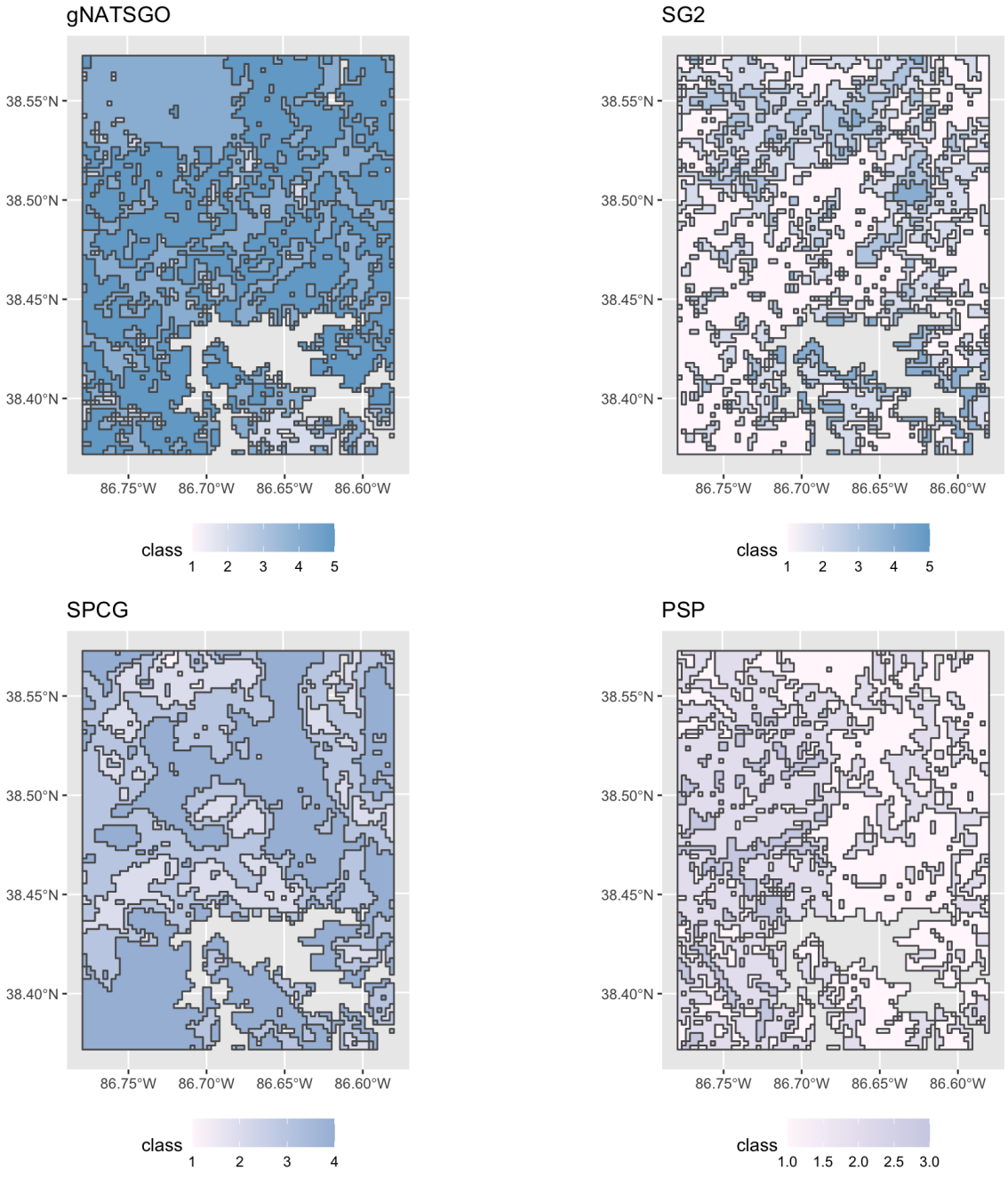


**Figure 77.** SOC classes, 5–15 cm, SW Indiana, detail

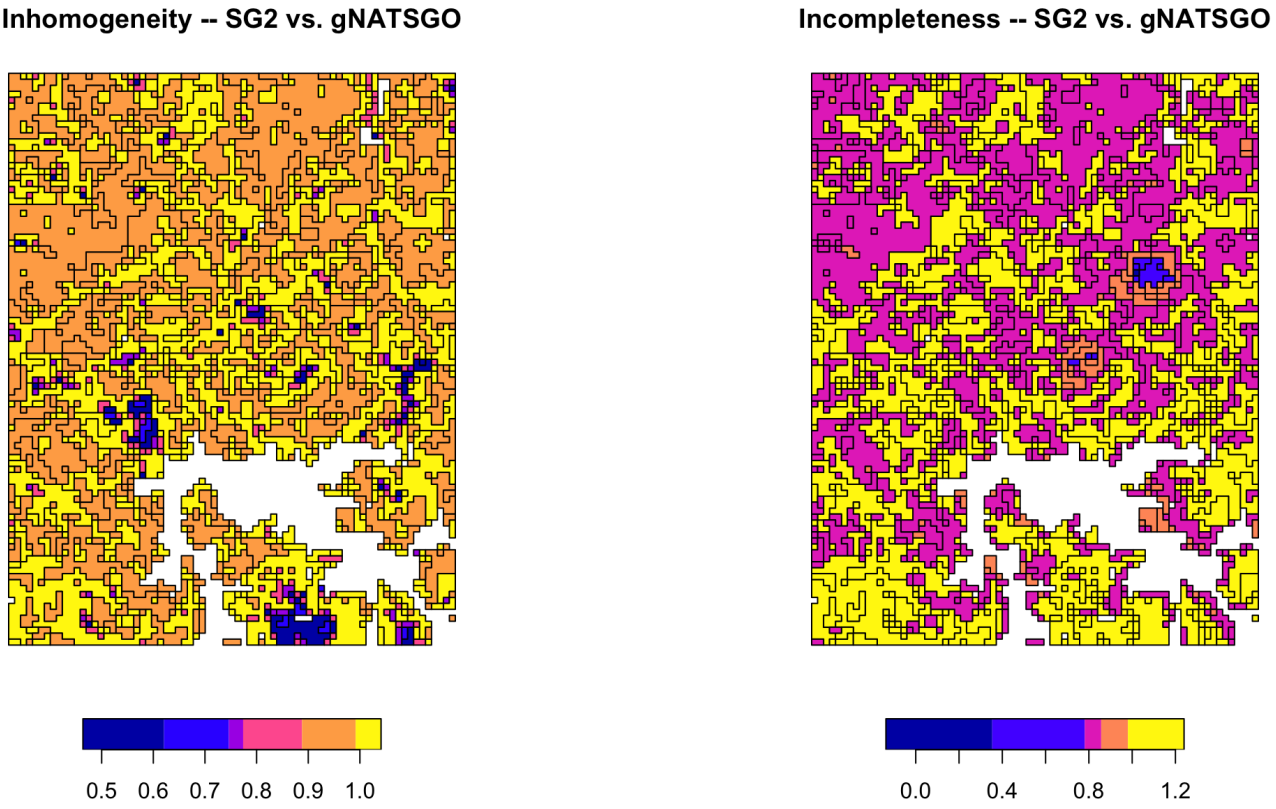


**Figure 78.** Homogeneity (left) and Completeness (right) of the SG2 SOC class map, with respect to gSSURGO SOC class map, 0–5 cm

(zone) predicted by gNATSGO is contained within the SG2 class (region). However, based on completeness, there seem to be more areas where less than one class predicted by SG2 is contained within gSSURGO. However, for the 5–15 cm depth increment both homogeneity and completeness show more disagreements suggesting that compartmentalization of the maps based on classes appear to be random with respect to each other.

### 4.1.6 Landscape metrics

Table 23 shows the statistics from the landscape metrics calculations.

The mean fractal dimension (`frac_mn`), an indication of the landscape complexity, are very similar among all products for both depth increments and close to 1 indicating that all patches are square. However, this indicator, which is scale dependent, could be misleading especially for the gSSURGO that was resampled to 100 m resolution for comparing with other DSM products. Similarly, the landscape shape index (`lsi`), a ratio of total length of edges of units/patches and total area of the landscape, another indicator of landscape complexity shows comparable values between all products, especially for the subsurface layer (5-15 cm), except for SG2 which shows more complexity with higher `lsi` values. The `lsi` for the surface layer (0-5 cm) is higher overall compared to the subsurface layer, with PSP having the highest value (18.5) and SG2 the lowest

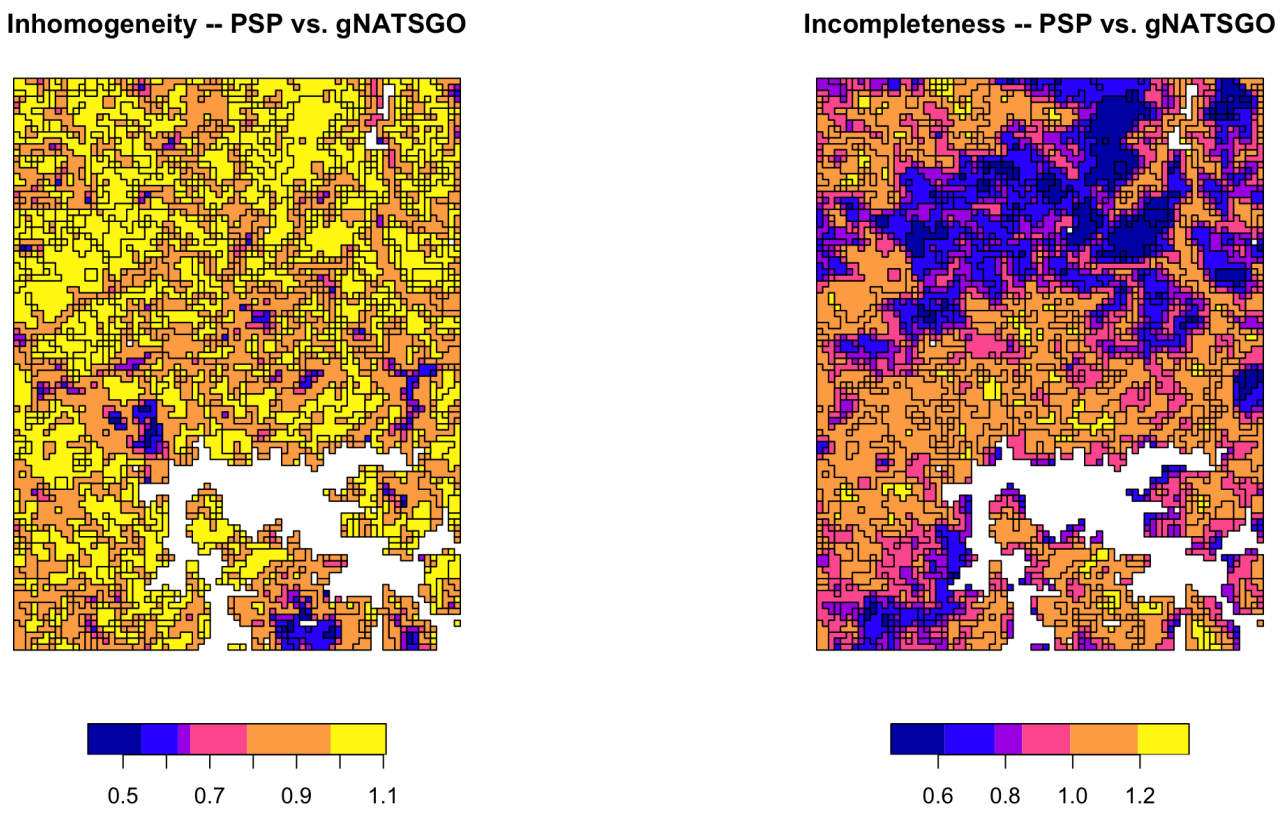


**Figure 79.** Homogeneity (left) and Completeness (right) of the SG2 SOC class map, with respect to gSSURGO SOC class map, 5–15 cm

| product | ai | frac_mn | lsi | shdi | shei |
|---|---|---|---|---|---|
| gNATSGO | 67.649 | 1.029 | 14.826 | 0.948 | 0.529 |
| SG2 | 74.202 | 1.034 | 12.16 | 0.83 | 0.516 |
| SPCG | 64.129 | 1.039 | 16.382 | 1.49 | 0.832 |
| PSP | 55.881 | 1.041 | 19.444 | 1.245 | 0.695 |

| product | ai | frac_mn | lsi | shdi | shei |
|---|---|---|---|---|---|
| gNATSGO | 73.416 | 1.03 | 12.565 | 0.944 | 0.586 |
| SG2 | 66.394 | 1.033 | 15.29 | 1.12 | 0.696 |
| SPCG | 80.907 | 1.041 | 9.68 | 1.045 | 0.754 |
| PSP | 72.854 | 1.04 | 12.685 | 0.903 | 0.822 |

**Table 23.** Landscape metrics statistics, SOC 0–5 cm (top), 5–15 cm (bottom). `frac_mn`: Mean Fractal Dimension; `lsi`: Landscape Shape Index; `shdi`: Shannon Diversity; `shei`: Shannon Evenness; `ai`: Aggregation Index

| | gNATSGO | SG2 | SPCG | PSP |
|---|---|---|---|---|
| gNATSGO | 0.000 | 0.979 | 0.374 | 0.391 |
| SG2 | 0.979 | 0.000 | 0.883 | 0.983 |
| SPCG | 0.374 | 0.883 | 0.000 | 0.203 |
| PSP | 0.391 | 0.983 | 0.203 | 0.000 |

| | gNATSGO | SG2 | SPCG | PSP |
|---|---|---|---|---|
| gNATSGO | 0.000 | 0.560 | 0.705 | 0.919 |
| SG2 | 0.560 | 0.000 | 0.548 | 0.799 |
| SPCG | 0.705 | 0.548 | 0.000 | 1.005 |
| PSP | 0.919 | 0.799 | 1.005 | 0.000 |

**Table 24.** Jensen-Shannon distance beween co-occurence vectors; 0–5 cm (top); 5–15 cm (bottom)

(11.6). Higher values indicate complex boundaries; however, the indicator does not show the spatial pattern of the boundaries and whether or not they represent landscape processes like erosion and depositional processes that dominate at the hillslope scale. Both Shannon diversity (`shdi`) and evenness indices (`shei`) show similar results as `frac_mn` and `lsi`. Despite some differences between products, overall, DSM products perform better regarding `shei`, showing high landscape diversity compared to gSSURGO. However, this particular index does not depend on the number of classes and does not account for spatial contiguity. Both features of this index would affect gSSURGO more than DSM products, especially given the sensitivity or dependence of gSSURGO on soil landscape model and how resampling to 100 m may affect the integrity of the landscape in this area. The average slope length from summit to toeslope in this area is between 100 and 150 m and with multiple map units and soils occurring over this distance. The quantitative similarity comparison based on the Jensen-Shannon distance (Table 24) shows that gSSURGO is different from DSM products for both soil depths. For the surface layer (0-5 cm) PSP and SPCG show a greater degree of similarity between each other and with gSSURGO compared to SG2 that is highly dissimilar with gSSURGO and PSP and SPCG. For the 5–15 cm soil layer all DSM products are dissimilar in relation to each other and gSSURGO.

Table 24 shows the Jensen-Shannon distance beween co-occurence vectors of the four products.

The quantitative similarity comparison based on the Jensen-Shannon distance (Table 24) shows that gSSURGO is different from DSM products for both soil depths. For the surface layer (0-5 cm) PSP and SPCG show a greater degree of similarity between each other and with gSSURGO compared to SG2 that is highly dissimilar with gSSURGO and PSP and SPCG. For the 5–15 cm soil layer all DSM products are dissimilar in relation to each other and gSSURGO.

### 4.2 Local spatial patterns

As previously discussed, the selected area represents an erosion and depositional model with deeper soils on summits followed by eroded steep slopes with shallower soils and floodplains with deeper soils. More importantly, the erosion and depositional processes occur within 100 to 150 m, which challenges the relationship between grid resolution and soil landscape/slope models.

The interest here is to see how well DSM methods at relatively fine resolution reproduce known relations at the local geomorphic level, e.g., hillslopes, transects across valleys with multiple terrace levels, and within farms. It has been claimed

that DSM at 30 m resolution is sufficient for management of, or even within, individual farm fields. The only DSM product which predicts at this resolution is PSP.

We examine this first qualitatively, i.e., by visual inspection, and then quantitatively, mostly following the methods of the regional assessment.

### 4.2.1 Qualitative assessment

Fig. 80 shows the land use land cover and SOC concentration of the 0–5 cm layer (top) and 5–15 cm layer (bottom) for disaggregated PSP and gSSURGO overlain on the original polygons from which it was derived, in a hilly landscape northwest of Lake Patoka, just east of the hamlet of Cuzco, IN. SOC concentrations are shown by the colour, from low (light brown) to high (dark brown).

This figure reveals clear dissimilarities between gSSURGO and DSM products at the landscape scale. The spatial distribution of SOC for both depths for gSSURGO aligns with major landscape positions and their associated vegetation. The higher SOC on the slopes coincides with forest, while lower SOC with summits that are under pasture and floodplains that are under corn and soybean rotation. Contrary to gSSURGO, the spatial distribution of SOC for PSP appears random often showing higher SOC content for floodplains. SG2 and SPGC100 (not shown) showed similar SOC distribution with PSP and with a coarser resolution.

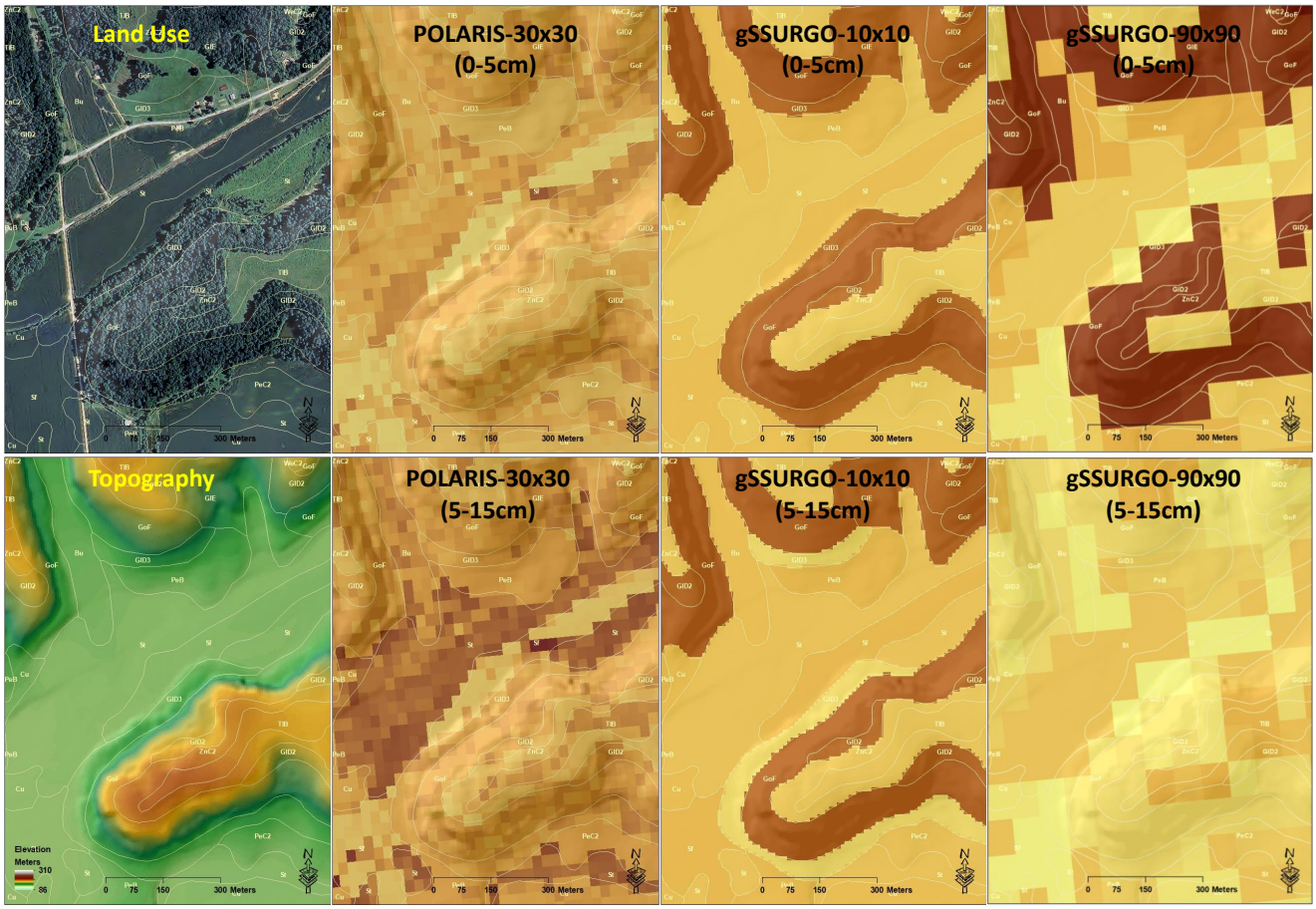


**Figure 80.** Land use, topography, and predicted SOC concentrations at two depth intervals, by PSP and gSSURGO at two resolutions. Centre of image $-86°42'23"\text{E}, 38°28'44"N$

### 4.2.2 Quantitative assessment

To see the fine differences at this high resolution, we concentrate on a $0.15 \times 0.15°$ subtile in an area near Lake Patoka, IN with lower-right corner at $(-86.61°\text{E}, 38.44°\text{N})$ and evaluate SOC, as in the regional assessment (§4.1).

As with the results from the regional pattern comparisons, the DSM products under-predict the SOC compared to gSSURGO. However, the under-predictions are greater at local levels. For example, on average, the DSM products under predict SOC by 10% compared to only 6% at the regional level. Similar trends are observed for each depth increment with under prediction values being larger at local level compared to regional level. Similar trends are observed for RMSD. Even after adjusting for the mean difference (accounting for bias), the under predictions are higher at local level for both depth increments compared to regional levels. The mean adjusted RMSD at local level for 0–5 cm depth increment is 6.1% compared to 4.6% at regional level.

Table 25 shows the statistical differences between gSSURGO (reference) and the DSM products, along with the predictions of SOC in the two depth intervals. Fig. 81 shows the pairwise Pearson correlations between the maps.

At local level, the DSM products are poorly correlated with gSSURGO (Fig. 74). The highest correlation is observed between gSSURGO and PSP for 0–5 cm depth increment ($r < 0.5$). Also, the DSM products are poorly correlated with each other. The spatial distribution of SOC shows substantial differences between all products for both soil depth increments (Fig. 75 and 76). gSSURGO shows finer spatial details compared to DSM products. The gSSURGO pattern are more consistent with the soil-landscape model compared to the DSM products, however, administrative boundaries still compartmentalize the gSSURGO spatial patterns.

| DSM_product | MD | RMSD | RMSD.Adjusted |
|---|---|---|---|
| SG2 | 1242.451 | 1395.062 | 634.439 |
| PSP | 758.777 | 957.032 | 583.239 |

| DSM_product | MD | RMSD | RMSD.Adjusted |
|---|---|---|---|
| SG2 | 1205.983 | 1320.576 | 538.077 |
| PSP | 525.447 | 753.045 | 539.427 |

**Table 25.** Statistical differences between gSSURGO and DSM products, SOC %, 0–5 cm (left), 5–15 cm (right)

Figs. 82 and 83 show gSSURGO (reference) along with the predictions of SOC concentration in the two depth intervals of the DSM products. Figs. 84 and 85 show these as difference maps.

The spatial distribution of differences between gSSURGO and PSP or SPCG shows that both DSM products under predict the SOC, especially for the surface layer (Fig. 77). The under predictions are greater for sloping areas compared to summits and floodplains. Similar trends are observed for the 0-15 cm layer (Fig. 78), however, the differences due to political boundaries (i.e., soil surveys of different vintages and with different standards) are more visible. Additionally, PSP overestimates the SOC, especially for floodplains and to a lesser degree for summits.

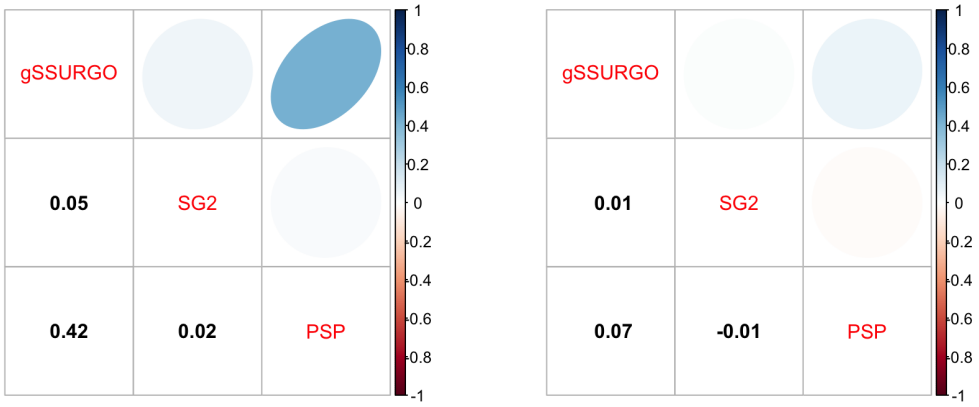


**Figure 81.** Pearson correlations between local products, SOC %, 0–5 cm (left), 5–15 cm (right)

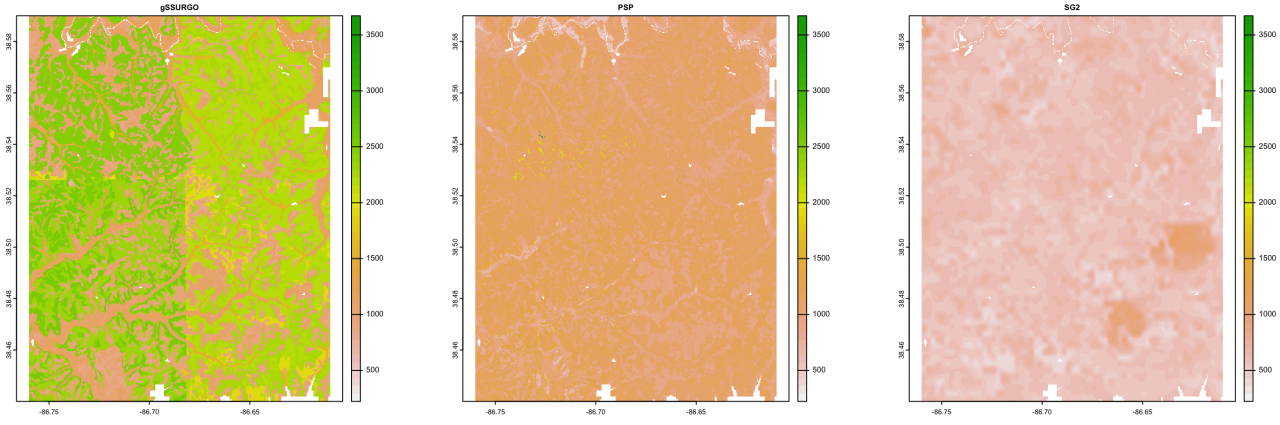


**Figure 82.** Topsoil (0-5 cm) SOC %, according to gSSURGO and DSM products

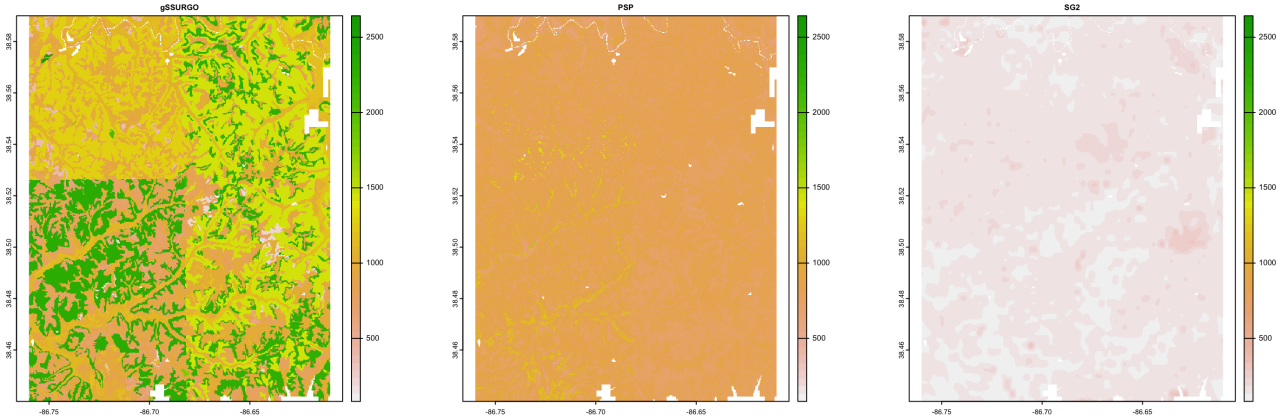


**Figure 83.** Subsoil (5-15 cm) SOC %, according to gSSURGO and DSM products

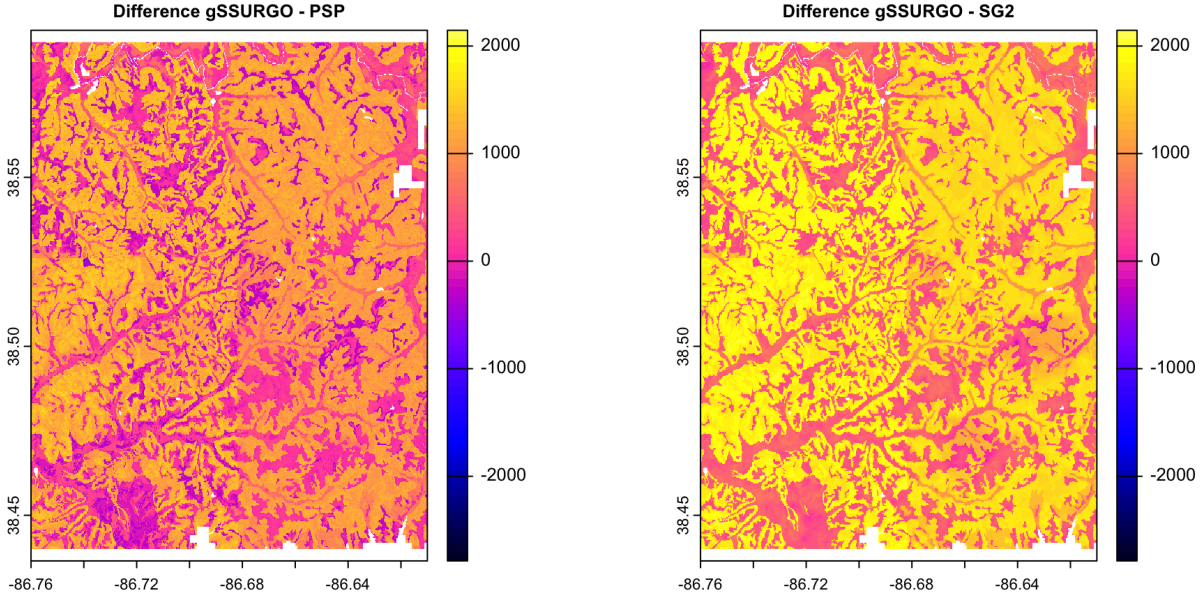


**Figure 84.** Difference between gSSURGO and DSM products, SOC %, 0–5 cm

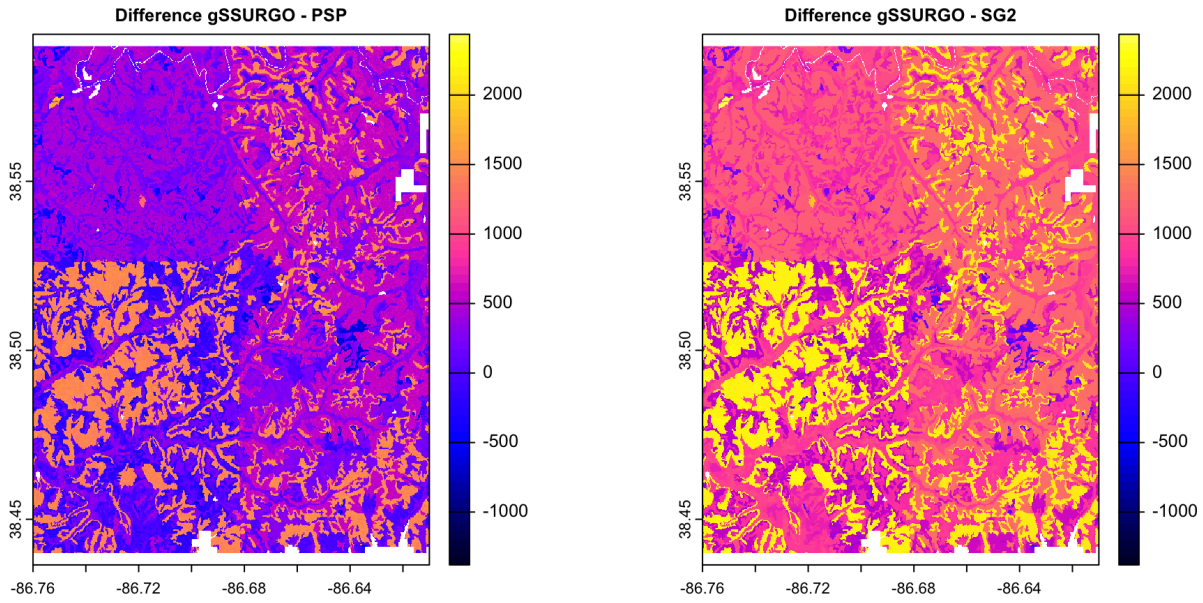


**Figure 85.** Difference between gSSURGO and DSM products, SOC %, 5–15 cm

### 4.2.3 Class maps

Fig. 86 shows the topsoil and subsoil SOC, respectively, classified into eight histogram-equalized classes. Class limits for the surface soil in this area are approximately 5.56, 6.08, 8.85, 10.26, 11.26, 12.63, 22.04 with the extreme values of 3.44 and 34.24 %, and for the subsoil are approximately 1.42, 1.61, 7.29, 8.20, 8.72, 10.15, 14.14 with the extreme values of 1.00 and 25.62 %. The SOC content decreases from surface to sub-surface across all classes. gSSURGO and PSP maintain overall a higher number of classes compared to SG2. However, the number of classes with lower SOC values is higher for PSP compared to gSSURGO, while SG2 has not only the lowest number of classes but also the classes with the lowest SOC content. The spatial patterns of SOC classes show that DSM products overall underestimate the SOC compared to gSSURGO.

### 4.2.4 Local spatial autocorrelation

The local variograms and their fitted exponential models are shown in Fig. 87. Table 26 shows their statistics. For the surface layer (0-5 cm) PSP has the shortest range (375) compared to gSSURGO (2400 m) and SG2 (2196 m). However, the structural sill for PSP (14,346.98) is twice as big compared to SG2 (7064.98 m). For the subsurface layer (5-15 cm) the sill for gSSURGO and PSP are comparable (399 vs 336) but much less compared to SG2 (1632 m). Also, the structural sill is the highest for gSSURGO (220575 m). Different from the regional comparisons, the variogram parameters offer a complex picture of smoothing effects (long range and low sill) and scale versus grid resolution mismatches particularly at the soil landscape.

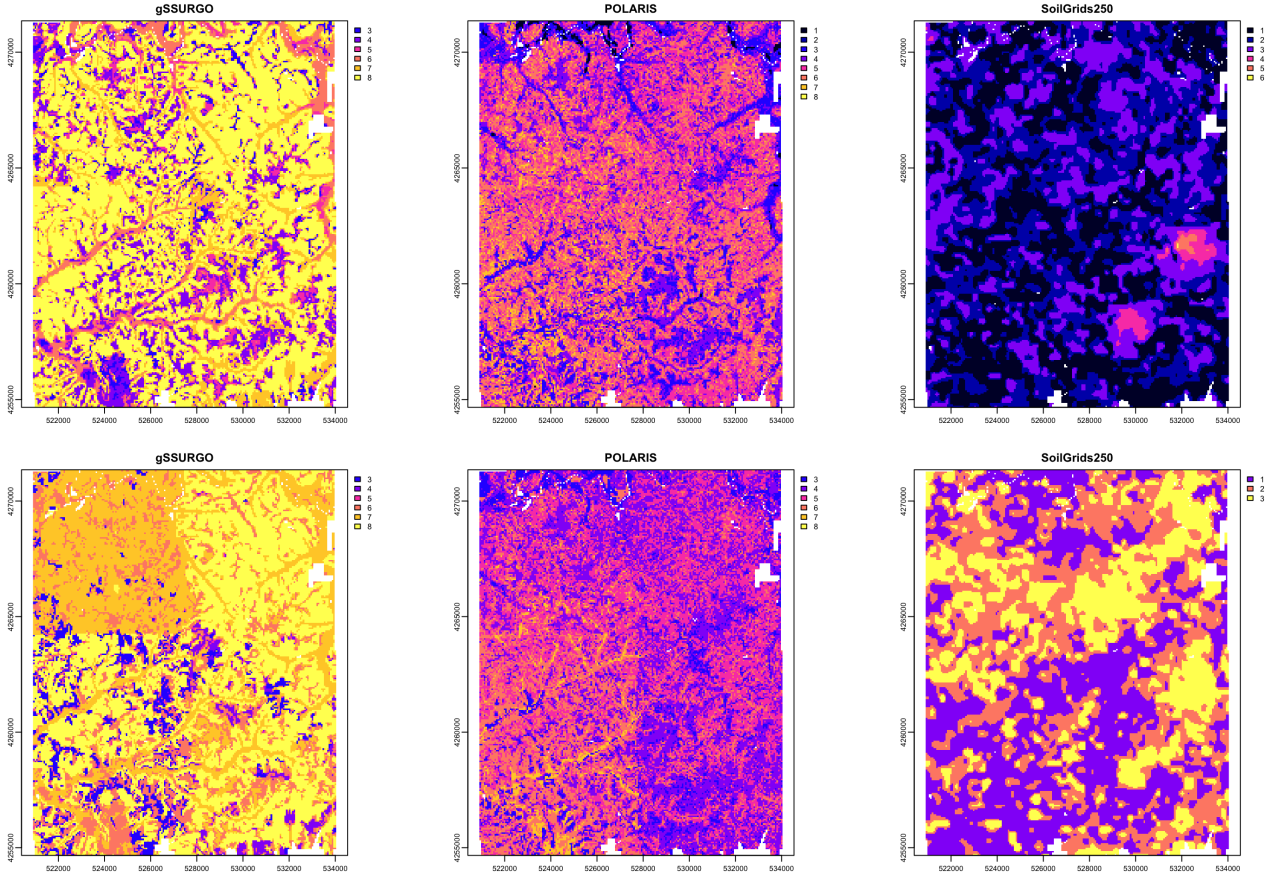


**Figure 86.** SOC classes, 0–5 cm (top), 5–15 cm (bottom), Indiana, detail. Coordinates are UTM 16N meters

| Product | Effective range | Structural Sill | Proportional Nugget |
|---|---|---|---|
| gSSURGO | 2400.00 | 0.00 | |
| SG2 | 2196.00 | 7064.95 | 0.00 |
| PSP | 375.00 | 14346.98 | 0.19 |

| Product | Effective range | Structural Sill | Proportional Nugget |
|---|---|---|---|
| gSSURGO | 399.00 | 220575.06 | 0.02 |
| SG2 | 1632.00 | 426.24 | 0.00 |
| PSP | 336.00 | 3798.49 | 0.22 |

**Table 26.** Fitted variogram parameters, SOC 0–5 cm (top), 5–15 cm (bottom). Effective range in $\mathrm{m}$; structural sill in $(\%x10)^2$, proportional nugget on $[0 \ldots 1]$

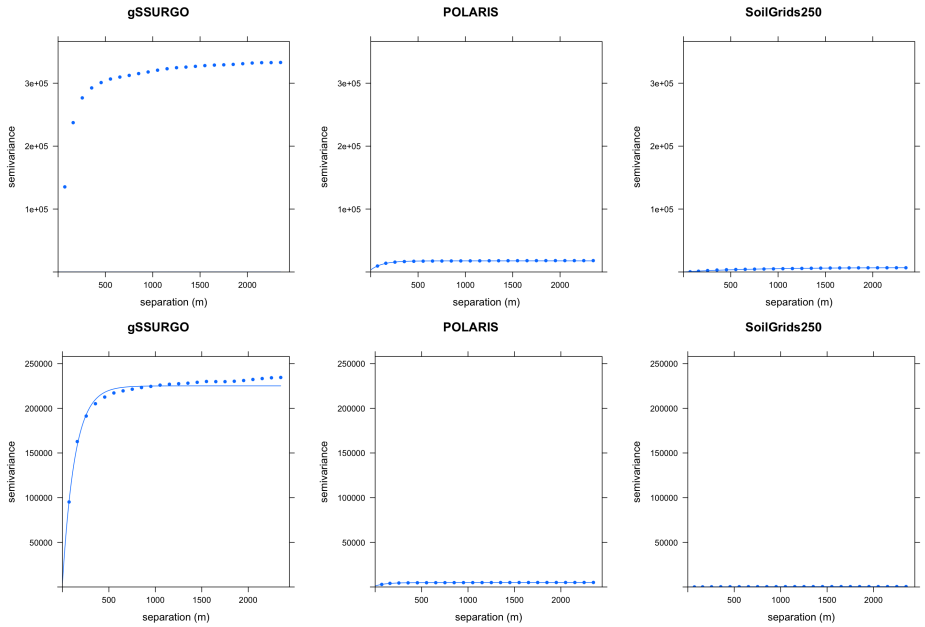


**Figure 87.** Fitted variograms, SOC 0–5 cm (top), 5–15 cm (bottom), Indiana. Semivariance units $(\%x10)^2$

| product | ai | frac_mn | lsi | shdi | shei |
|---|---|---|---|---|---|
| gSSURGO | 76.610 | 1.051 | 63.755 | 1.483 | 0.828 |
| SG2 | 92.809 | 1.058 | 20.968 | 1.152 | 0.643 |
| PSP | 56.027 | 1.052 | 117.986 | 1.494 | 0.718 |

| product | ai | frac_mn | lsi | shdi | shei |
|---|---|---|---|---|---|
| gSSURGO | 81.699 | 1.050 | 50.284 | 1.330 | 0.742 |
| SG2 | 93.956 | 1.056 | 17.869 | 1.082 | 0.985 |
| PSP | 61.331 | 1.047 | 103.958 | 1.327 | 0.741 |

**Table 27.** Landscape metrics statistics, SOC 0–5 cm (left); 5–15 cm (right). `frac_mn`: Mean Fractal Dimension; `lsi`: Landscape Shape Index; `shdi`: Shannon Diversity; `shei`: Shannon Evenness; `ai`: Aggregation Index

### 4.2.5 Landscape metrics

Table 27 shows the statistics from the landscape metrics calculations.

As with the regional scale, the mean fractal dimension `frac_mn` are very similar among all products for both depth increments and close to 1 indicating a complex landscape with almost all patches being square (Table 27). The indicator is scale dependent, which could be more consequential for resampled gSSURGO at 100 m for this landscape. The mean fractal dimension `lsi` values were higher for PSP for both soil layers indicating higher complexity. However, the complexity was not associated with soil landscape patterns; it rather reflects the PSP approach to predicting soil properties and note necessarily landscape processes like erosion and deposition that are major drivers in these landscapes. Both Shannon diversity `shei` and evenness indices `ai` show similar results as `frac_mn` and `lsi`, especially for PSP versus gSSURGO.

| | gSSURGO | SG2 | PSP |
|---|---|---|---|
| gSSURGO | 0.000 | 0.434 | 0.251 |
| SG2 | 0.434 | 0.000 | 0.458 |
| PSP | 0.251 | 0.458 | 0.000 |

| | gSSURGO | SG2 | PSP |
|---|---|---|---|
| gSSURGO | 0.000 | 1.225 | 0.436 |
| SG2 | 1.225 | 0.000 | 1.285 |
| PSP | 0.436 | 1.285 | 0.000 |

**Table 28.** Jensen-Shannon distance beween co-occurence vectors; 0–5 cm (left); 5–15 cm (right)

The quantitative similarity comparison based on the Jensen-Shannon distance (Table 28) shows that gSSURGO and PSP are more similar compared to gSSURGO versus SG2 for both soil layers. PSP and SG2 are dissimilar for the 5–15 cm soil layer.

Table 28 shows the Jensen-Shannon distance beween co-occurence vectors of the four products. The quantitative similarity comparison based on the Jensen-Shannon distance (Table 28) shows that gSSURGO and PSP are more similar compared to gSSURGO versus SG2 for both soil layers. PSP and SG2 are dissimilar for the 5–15 cm soil layer.

### 4.3 Summary (SW Indiana)

We compared the most recent and widely used DSM grid-based products (PSP, SG2 and SPCG) with gSSURGO polygon-based maps using quantitative and qualitative metrics. The quantitative analysis showed that the DSM products overall generated narrower ranges for the SOC and decreased the spatial variability compared to the native gSSURGO. Poor correlations were observed between DSM products and gSSURGO and among DSM products. Also, the spatial distribution of SOC for DSM products was substantially different for both soil depth increments when compared to gSSURGO. Based on qualitative assessment at regional level (coarse scale), PSP and gSSURGO spatial patterns were somewhat similar compared to SG2 and SPGC100. However, for gSSURGO artifacts related to political and administrative boundaries were still visible. At local scale, gSSURGO showed finer spatial details compared to DSM products and with patterns that aligned with soil-landscape relationships. For gSSURGO, higher values of SOC were observed for side slopes under forest compared to summits and floodplains, while for PSP the spatial distribution of SOC was random. The grid size may have played a role in the spatial distribution of SOC, especially for SG2 and SPGC100. However, even when gSSURGO was resampled to 90 x 90 m grid size per GlobalSoilMap specifications (Science Committee, 2012), the soil landscape relationship spatial patterns persisted, though to a lesser degree. Although, all DSM products were based on gSSURGO and point measured data, the underlying assumptions about the soil-landscape and scale relationship were largely ignored This led to either random spatial pattern predictions (PSP) or very coarse spatial predictions (SG2, SPGC100) with little utility for supporting management decisions at soil-landscape scale.

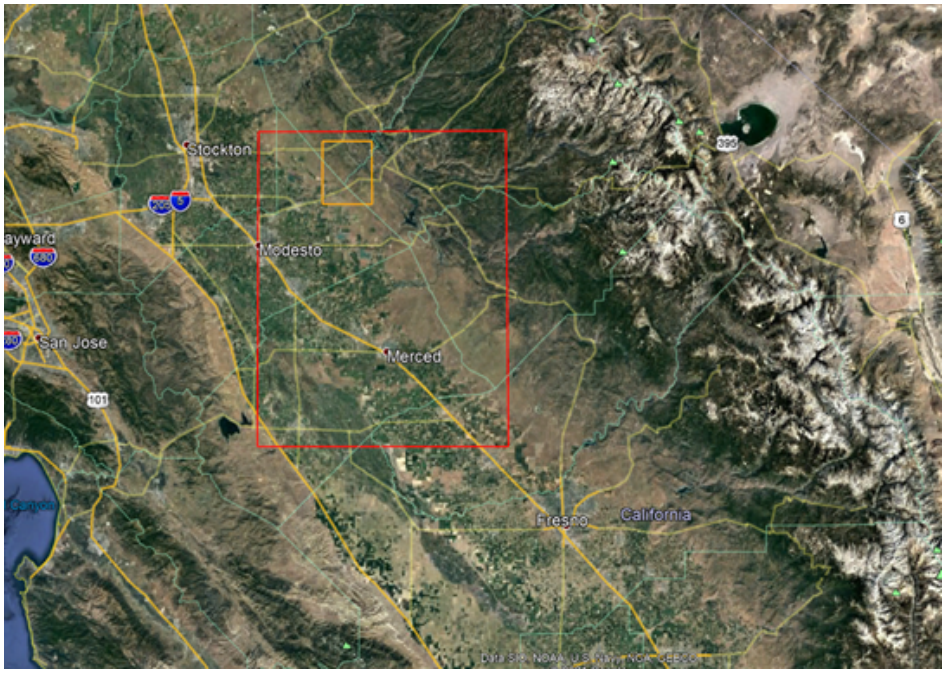


**Figure 88.** California study area

## 5 California

This area, bounding box (-121 – -120° E), (37–38° N), centred north of Merced CA in California's Central Valley, was selected because it is a transition zone between strongly-contrasting soil landscapes. Fig. 88 shows the study area and the sub-area used for local comparisons.

The property chosen for analysis is sand concentration in two upper subsoil GlobalSoilMap.net layers, namely 5–15 and 15-30 cm layers. This property and depths were selected due to the strong contrasts in parent materials in the area, as well as redistribution by erosion and deposition, e.g., into large alluvial fans.

## 5.1 Regional spatial patterns

### 5.1.1 Regional maps

Figs. 89 and 90 show gNATSGO (reference) along with the predictions of sand concentration in the two depth intervals (5-15 cm, 15-30 cm, respectively) of the other products.

Figs. 91 and 92 shows their histograms, and Fig. 93 the pairwise Pearson correlations between all maps.

Table 29 shows the statistical differences, and Figs. 94 and 95 show the differences as maps.

| Product | MD | RMSD | RMSD.Adjusted |
|---|---|---|---|
| SG2 | 143.433 | 227.74 | 176.896 |
| PSP | -17.551 | 125.901 | 124.672 |
| SPCG | 81.509 | 169.234 | 148.312 |

| Product | MD | RMSD | RMSD.Adjusted |
|---|---|---|---|
| SG2 | 140.55 | 227.329 | 178.673 |
| PSP | -13.987 | 127.045 | 126.272 |
| SPCG | 91.206 | 176.333 | 150.913 |

**Table 29.** Statistical differences between DSM products, sand %, 5–15 cm (left), 15-30 cm (right)

The DSM products under-predict the sand content for both soil depths, except for PSP, which slightly over predicts the sand content by only 1.7 % and 1.3% for 5–15 and 15-30 cm depth intervals. SG2 under-predicts the most with about 14 % for both depths compared with SPGC with 8.1 % and 9.1 % for 5–15 and 15-30 cm depths intervals. Similar trends are observed for RMSD and adjusted RMSD (unbiased). The RMSD values almost double compared to MD varying from 12 % (PSP, both depths) to 28 % (SG2, both depths). The unbiased differences are slightly less compared to RMSD and comparable between DSM and depths. The distribution of sand content for gNATSGO for both depths is wider (0-100 %) with a slight bi-modal shape compared to DSM products that show narrower ranges and uni-modal shape. SG2 and SPCG, in particular, have a narrower range distribution from 15 % to 70 % and with peaks centered around 35 % and 40 %. gNATSGO and PSP have somewhat similar distributions with PSP showing slightly narrower ranges and a weak bi-modal distribution. These slight similarities between gNATSGO and PSP are also reflected by the Pearson correlation coefficients that are higher for gNATSGO vs PSP ($\approx 0.75$, both depths) compared to SG2 ($\approx 0.2$) and SPCG ($\approx 0.4$). PSP and SG2 are the least correlated for both depths. As intuitive as the overall differences are, their spatial expression provides a real context for their interpretation. The spatial distribution of sand content for both depths is different among all models. gNATSGO and PSP are similar to a certain degree, at least at this regional scale, although gNATSGO shows more detail. SG2 and SPCG, on the other hand, show not only less spatial detail, but also narrower spatial distribution range, especially SG2. SPGC only slightly distinguishes the alluvial fans with higher sand content coming off the foothills of Sierra Nevada, while SG misses them entirely. As expected, the spatial difference between gNATSGO and DSM products are higher for SG2 and SPGC vs gNATSGO compared to PSP vs gNATSGO, especially for the alluvial fans. For example, for both depths, SG2 and SPCG underestimate the sand content for alluvial fans by 20 to 30 % sand content, while PSP to a lesser degree by 5 to 10 %. The opposite seems to be the true for the Sierra Nevada foothills and the mountainous areas.

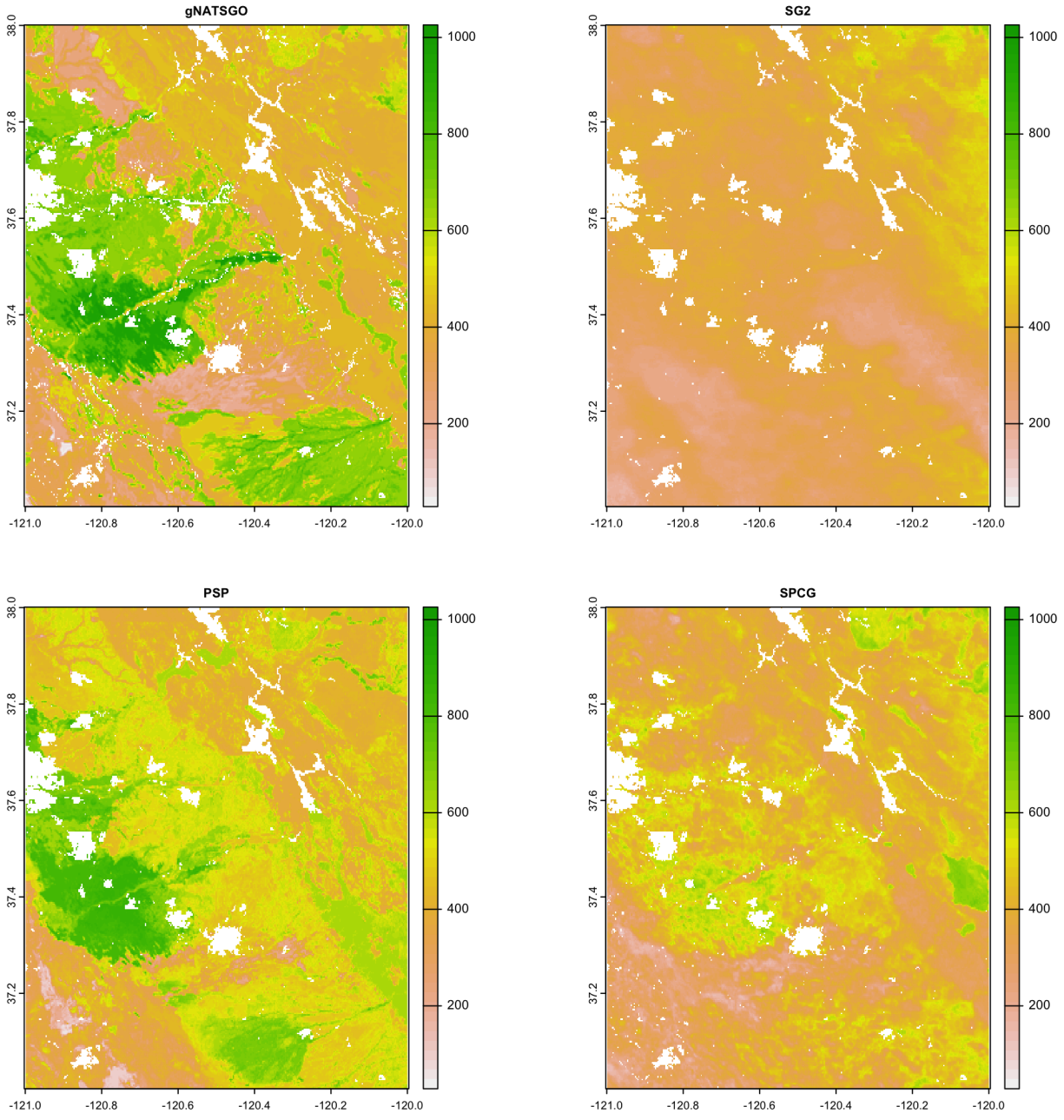


**Figure 89.** 5-15 cm sand %%, according to different DSM products

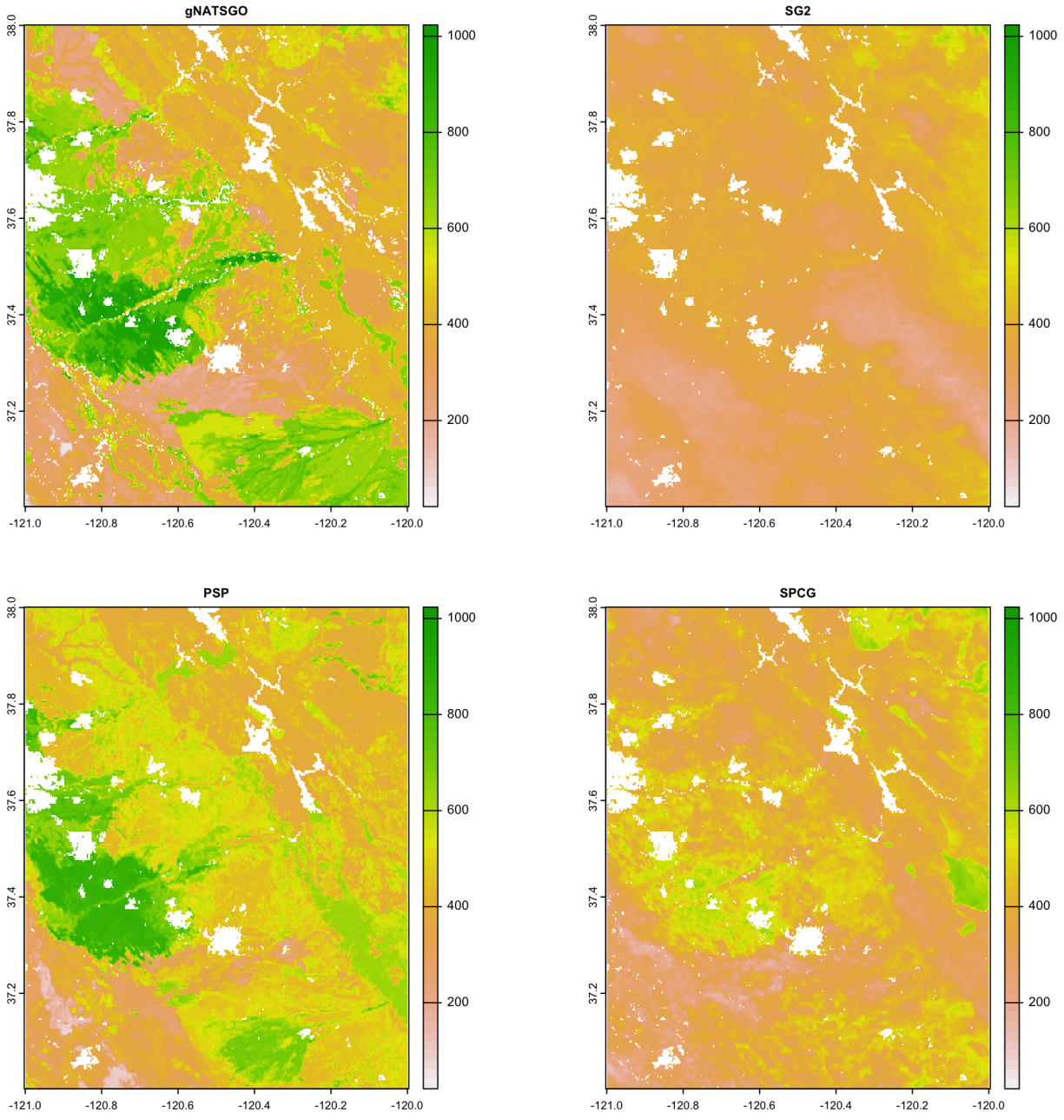


**Figure 90.** 15-30 cm sand %%, according to different DSM products

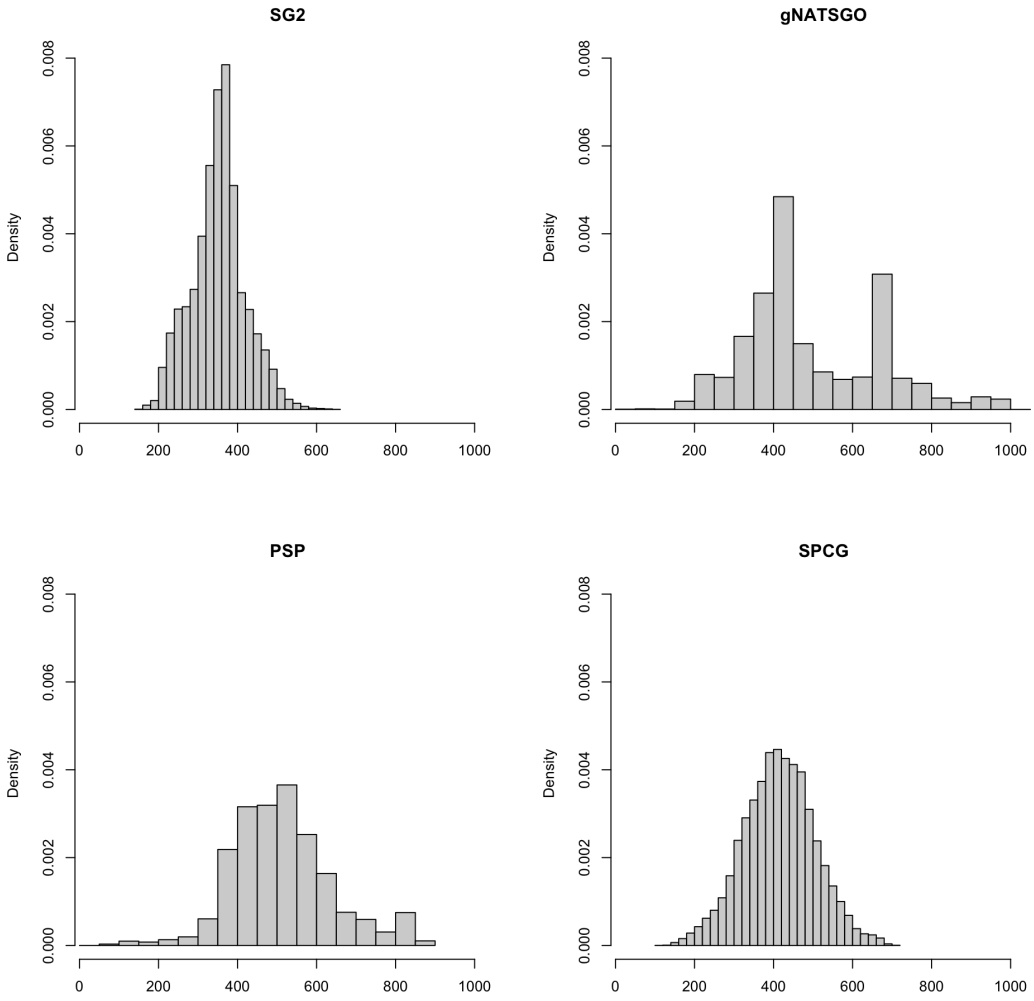


**Figure 91.** Histograms of 5–15 cm sand %%, according to different DSM products

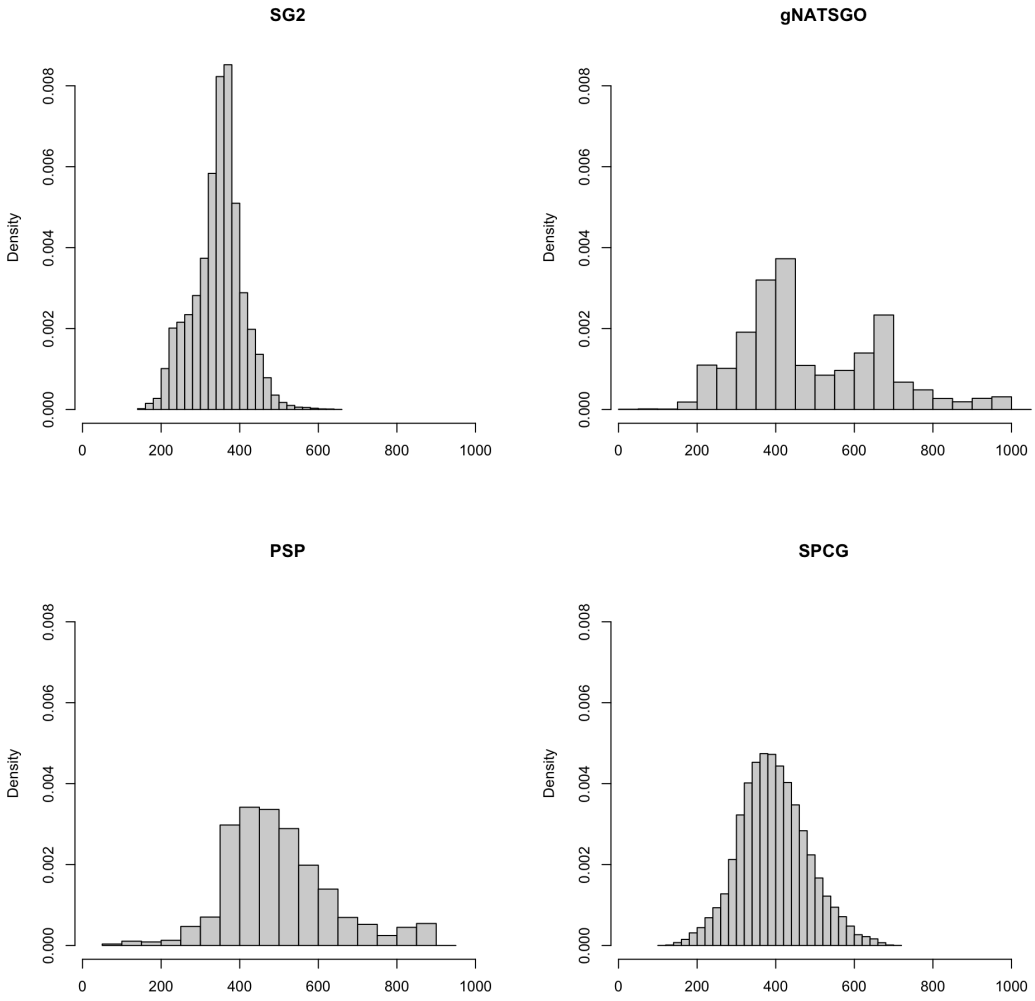


**Figure 92.** Histograms of 15-30 cm sand %%, according to different DSM products

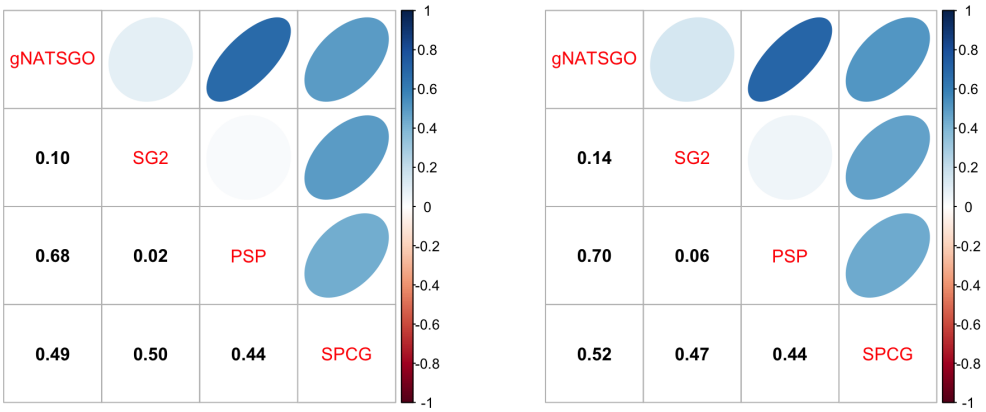


**Figure 93.** Pearson correlations between DSM products, sand %, 5–15 cm (left), 15-30 cm (right)

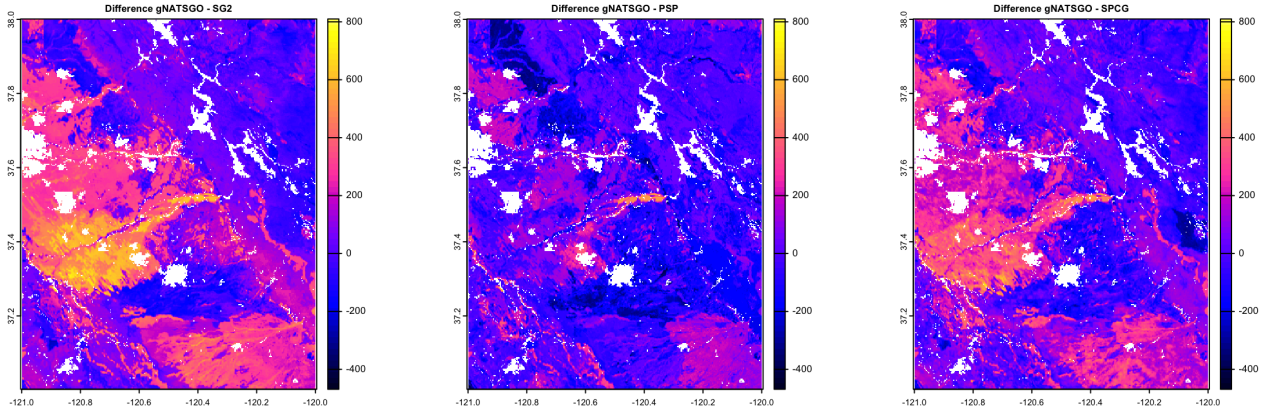


**Figure 94.** Difference between gSSURGO and other DSM products, sand %, 5–15 cm

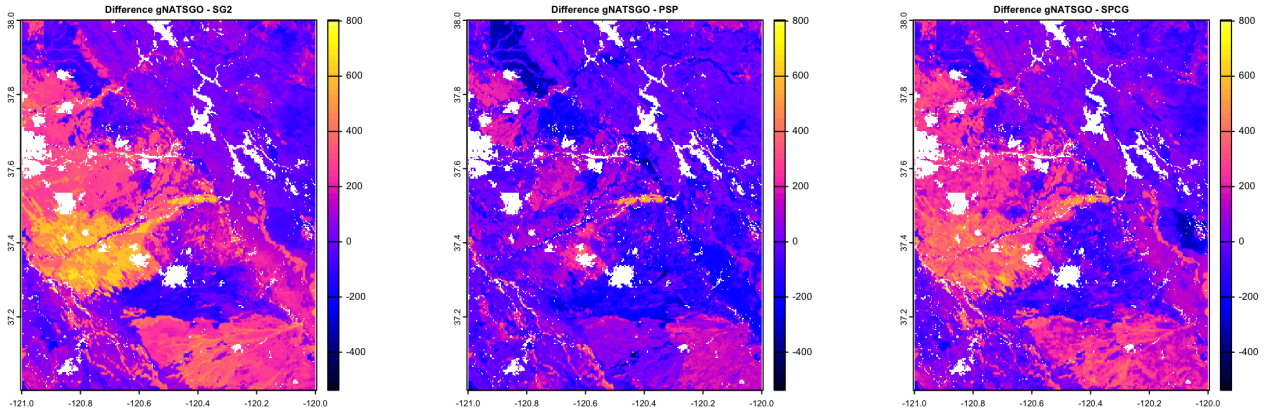


**Figure 95.** Difference between gSSURGO and other DSM products, sand %, 15-30 cm

### 5.1.2 Uncertainty

The 5%, 50%, and 95% prediction quantile maps are shown in Figs. 96 (SG2) and 97 (PSP) for 5–15 cm and 15-30 cm; each figure has its own stretch. The "low", "representative" and "high" values from gNATSGO are shown in Fig. 98. The large area of "unknown" (white areas in the "low" and "high" figures) is because no limits have been defined for the soil series covering these areas.

Figs. 99 shows the inter-quartile range 5–95% (IQR), along with the low-high range for gNATSGO (in the areas where these are defined), for the two products at the two depth intervals. The inter-quartile predictions (IQP) for SG2 are relatively lower and show less spatial heterogeneity compared to PSP for both depths. Similarly, the inter-quartile range (IQR) for SG2 shows less spatial variability and smaller range compared to PSP for both depths. The IQR for SG2 is predominately in the 40-60 % range for sand content for both depths compared to PSP with a slightly wider range that is between 35 and 65 % for the majority of the area. The IQR range difference between SG2 and PSP for both depths shows that compared to PSP, SG2 over predicts sand content for the valley and foothills by a wide margin (5 to 50 %) but under predicts for the mountainous area. Interestingly, the area between over and under predictions occurs along the boundary between two Major Land Resource Areas (MLRA) 17-Sacramento and San Joaquin Valley and 18-Sierra Nevada Foothills.

Fig. 100 shows the spatial differences between the two IQR at the two depth intervals. PSP has more areas with a wide IQR than SG2, especially along the MLRA boundary area.

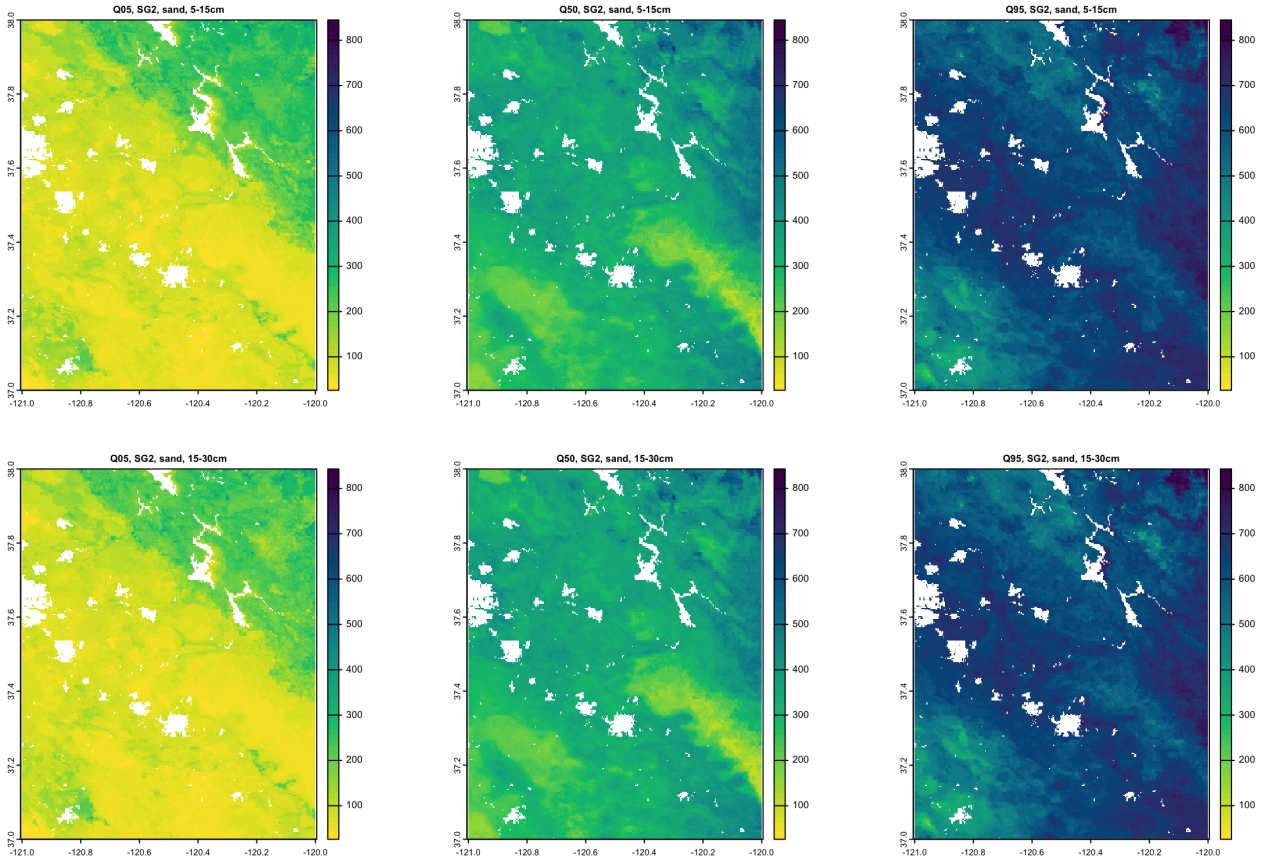


**Figure 96.** Quantiles of the prediction, SG2, sand %x10, 5–15 cm (top), 15–30 cm (bottom)

### 5.1.3 Class maps

Figs. 101 (5-15 cm) and 102 (15-30 cm) show the sand concentration, classified into eight histogram-equalized classes in a small 0.2 x 0.2° sub-area, with limits $(-120.74 \cdots -120.54)°$ E, $(37.77 \cdots 37.97)°$ N, centred W of Lake Tulloch CA (the unmapped area). Note that each depth interval has a separate histogram equalization.

Class limits from histogram equalization are approximately 353, 372, 388, 405, 425, 447, and 485 %x10 (5-15 cm) and 339, 357, 372, 387, 406, 432, and 479 %x10 (15-30 cm). There are substantial differences in the distribution of classes between gNATSGO and DSM products. gNATSGO and PSP show more areas in the highest sand content classes compared to SG2 and SPCG for both soil depths. However, the distribution patterns between gNATSGO and PSP are obvious, especially for the alluvial fan across the foothills and the foothill valley. PSP exaggerates the extend of the classes with the highest sand content, especially for the southwest corner in comparison to gNATSGO, which shows patterns that match with the geomorphology setting of this particular area.

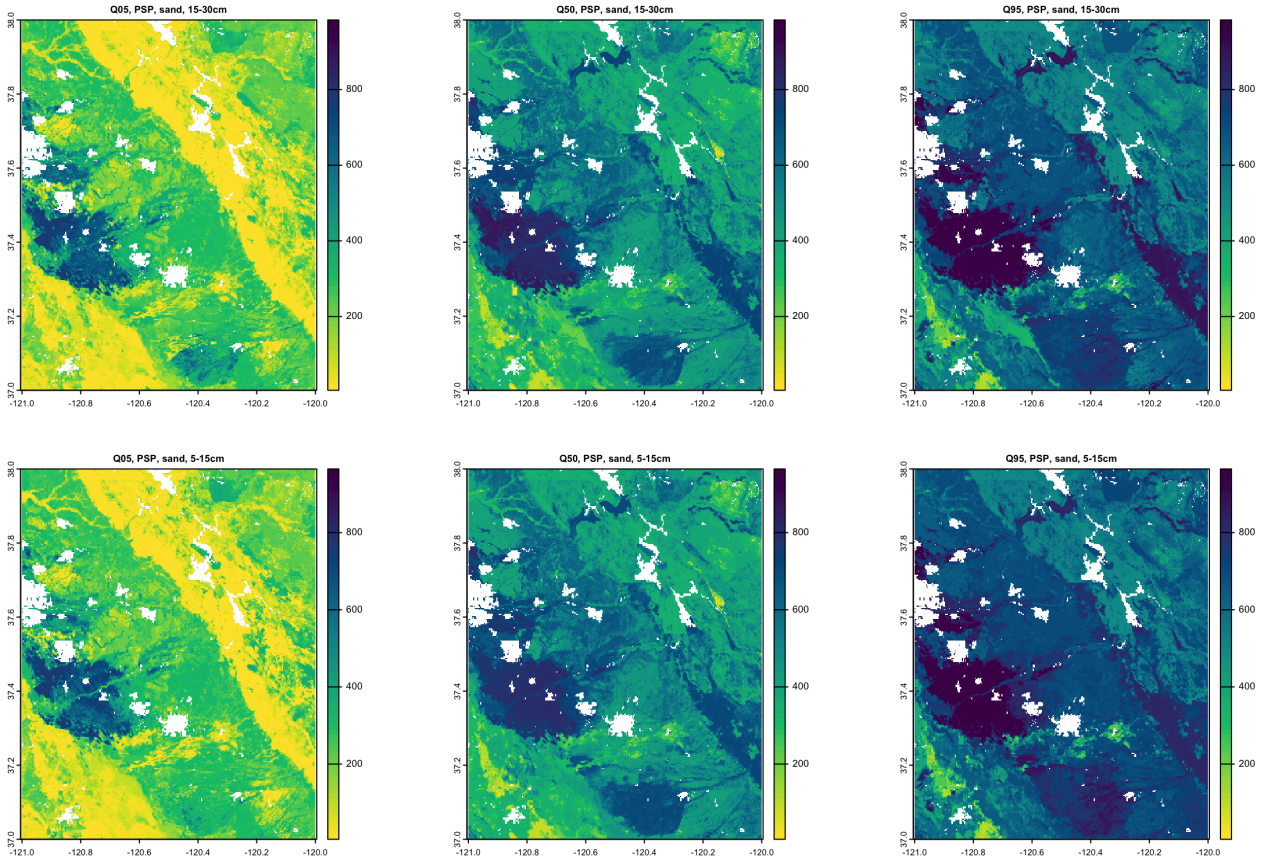


**Figure 97.** Quantiles of the prediction, PSP, sand %x10, 5–15 cm (top), 15–30 cm (bottom)

### 5.1.4 Local spatial autocorrelation

The local variograms and their fitted exponential models are shown in Figs. 103 (5-15 cm) and 103 (15-30 cm). Table 30 shows their statistics.

gNATSGO has the lowest effective range compared to DSM, but comparable with PSP. However, PSP has a lower structural sill showing some smoothing effects due to the modelling approach (DSMART) used by PSP. SG2 has the highest effective range and lowest structural sill due to the use of global covariates for the predictions and their coarse resolution.

### 5.1.5 V-measure

Table 31 shows the statistics from several V-measure comparisons, based on the histogram-equalized class maps. There is little correspondence between the maps.

| Product | Effective range | Structural Sill | Proportional Nugget |
|---|---|---|---|
| gNATSGO | 6027.00 | 6256.22 | 0.00 |
| SG2 | 13899.00 | 826.62 | 0.00 |
| SPCG | 9666.00 | 2396.85 | 0.00 |
| PSP | 6474.00 | 4398.32 | 0.00 |

| Product | Effective range | Structural Sill | Proportional Nugget |
|---|---|---|---|
| gNATSGO | 6450.00 | 7546.86 | 0.00 |
| SG2 | 10467.00 | 672.15 | 0.00 |
| SPCG | 9504.00 | 2088.83 | 0.00 |
| PSP | 6318.00 | 5077.22 | 0.00 |

**Table 30.** Fitted variogram parameters, sand 5–15 cm (top), 15-30 cm (bottom). Effective range in $\mathrm{m}$; structural sill in $(\%\%x10)^2$, proportional nugget on $[0 \dots 1]$

| DSM_products | V_measure | Homogeneity | Completeness |
|---|---|---|---|
| gNATSGO vs. SG2 | 0.0298 | 0.028 | 0.0318 |
| gNATSGO vs. SPCG | 0.0435 | 0.0451 | 0.042 |
| gNATSGO vs. PSP | 0.0906 | 0.0866 | 0.0951 |
| SPCG vs. SG2 | 0.0437 | 0.0397 | 0.0485 |

| DSM_products | V_measure | Homogeneity | Completeness |
|---|---|---|---|
| gNATSGO vs. SG2 | 0.031 | 0.0289 | 0.0334 |
| gNATSGO vs. SPCG | 0.0682 | 0.0665 | 0.0699 |
| gNATSGO vs. PSP | 0.0945 | 0.085 | 0.1063 |
| SPCG vs. SG2 | 0.0602 | 0.0574 | 0.0632 |

**Table 31.** V-measure statistics, sand %% 5–15 cm (top), 15-30 cm (bottom)

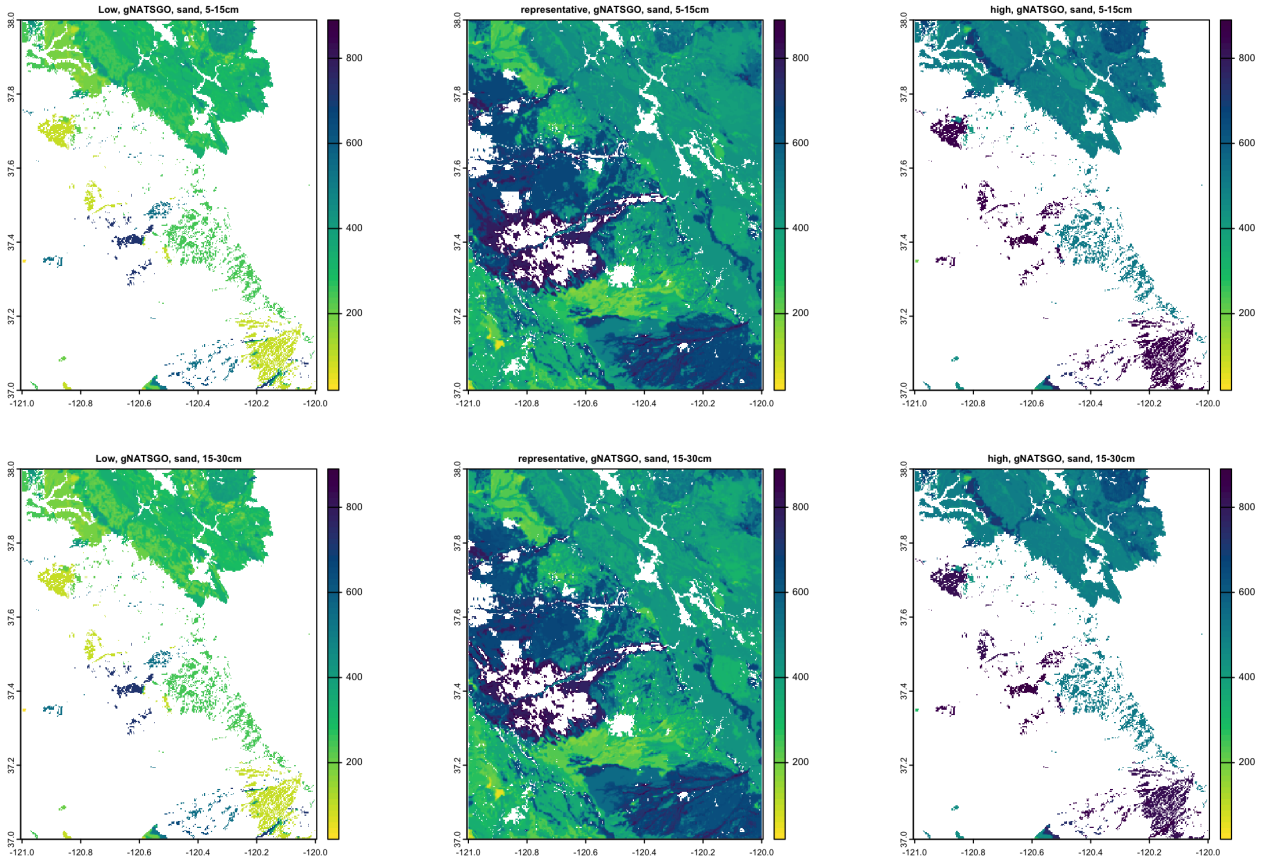


**Figure 98.** Low, representative, high values from gNATSGO, pHx10, 0–5 cm

Figs. 105 (5-15 cm) and 106 (15-30 cm) show the computed homogeneity and completeness of the SG2 sand class map, with respect to the gSSURGO sand class map. There is no spatial association overall between all maps with values being less than 0.1 for both soil depths (Table 31). Both homogeneity and completeness show similar disagreements indicating that the compartmentalization of the maps using classes seem to be random in relation to each other. Spatially, only few areas show some degree of homogeneity for both SG2 vs gNATSGO and PSP vs gNATSGO (areas in yellow with values close to 1). This means that areas (zones) in the first map SG2 or PSP are entirely within areas (region) of gNATSGO. However, many areas show less homogeneity and completeness, especially for the alluvial fan for PSP vs gNATSGO.

### 5.1.6 Landscape metrics

Table 32 shows the statistics from the landscape metrics calculations.

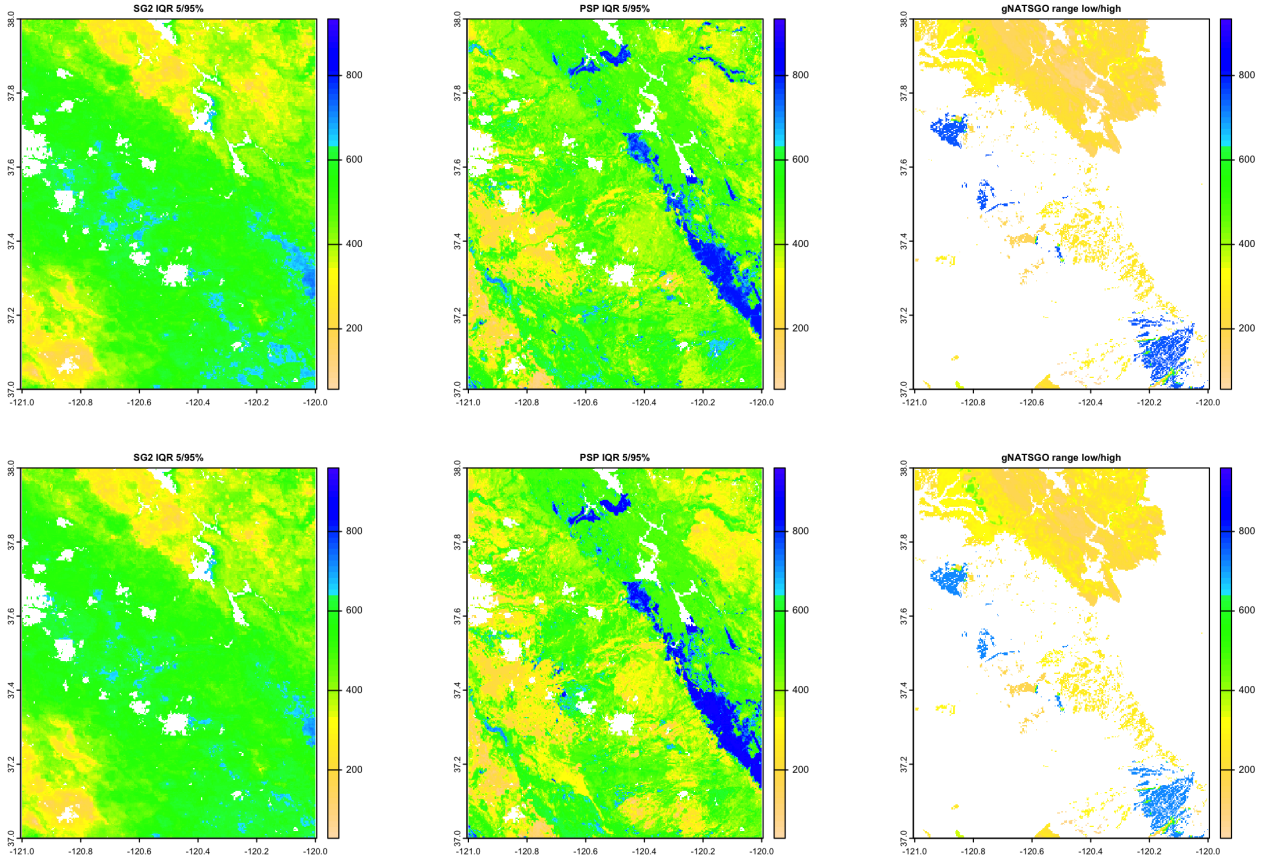


**Figure 99.** Inter-quartile ranges of the prediction, sand %x10, 5–15 cm (top), 15–30 cm (bottom)

The landscape aggregation index values `ai`, for the 5–15 cm layer are the lowest for SPCG (54) and comparable with gNATSGO (57)and PSP (60) showing higher landscape desegregation compared to SG2 (74). For 15 to 30 cm layer,, SG2 shows less desegregation (68) compared to the other products. gNATSGO (53) and SPCG (57) have the highest degree of desegregation with PSP (63) being closer to SG2. The mean fractal dimension values `frac_mn` are close to 1 and very similar between all maps and both depths indicating that all patches are square. However, because `frac_mn` is scale dependent, it interpretation with regard to gNATSGO should be interpreted with caution because gNATSGO was re sampled from a finer resolution to 100 m for the calculation of all these indexes. The landscape shape index `lsi` values are generally low and similar for all maps varying from 10 (SG2; 5–15 cm) 17.4 (gNATSGO; 15-30 cm). Both Shannon Diversity `shdi` and Shannon Evenness `shei` values show similar trends like `frac_mn` and `lsi` for all products. They point to a diverse landscape but there are some differences, especially for the 15-30 cm soil layer. Thus, PSP shows the lowest diversity (`shdi` = 1.54;`shei` = 0.74) while gNATSGO shows the highest (`shdi` = 1.93;`shei` = 0.93).

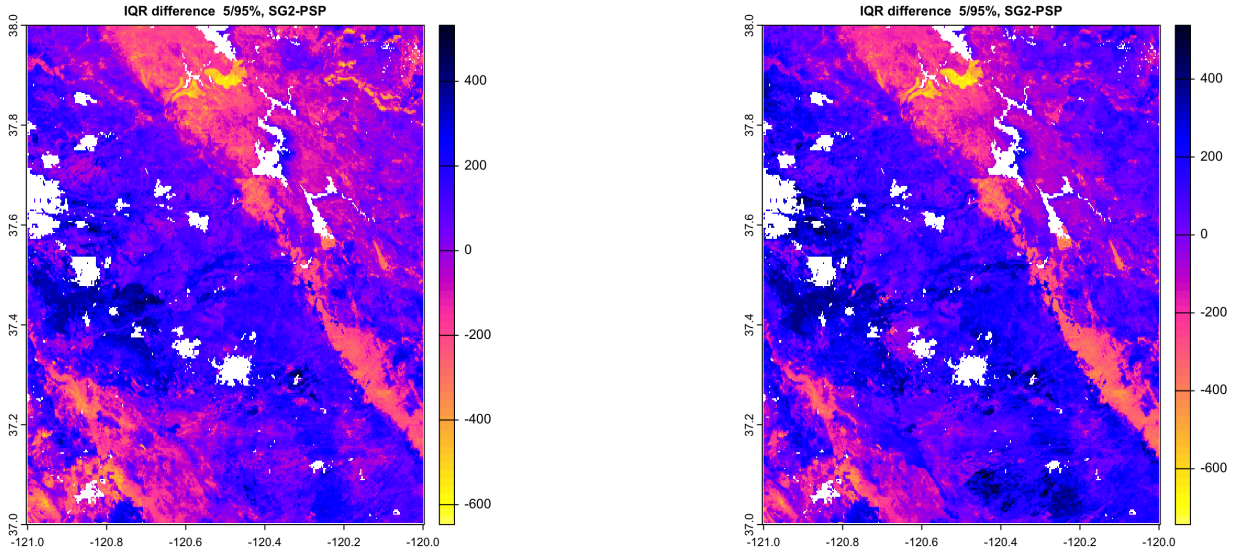


**Figure 100.** Difference between Inter-quantile ranges 0.05–0.95, Δ(sand %x10) 5–15 cm (left), 15–30 cm (right)

| product | ai | frac_mn | lsi | shdi | shei |
|---|---|---|---|---|---|
| gNATSGO | 56.817 | 1.031 | 16.119 | 1.817 | 0.874 |
| SG2 | 74.09 | 1.046 | 10.353 | 1.598 | 0.768 |
| SPCG | 53.763 | 1.045 | 17.178 | 1.951 | 0.938 |
| PSP | 59.779 | 1.038 | 14.938 | 1.655 | 0.851 |

| product | ai | frac_mn | lsi | shdi | shei |
|---|---|---|---|---|---|
| gNATSGO | 53.363 | 1.034 | 17.437 | 1.925 | 0.926 |
| SG2 | 67.599 | 1.05 | 12.482 | 1.666 | 0.856 |
| SPCG | 56.941 | 1.044 | 16.089 | 1.832 | 0.881 |
| PSP | 62.673 | 1.039 | 13.985 | 1.54 | 0.74 |

**Table 32.** Landscape metrics statistics, sand % 5–15 cm (top), 15-30 cm (bottom). `frac_mn`: Mean Fractal Dimension; `lsi`: Landscape Shape Index; `shdi`: Shannon Diversity; `shei`: Shannon Evenness; `ai`: Aggregation Index

| | gNATSGO | SG2 | SPCG | PSP |
|---|---|---|---|---|
| gNATSGO | 0.000 | 0.400 | 0.196 | 0.560 |
| SG2 | 0.400 | 0.000 | 0.086 | 0.560 |
| SPCG | 0.196 | 0.086 | 0.000 | 0.524 |
| PSP | 0.560 | 0.560 | 0.524 | 0.000 |

| | gNATSGO | SG2 | SPCG | PSP |
|---|---|---|---|---|
| gNATSGO | 0.000 | 0.692 | 0.205 | 0.086 |
| SG2 | 0.692 | 0.000 | 0.521 | 0.818 |
| SPCG | 0.205 | 0.521 | 0.000 | 0.397 |
| PSP | 0.086 | 0.818 | 0.397 | 0.000 |

**Table 33.** Jensen-Shannon distance beween co-occurence vectors; 5–15 cm (top); 15-30 cm (bottom)

Table 33 shows the Jensen-Shannon distance beween co-occurence vectors of the four products.

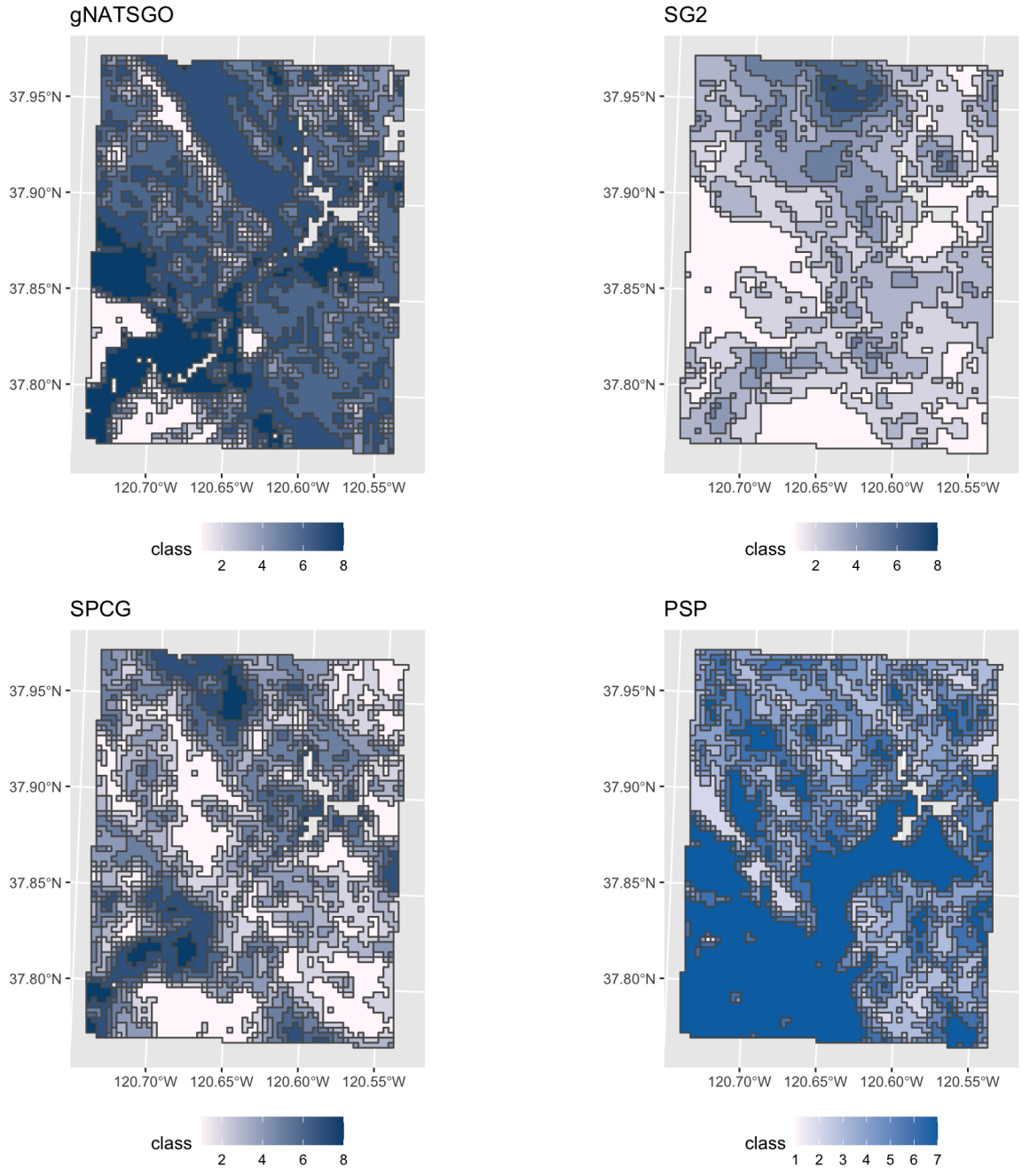


**Figure 101.** sand % classes, 5–15 cm, CA, detail

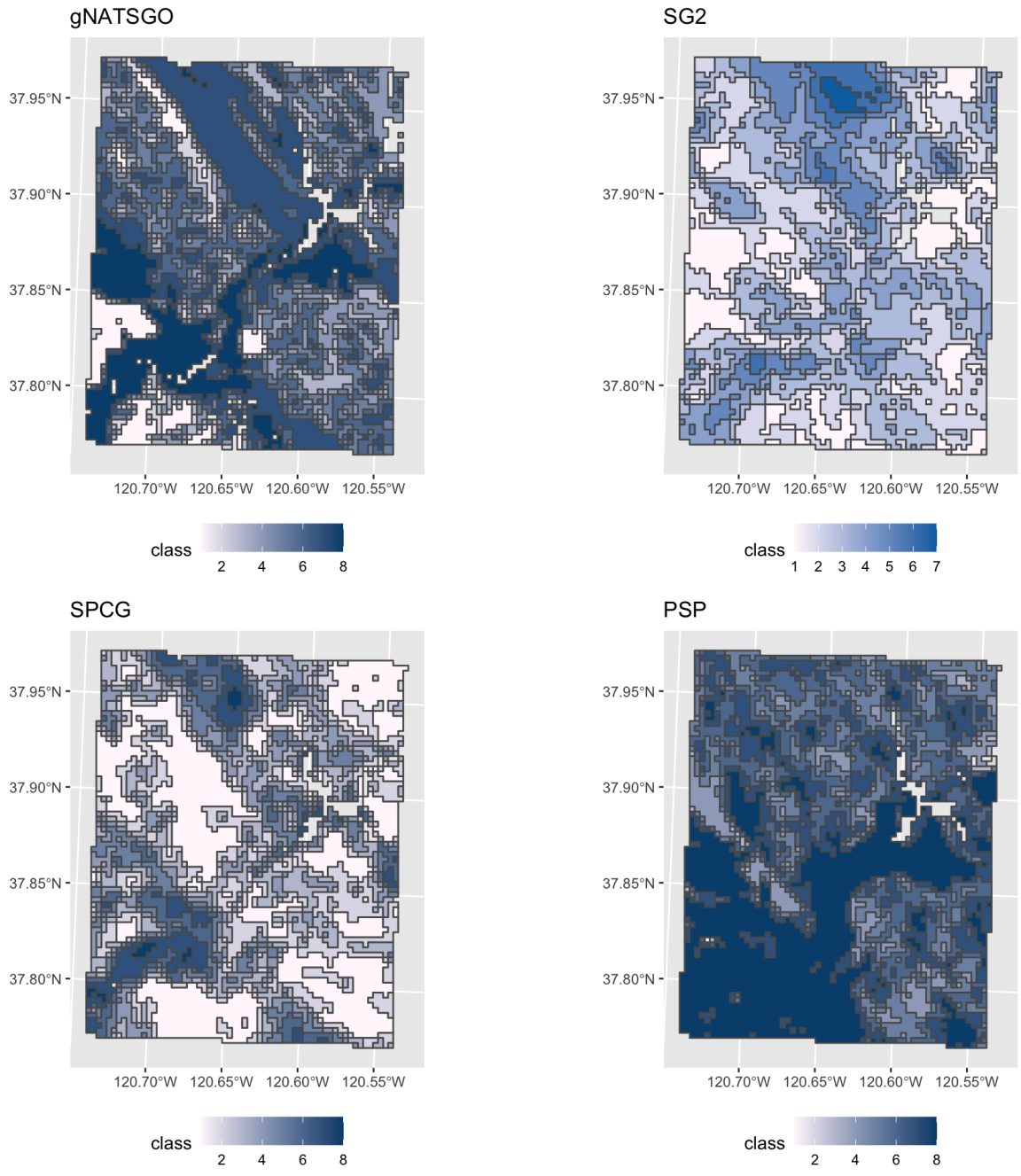


**Figure 102.** sand % classes, 15-30 cm, CA, detail

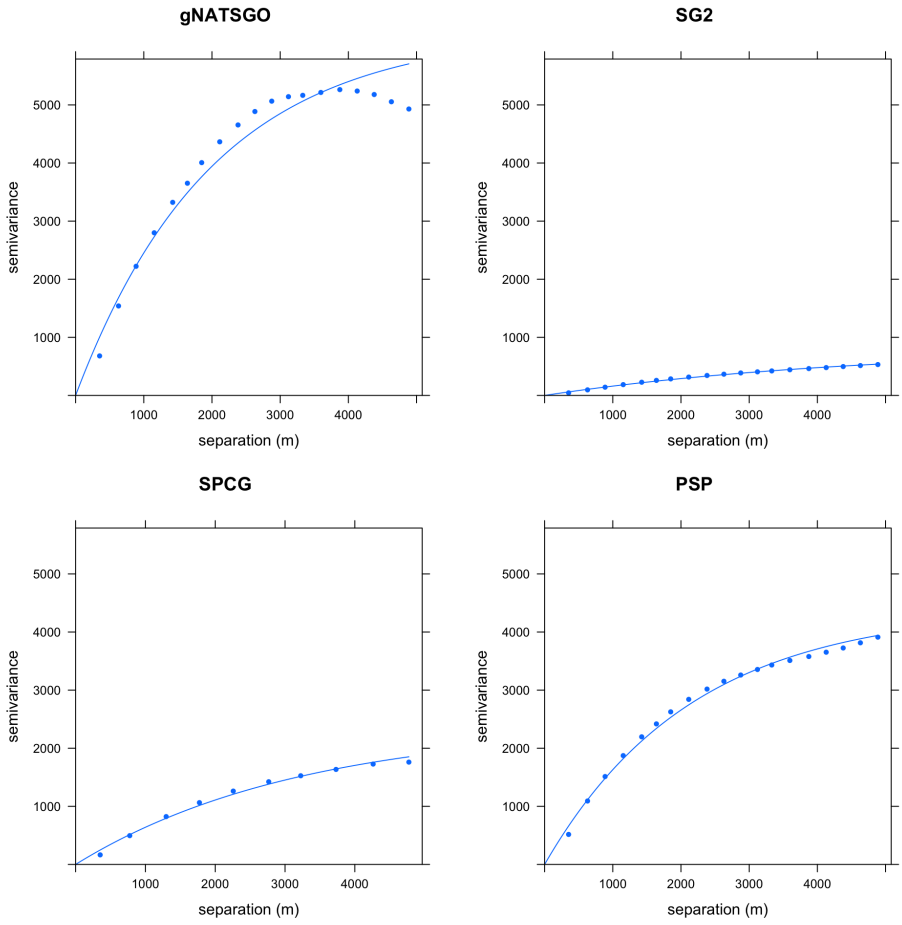


**Figure 103.** Fitted variograms, sand 5–15 cm (top), 15-30 cm (bottom), California. Semivariance units $(\%x10)^2$

The co-occurence vector based on Jensen-Shannon distance between pairs of adjacent cells for each category in a local landscape shows low and various degrees of similarity between products. The highest dissimilarity values are for PSP vs SG2 (0.82; 15-30 cm), while the highest similarity is found between SPGC vs SG2 (0.086) and gNATSGO vs PSP (0.087) both for 15-30 cm soil layer.

The indices showing the diversity of maps with respect to the landscape and similarities and dissimilarities point towards some differences between all maps. However, the interpretation of these differences is more meaningful if the right context is provided. Because all DSM products are either derived from gNATSGO or use data sources that were utilized for making gNATSGO, it suffices to use gNATSGO and the soil landscape model it is based upon to asses the loyalty of DSM products and their assumptions to the soil landscape model.

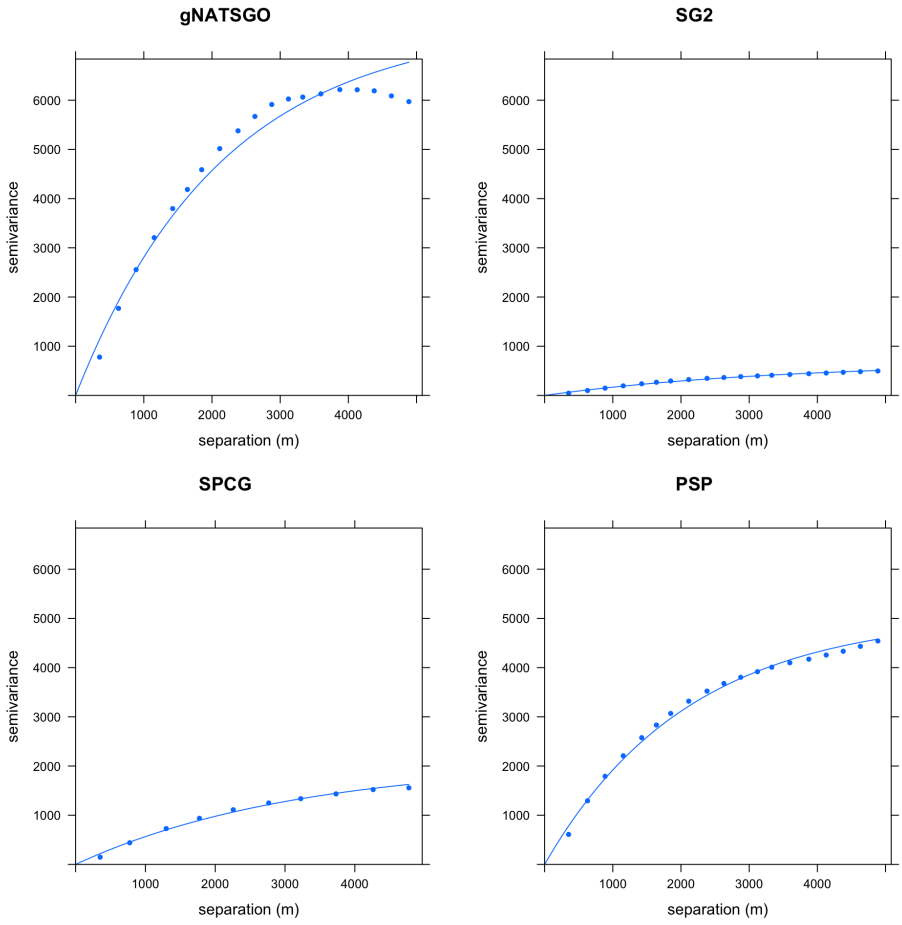


**Figure 104.** Fitted variograms, sand 5–15 cm (top), 15-30 cm (bottom), California. Semivariance units $(\%x10)^2$

## 5.2 Local spatial patterns

### 5.2.1 Qualitative assessment

Fig. 107 shows the sand concentration of the 5–15 cm layer for (top) the gridded SSURGO overlain on the original polygons from which it was derived, and (bottom) the disaggregated PSP grid cells in a rolling landscape about 8 km E of Knights Ferry, CA. Red colours are low sand, yellowish colours are high sand.

The gSSURGO product follows the SSURGO lines exactly. In this survey area the map units are complexes, for example map unit 7076 “Bonanza-Loafercreek-Gopheridge complex, 15–30% slopes”, with contrasting components, almost all loamy *Ultic Haploxeralfs*, but with varying family particle-size classes. Thus the gSSURGO prediction is averaged over the components. It also appears to show poor correspondence between some map unit boundaries and landscape features. However, PSP hardly

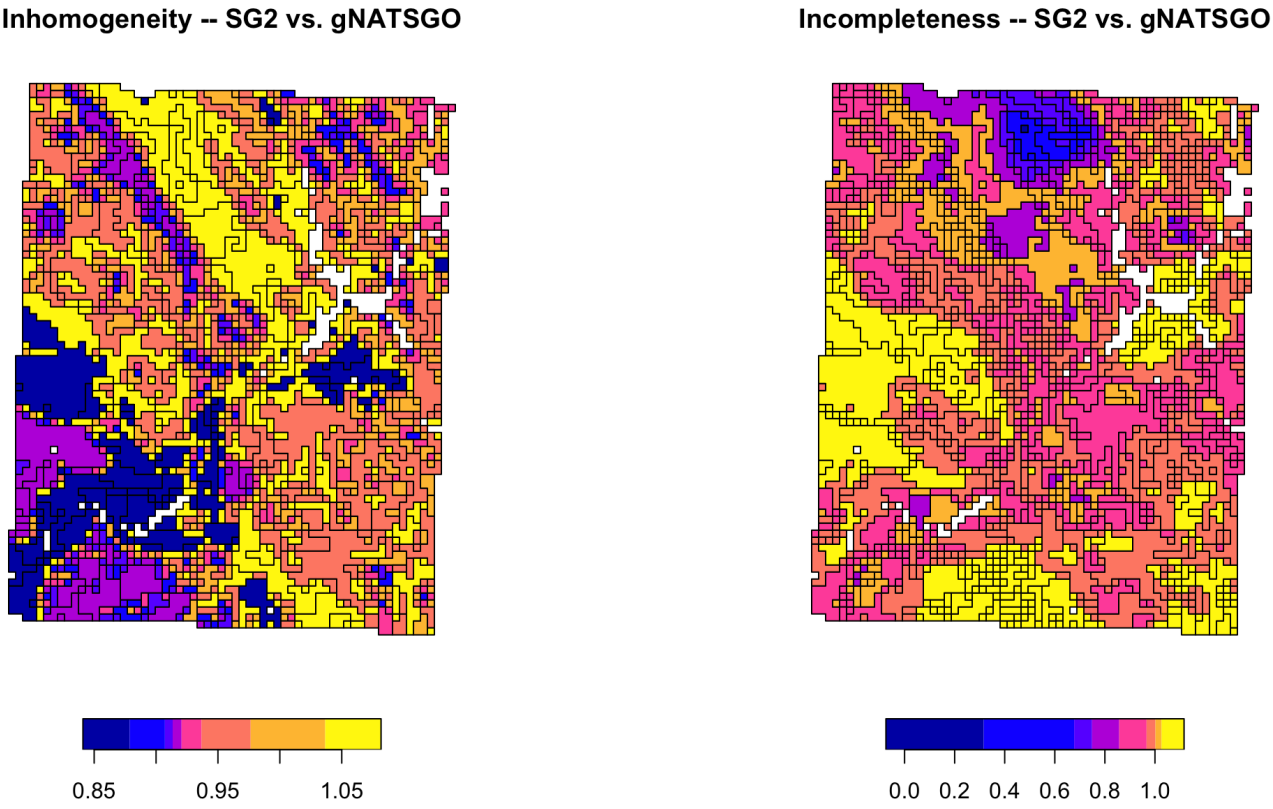


**Figure 105.** Homogeneity (left) and Completeness (right) of the SG2 sand class map, with respect to gSSURGO sand class map, 0–5 cm

follows the map unit lines, and identifies contrasts in sand concentration across the landscape, by disaggregating the gSSURGO polygons. The landscape relations, if any, are not obvious.

### 5.2.2 Quantitative assessment

To see the fine differences at this high resolution, we concentrate on a $0.15 \times 0.15°$ subtile with lower-right corner $(-120.54°\mathrm{E}, 37.77°\mathrm{N})$ and evaluate sand concentration, as in the regional assessment (§5.1). This is the same lower-right corner used for the assessment of class maps at regional scale.

### 5.2.3 Class maps

Fig. 108 shows the sand concentration for the two layers classified into eight histogram-equalized classes. Class limits for the 5–15 cm layer in this area are approximately 356, 373, 380, 395, 439, 452, 544 with the extreme values of 130 and 979 %%, and for the 15-30 cm layer approximately 349, 362, 373, 375, 413, 450, 555 with the extreme values of 122 and 979 %%.

SG2 is less detailed than the other two products with a smaller number of classes. More importantly, the pattern of the spatial distribution is very coarse and misses significant landscape features. On the other hand, PSP and gSSURGO show fine spatial

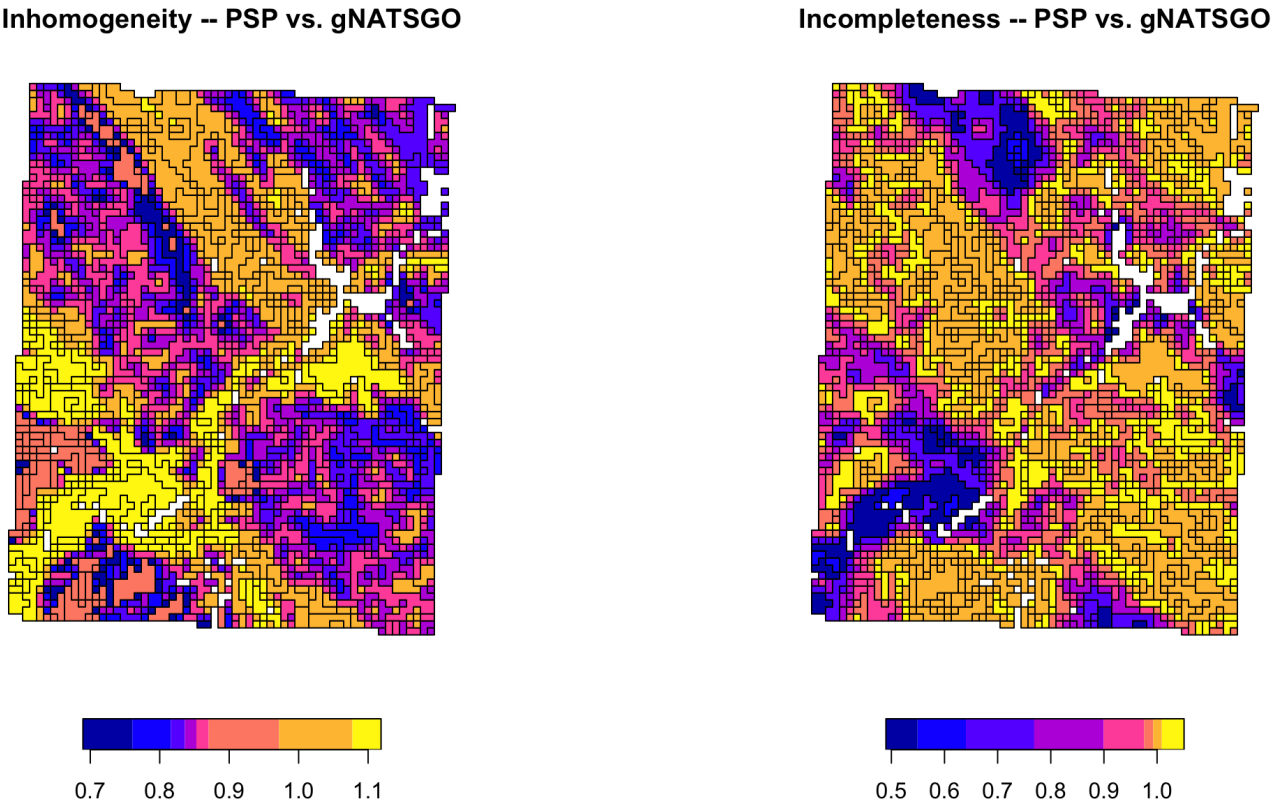


**Figure 106.** Homogeneity (left) and Completeness (right) of the SG2 sand class map, with respect to gSSURGO sand class map, 5–15 cm

patterns and have the same number of classes. However, for PSP classes with higher sand content are overextended, especially around the alluvial fan, while the distribution of classes for the rest of the area appears quite random compared to gSSURGO.

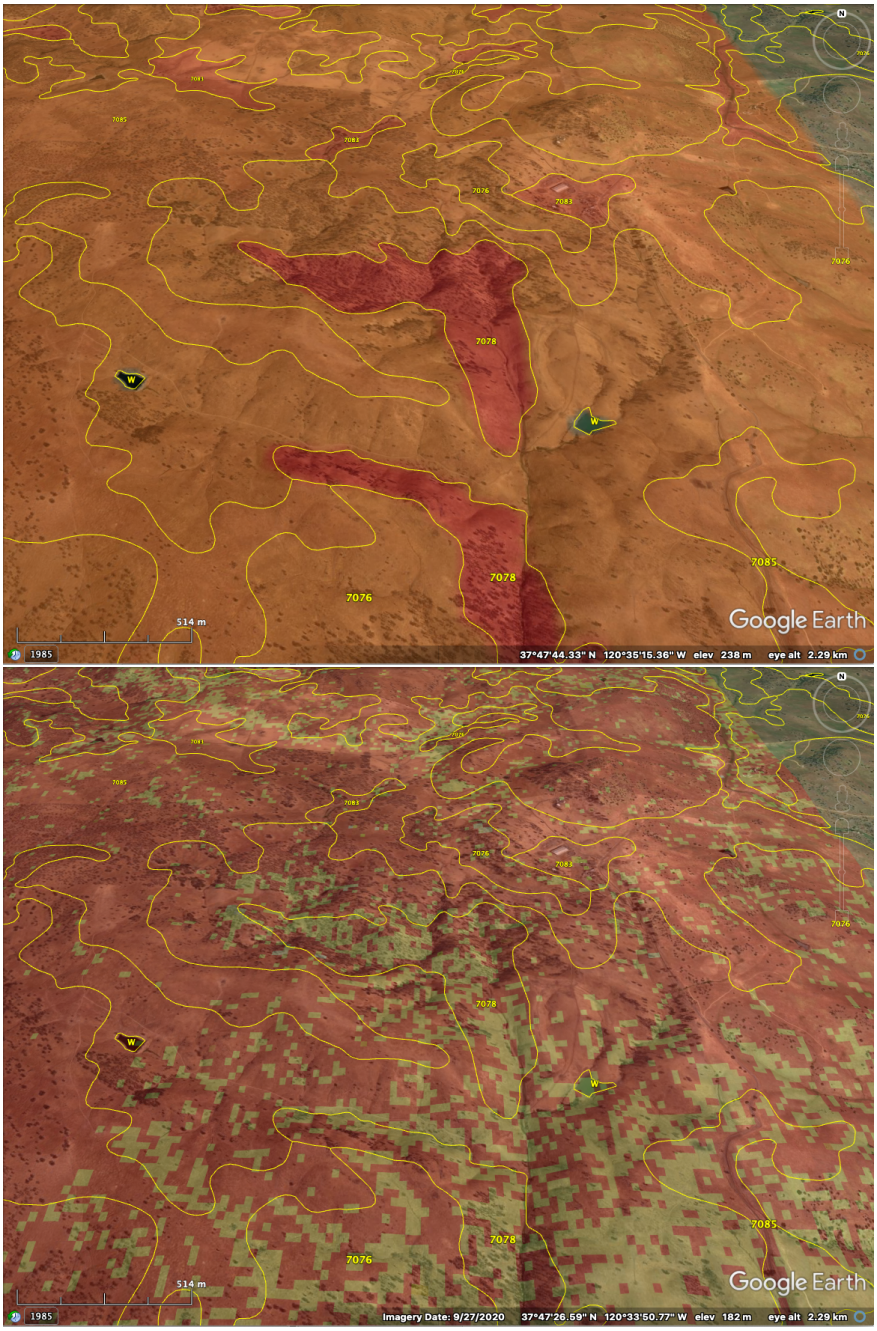


**Figure 107.** Ground overlay from gSSURGO (top) and PSP (bottom), sand % 5–15 cm, with SSURGO polygons from SoilWeb. Centre of image $-122°33'50"\mathrm{E}, 37°47'25"N$; view azimuth 0°

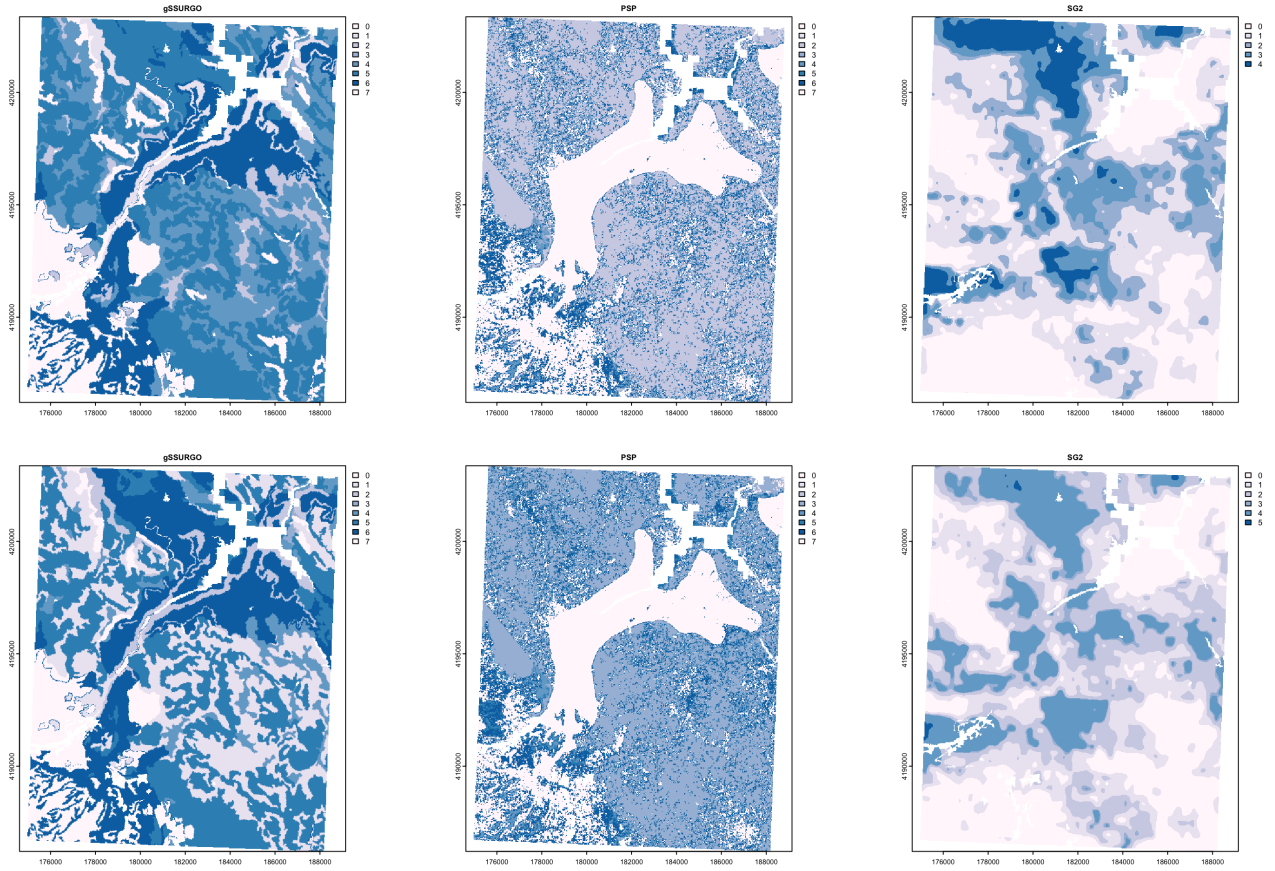


**Figure 108.** Sand classes, 5–15 cm (top), 15-30 cm (bottom), California, detail. Coordinates are UTM 11N meters

### 5.2.4 Local spatial autocorrelation

The local variograms and their fitted exponential models are shown in Fig. 109. Table 34 shows their statistics.

The differences between DSM and gSSURGO with regard to variagram parameters are more obvious at the local scale. gSSURGO has the smallest effective range compared to SG2 and PSP indicating a finer scale structure at local level. The structural sill is the lowest for SG2 showing a large degree of smoothing, while PSP and gSSURGO are relatively comparable. However, as expected, PSP has higher proportional nugget values compared to gSSURGO, most likely do to the uncertainty from the DSMART algorithm.

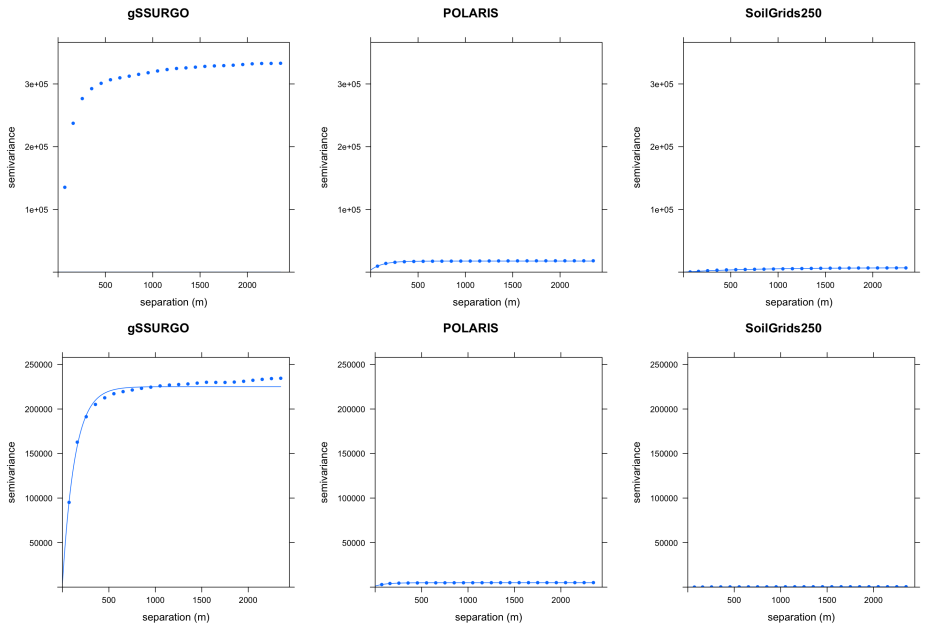


**Figure 109.** Fitted variograms, sand classes, 5–15 cm (top), 15-30 cm (bottom), California, detail. Semivariance units $(\%x10)^2$

| Product | Effective range | Structural Sill | Proportional Nugget |
|---|---|---|---|
| gSSURGO | 1179.00 | 3974.90 | 0.07 |
| SG2 | 11460.00 | 709.34 | 0.00 |
| PSP | 2742.00 | 5272.63 | 0.32 |

| Product | Effective range | Structural Sill | Proportional Nugget |
|---|---|---|---|
| gSSURGO | 1386.00 | 5064.06 | 0.07 |
| SG2 | 9882.00 | 653.03 | 0.00 |
| PSP | 2679.00 | 6276.97 | 0.32 |

**Table 34.** Fitted variogram parameters, sand classes, 5–15 cm (top), 15-30 cm (bottom), California, detail. Effective range in $\mathrm{m}$; structural sill in $(\%x10)^2$, proportional nugget on $[0 \ldots 1]$

| product | ai | frac_mn | lsi | shdi | shei |
|---|---|---|---|---|---|
| gSSURGO | 89.313 | 1.035 | 30.427 | 1.696 | 0.815 |
| SG2 | 95.778 | 1.064 | 13.485 | 1.491 | 0.927 |
| PSP | 64.926 | 1.038 | 93.638 | 1.486 | 0.714 |

| product | ai | frac_mn | lsi | shdi | shei |
|---|---|---|---|---|---|
| gSSURGO | 87.140 | 1.045 | 36.198 | 1.747 | 0.840 |
| SG2 | 94.904 | 1.078 | 15.935 | 1.477 | 0.824 |
| PSP | 64.973 | 1.043 | 93.461 | 1.475 | 0.709 |

**Table 35.** Landscape metrics statistics, sand 5–15 cm (left); 15-30 cm (right). `frac_mn`: Mean Fractal Dimension; `lsi`: Landscape Shape Index; `shdi`: Shannon Diversity; `shei`: Shannon Evenness; `ai`: Aggregation Index

| | gNATSGO | SG2 | SPCG | PSP |
|---|---|---|---|---|
| gNATSGO | 0.000 | 0.400 | 0.196 | 0.560 |
| SG2 | 0.400 | 0.000 | 0.086 | 0.560 |
| SPCG | 0.196 | 0.086 | 0.000 | 0.524 |
| PSP | 0.560 | 0.560 | 0.524 | 0.000 |

| | gNATSGO | SG2 | SPCG | PSP |
|---|---|---|---|---|
| gNATSGO | 0.000 | 0.692 | 0.205 | 0.086 |
| SG2 | 0.692 | 0.000 | 0.521 | 0.818 |
| SPCG | 0.205 | 0.521 | 0.000 | 0.397 |
| PSP | 0.086 | 0.818 | 0.397 | 0.000 |

**Table 36.** Jensen-Shannon distance beween co-occurence vectors; 0–5 cm (left); 5–15 cm (right)

### 5.2.5 Landscape metrics

Table 35 shows the statistics from the landscape metrics calculations. PSP shows a much finer structure than gSSURGO, due to its disaggregation algorithm. Unsurprisingly, SG2 is much coarser, due to its 250 m resolution.

Table 36 shows the Jensen-Shannon distance beween co-occurence vectors of the four products.

The landscape aggregation index values `ai`, for both 5–15 cm and 15-30 cm layers are the lowest for PSP (68 and 70) and the highest for gSSURGO (89) and SG2 (98) showing higher landscape desegregation for PSP. The mean fractal dimension values `frac_mn` are close to 1 and very similar between all maps and both depths indicating that all patches are square. The landscape shape index `lsi` values are generally low for both soil layers, especially for SG2 13 and 16. PSP has the highest values (86 and 80) compared to gSSURGO (32 and 35). However, the index does not provide spatially explicit indication of how shapes conform to the landscape. Both Shannon Diversity `shdi` and Shannon Evenness `shei` values show similar trends like `frac_mn` and `lsi` for all products. They show a diverse landscape with values varying from 0.6 (PSP; 15-30 cm) to 0.93 (SG2; 5–15 cm). PSP shows the lowest diversity (`shdi` = 1.24;`shei` = 0.60) while gNATSGO shows the highest (`shdi` = 1.76).

The co-occurence vector based on Jensen-Shannon distance between pairs of adjacent cells for each category in a local landscape shows low and various degrees of similarity between products and are very similar to the ones from the regional comparison. The highest dissimilarity values are for PSP vs SG2 (0.82; 15-30 cm), while the highest similarity is found between SPGC vs SG2 (0.086) and gNATSGO vs PSP (0.087) both for 15-30 cm soil layer.

### 5.3 Summary (CA)

Overall, in this area, and for this soil property, the DSM products do not give a satisfactory picture of the soil geography. Some of the main problems are as follows.

(1) There are substantial differences overall in mean predicted sand content, about $15\%$ (SG2), $9\%$ (SPCG), and $< -2\%$ (PSP). All DSM products narrow the distribution.

(2) None of the DSM products succeeded in reproducing important features of the spatial distribution of sand in this landscape, primarily because of the absence of surficial geology representing the source and sink for erosion, transport and deposition. SG2 misses almost all of the spatial pattern, especially the alluvial fans. SPCG is only a bit better, despite using SSURGO parent material and drainage class. PSP finds the overall pattern, due to its dependence on SSURGO, but blurs the pattern. There are gross differences between variograms. The DSMART disaggregation by PSP of a complex does not show obvious relation to landscape.

(3) There is quite high uncertainty in the two DSM products that provide it. The 5-95% inter-quantile range is 20-80% sand, with a strong spatial pattern of narrow and wide ranges.

In conclusion, for this area and property, it is clear that conventional soil survey, based on geomorphic interpretation of the soil landscape, clearly outperforms the DSM methods compared here.

## 6 Conclusions

The increase of measured and auxiliary soil data along with computer processing power and algorithms has led to the emergence of alternative predictive soil maps, several of which are examined in this report. These products address the needs of users, especially modelers and forecasters, for maps that are consistent and reproducible over large areas beyond county, state, and country boundaries. However, these advantages for the DSM products may come at the expense of loss of information and level of detail that traditional soil maps offer. Also, DSM products may violate or compromise the integrity of soil landscape relationships and their underlying physical, biological, and chemical principles, as understood by field soil surveyors.

The above analysis shows clearly that DSM is no substitute for field survey. Soil geography is often subtle, as field surveyors well know. It can be challenging to form a proper mental model of the soil-landscape relations in a survey area, so it is not surprising that using proxies (environmental covariates) rather than direct observation is not as accurate. This is known from cross-validation or other numerical evaluation exercises of point observations and their DSM predictions. Here we show that the spatial patterns are also not well-reproduced. This is especially relevant for earth surface models that use groups of grid cell predictions and their spatial contiguity, for example, watershed hydrology.

On the other hand, not all soil surveyors are equally competent, and the actual soil observations (augerings, profiles) are few, so that the consistent DSM approach may be more accurate in areas where surveyors were either less competent or where the soil-landscape relations were complex and difficult to map in the field. DSM can also smooth out sharp boundary lines between mapped polygons, when these are in nature gradual and where the STU included in the SMU on either side of the boundary are not too different.

Surprisingly, the inclusion of parent material and drainage class, and the use of only CONUS-wide covariates, did not improve predictive maps in the test areas. This is clear from the comparison of SPCG and SG2.

Geomorphology has proven to be a key component of soil survey, and DSM has great difficulties representing geomorphology, as opposed to landforms. If the landform and geomorphology are not congruent, and the DSM data source does not have a covariate to represent the geomorphology, several geomorphic units will be combined into similar predictions. A typical example is recently-glaciated terrain (Rossiter, 2016) where a given landform may have several geomorphic origins. A long linear low hill may be an esker, a lateral moraine, a drumlin, or thin till over a pre-existing rock structure. For example, in the Central New York example the valley trains of glacial outwash are in low positions, suggesting fine textures, but in fact have a large content of coarse fragments and coarser textures. They also have a pH derived from their source rocks carried by the glacier, not the rocks of the surrounding areas.

DSM also has problems identifying soil age. For example, in the North Carolina coastal plain example the different ages of the marine terraces are not clearly differentiated by the slight elevation differences separated by scarps, well-known to local soil surveyors. These age differences result in different degrees of development of the WRB Acrisols (USDA Soil Taxonomy Ultisols), especially the horizon thickness and in the oldest positions the development of plinthite gravel Daniels et al. (1999).

Perhaps the most important conclusion is that different DSM methods, with different training points and different algorithms, can produce quite different predictive soil maps. Comparing these with point-wise evaluation ("validation") gives an incomplete

picture of how the different methods represent the soil landscape, which is after all what dictates how the soil is used and managed.

The obvious limitation of this study is that it only examines a few of the many study areas, and in each one either one or a few of the mapped soil properties. The relative success of different DSM methods vs. field study and among themselves will surely differ greatly as these are changed. We encourage readers to apply the methods to their own study areas within the USA and to their soil properties of interest, to themselves evaluate the utility of the several DSM products, and indeed the utility of DSM in general. For this, we provide our analysis scripts as R Markdown documents (R Studio, 2020), see below.

*Code availability.* Source code as R Markdown documents are freely available without restriction at https://github.com/ncss-tech/compare-psm or at , or at Zenodo, doi:10.5281/zenodo.5512626. These can be used to (1) import all products to compare, as well as some others not considered in this study; (2) create ground overlays and corresponding KML files for display in Google Earth; (3) compare SG2 and PSP for $1 \times 1^{\circ}$ tiles; (4) compare SG2 with SPCG and gNATSGO for any rectangular tile; (5) compute landscape metrics and compare them between products for any subtile of these; (6) evaluate the success of PSP in disaggregating at 30 m resolution.

*Author contributions.* DGR conceptualized the approach, did most of the writing, and performed the central NY State and coastal plain NC case studies. DB performed the California case study; LZ performed the Indiana case study.

*Competing interests.* There are no competing interests.

## References


Abbott Jr., L. F., Farrell, K. M., Nickerson, J. G., and Gay, N. K.: Lithic Resources of the North Carolina Coastal Plain: Prehistoric Acquisition and Utilization Patterns, in: The Archaeology of North Carolina: Three Archaeological Symposia, edited by Ewen, C. R., Whyte, T. R., and Davis Jr., R. P. S., no. 30 in North Carolina Archaeological Council Publication, p. 51, North Carolina Archaeological Council, http://www.rla.unc.edu/NCAC/Publications/NCAC30/index.html, 2011.

Arrouays, D., Grundy, M. G., Hartemink, A. E., Hempel, J. W., Heuvelink, G. B., Hong, S. Y., Lagacherie, P., Lelyk, G., McBratney, A. B., McKenzie, N. J., d.L. Mendonca-Santos, M., Minasny, B., Montanarella, L., Odeh, I. O., Sanchez, P. A., Thompson, J. A., and Zhang, G.-L.: GlobalSoilMap: Towards a Fine-Resolution Global Grid of Soil Properties, Advances in Agronomy, 125, 93–134, 2014.

Arrouays, D., McBratney, A., Bouma, J., Libohova, Z., Richer-de-Forges, A. C., Morgan, C. L., Roudier, P., Poggio, L., and Mulder, V. L.: Impressions of Digital Soil Maps: The Good, the Not so Good, and Making Them Ever Better, Geoderma Regional, 20, e00 255, https://doi.org/10.1016/j.geodrs.2020.e00255, 2020.

Bloom, A. L.: Gorges History: Landscapes and Geology of the Finger Lakes Region, Paleontological Research Institution, Ithaca, New York, 2018.

Chaney, N., Minasny, B., Herman, J., Nauman, T., Brungard, C., Morgan, C., McBratney, A., Wood, E., and Yimam, Y.: POLARIS Soil Properties: 30-m Probabilistic Maps of Soil Properties over the Contiguous United States, Water Resources Research, 55, 2916–2938, https://doi.org/10.1029/2018WR022797, 2019.

Daniels, R. B., Gamble, E. E., and Wheeler, W. H.: Age of soil landscapes in the coastal plain of North Carolina, Soil Science Society of America Journal, 42, 98–105, https://doi.org/10.2136/sssaj1978.03615995004200010022x, 1978.

Daniels, R. B., Buol, S. W., Kleiss, H. J., and Ditzler, C. A.: Soil Systems in North Carolina, no. 314 in Technical Bulletin, North Carolina State University, Soil Science Dept, Raleigh, NC, 1999.

ISRIC - World Soil Information: SoilGrids – Global Gridded Soil Information, https://www.isric.org/explore/soilgrids, 2020.

IUSS Working Group WRB: World Reference Base for Soil Resources 2014; Update 2015. International Soil Classification System for Naming Soils and Creating Legends for Soil Maps, no. 106 in World Soil Resources Reports, FAO, Rome, http://www.fao.org/3/i3794en/I3794en.pdf, 2015.

McBratney, A. B., Mendon\ c{c}a Santos, M. L., and Minasny, B.: On Digital Soil Mapping, Geoderma, 117, 3–52, https://doi.org/10.1016/S0016-7061(03)00223-4, 2003.

Minasny, B. and McBratney, A. B.: Digital Soil Mapping: A Brief History and Some Lessons, Geoderma, 264, Part B, 301–311, https://doi.org/10.1016/j.geoderma.2015.07.017, 2016.

Natural Resources Conservation Service: Land Resource Regions and Major Land Resource Areas of the United States, the Caribbean, and the Pacific Basin, no. 296 in U.S. Department of Agriculture Handbook, US Government Printing Office, Washington, DC, https://www.nrcs.usda.gov/wps/portal/nrcs/detail/soils/survey/?cid=nrcs142p2_053624, 2006.

Natural Resources Conservation Service: SSURGO/STATSGO2 Structural Metadata and Documentation, https://www.nrcs.usda.gov/wps/portal/nrcs/detail/soils/survey/geo/?cid=nrcs142p2_053631, n.d.

New York State Geological Survey: Geologic Map of New York, New York State Geological Survey, Albany, NY, http://www.nysm.nysed.gov/research-collections/geology/gis, 1970.

New York State Geological Survey: Surficial Geologic Map of New York, New York State Geological Survey, Albany, NY, http://www.nysm.nysed.gov/research-collections/geology/gis, 1986.

North Carolina Geological Survey Section: Geologic Map of North Carolina, 1985, https://deq.nc.gov/about/divisions/energy-mineral-land-resources/north-carolina-geological-survey/ncgs-maps/1985-geologic-map-of-nc, 1985.

NRCS Soils: Gridded National Soil Survey Geographic Database (gNATSGO), https://www.nrcs.usda.gov/wps/portal/nrcs/detail/soils/survey/geo/?cid=nrcseprd1464625, 2020.

Poggio, L., de Sousa, L. M., Batjes, N. H., Heuvelink, G. B. M., Kempen, B., Ribeiro, E., and Rossiter, D.: SoilGrids 2.0: Producing Soil Information for the Globe with Quantified Spatial Uncertainty, SOIL, 7, 217–240, https://doi.org/10.5194/soil-7-217-2021, 2021.

R Studio: R Markdown, https://rmarkdown.rstudio.com/, 2020.

Ramcharan, A., Hengl, T., Nauman, T., Brungard, C., Waltman, S., Wills, S., and Thompson, J.: Soil Property and Class Maps of the Conterminous United States at 100-Meter Spatial Resolution, Soil Science Society of America Journal, 82, 186–201, https://doi.org/10.2136/sssaj2017.04.0122, 2018.

Rossiter, D. G.: Knowledge Is Power: Where Geopedologic Insights Are Necessary for Predictive Digital Soil Mapping, in: Geopedology, edited by Zinck, J. A., Metternicht, G., Bocco, G., and Valle, H. F. D., pp. 227–237, Springer International Publishing, https://doi.org/10.1007/978-3-319-19159-1_13, 2016.

Rossiter, D. G., Poggio, L., Beaudette, D., and Libohova, Z.: How Well Does Predictive Soil Mapping Represent Soil Geography? An Investigation from the USA, SOIL Discussions, https://doi.org/10.5194/soil-2021-80, 2021.

Rossiter, D. G., Poggio, L., Beaudette, D., and Libohova, Z.: How Well Does Digital Soil Mapping Represent Soil Geography? An Investigation from the USA, SOIL, https://doi.org/10.5194/soil-8-559-2022, 2022.

Science Committee: Specifications: Tiered GlobalSoilMap.Net Products; Release 2.3, Tech. rep., GlobalSoilMap.net, http://www.ozdsm.com.au/resources/GlobalSoilMap%20specs%20version%202point3.pdf, 2012.

Scull, P., Franklin, J., Chadwick, O., and McArthur, D.: Predictive Soil Mapping: A Review, Progress in Physical Geography, 27, 171–197, https://doi.org/10.1191/0309133303pp366ra, 2003.

Soil Survey Division Staff: Keys to Soil Taxonomy, US Government Printing Office, Washington, DC, twelfth edn., www.nrcs.usda.gov/wps/portal/nrcs/detail/soils/survey/class/, 2014.

Thompson, J. A., Kienast-Brown, S., D'Avello, T., Philippe, J., and Brungard, C.: Soils2026 and Digital Soil Mapping – A Foundation for the Future of Soils Information in the United States, Geoderma Regional, 22, e00 294, https://doi.org/10.1016/j.geodrs.2020.e00294, 2020.

Together with our partners we produce, gather, compile and serve quality-assured soil information at global, national and regional levels. We stimulate the use of this information to address global challenges through capacity building, awareness raising and direct cooperation with users and clients.

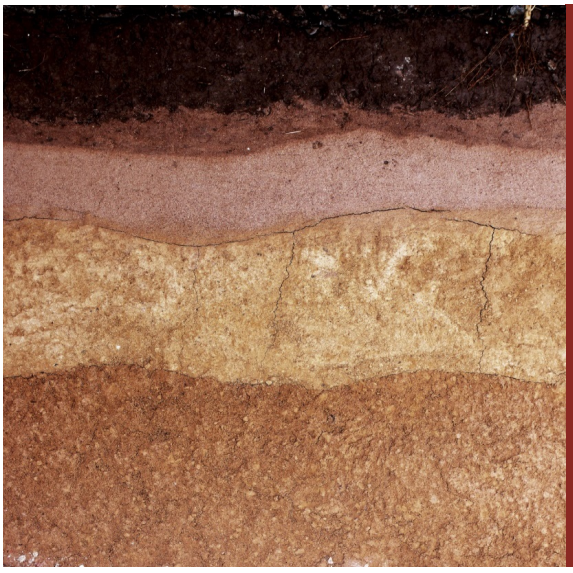

www.isric.org